
A systematic study of Galactic infrared bubbles along the Galactic plane with AKARI and Herschel

Misaki HANAOKA¹, Hidehiro KANEDA¹, Toyoaki SUZUKI¹, Takuma KOKUSHO¹, Shinki OYABU¹, Daisuke ISHIHARA¹, Mikito KOHNO¹, Takuya FURUTA¹, Takuro TSUCHIKAWA¹ and Futoshi SAITO¹

¹Graduate School of Science, Nagoya University, Furo-cho, Chikusa-ku, Nagoya 464-8602, Japan

*E-mail: hanaoka@u.phys.nagoya-u.ac.jp, kaneda@u.phys.nagoya-u.ac.jp

Received (reception date); Accepted (acceptation date)

Abstract

Galactic infrared (IR) bubbles, which have shell-like structures in the mid-IR wavelengths, are known to contain massive stars near their centers. IR bubbles in inner Galactic regions ($|l| \leq 65^\circ$, $|b| \leq 1^\circ$) have so far been studied well to understand the massive star formation mechanisms. In this study, we expand the research area to the whole Galactic plane ($0^\circ \leq l < 360^\circ$, $|b| \leq 5^\circ$), using the AKARI all-sky survey data. We limit our study on large bubbles with angular radii of $>1'$ to reliably identify and characterize them. For the 247 IR bubbles in total, we derived the radii and the covering fractions of the shells, based on the method developed in Hattori et al. (2016). We also created their spectral energy distributions, using the AKARI and Herschel photometric data, and decomposed them with a dust model, to obtain the total IR luminosity and the luminosity of each dust component, i.e., polycyclic aromatic hydrocarbons (PAHs), warm dust and cold dust. As a result, we find that there are systematic differences in the IR properties of the bubbles between inner and outer Galactic regions. The total IR luminosities are lower in outer Galactic regions, while there is no systematic difference in the range of the shell radii between inner and outer Galactic regions. More IR bubbles tend to be observed as broken bubbles rather than closed ones and the fractional luminosities of the PAH emission are significantly higher in outer Galactic regions. We discuss the implications of these results for the massive stars and the interstellar environments associated with the Galactic IR bubbles.

Key words: infrared: ISM — ISM: bubbles — star: formation — star: massive

1 Introduction

A large number of Galactic infrared (IR) bubbles, which have shell-like structures, are known to exist along the Galactic plane. Churchwell et al. (2006, 2007) cataloged about 600 objects which are located in inner Galactic regions ($|l| \leq 65^\circ$, $|b| \leq 1^\circ$), using the 8 μm band images of the Galactic Legacy Infrared Mid-plane Survey Extraordinaire (GLIMPSE; Benjamin et al. 2003; Churchwell et al. 2009) program with

Spitzer. In this catalog, the IR bubbles are classified into two categories, broken and closed bubbles, by their visual morphologies. More recently, Simpson et al. (2012) created a catalog of 5106 IR bubbles with such information as the position, the radius and the thickness of each IR bubble.

The 8 μm band brightness is dominated by the emission from polycyclic aromatic hydrocarbons (PAHs), which are present ubiquitously in photodissociation regions (PDRs). The

shell structures of the IR bubbles are clearly seen in the PAH emission. Within the PAH shells, ionized gases are distributed, emitting the $24\ \mu\text{m}$ emission which traces hot dust. Deharveng et al. (2010) investigated 102 IR bubbles which were cataloged by Churchwell et al. (2006). They showed that 86% of the sample objects enclose H II regions using the Spitzer 8 and $24\ \mu\text{m}$ and the radio-continuum data. Thus, most of the IR bubbles possess ionizing massive stars near the centers of the PAH shells.

These IR bubbles are likely to be formed by the central massive stars. Typical massive star formation mechanisms are “collect and collapse”, “globule squeezing” and “cloud-cloud collision (CCC)” (e.g., Elmegreen 1998; Zinnecker & Yorke 2007). The former two mechanisms compress the interstellar media (ISM) at the edge of the H II regions and clumps by radiation from the pre-existing massive stars (e.g., Deharveng et al. 2010; Dale et al. 2007). The CCC mechanism is triggered by collision between two molecular clouds, making dense cores on the collision surface. Habe and Ohta (1992) simulated the CCC process and found that head-on collisions between the clouds can produce massive stars. Recently, several pieces of evidence for massive star formation likely triggered by CCC have been observed for a number of IR bubbles (e.g., Torii et al. 2015; Baug et al. 2016; Hattori et al. 2016; Ohama et al. 2018; Fukui et al. 2018). Massive stars are often obscured heavily and thus mid- and far-IR observations are crucial.

In the previous study (Hattori et al. 2016), the IR flux densities of each bubble were estimated by using six images in the 9, 18, 65, 90, 140 and $160\ \mu\text{m}$ bands of the AKARI all-sky survey data. They showed a tight correlation between the total IR luminosity and the shell radius, which followed the conventional picture of the Strömgen sphere. They also obtained the central position and the shell radius of each object and established the quantitative criteria for classification of the shell morphologies. Then, they found that large broken bubbles tend to have higher total IR luminosities, lower fractional luminosities of the PAH emission and dust heating sources located nearer to the shells. Based on these results, Hattori et al. (2016) suggested that many of the large broken bubbles might have been formed by the CCC mechanism.

In the previous studies including ours, IR bubbles in inner Galactic regions ($|l| \leq 65^\circ$, $|b| \leq 1^\circ$) have been investigated intensively, whereas those in outer Galactic regions have not been investigated. We expand the previous studies to the whole Galactic plane ($0^\circ \leq l < 360^\circ$, $|b| \leq 5^\circ$) to obtain the morphologies and the IR luminosities of the IR bubbles in outer Galactic regions as well. We also add the far-IR and submillimeter wavelength data using the Herschel infrared Galactic plane survey (Hi-GAL; Molinari et al. 2010, 2016) to improve the estimation of the IR luminosity. Then, we obtain the properties of the IR bubbles along the whole Galactic plane and discuss the ef-

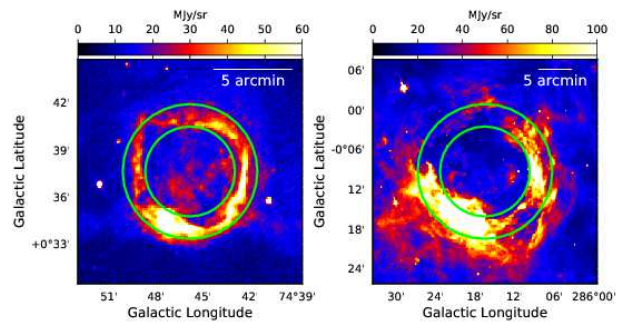


Fig. 1. Examples of the AKARI $9\ \mu\text{m}$ band images of the IR bubbles newly found in this work, (left) closed and (right) broken bubbles. The green annular regions are defined as the shell regions which are used for morphology characterization. The color scales are given in units of MJy sr^{-1} .

fects of the massive stars and the interstellar environments on the properties of the IR bubbles in inner and outer Galactic regions.

2 Observation and data analysis

We searched for new IR bubbles in outer Galactic regions ($|l| > 65^\circ$, $|b| \leq 5^\circ$) and high-latitude inner Galactic regions ($|l| \leq 65^\circ$, $1^\circ < |b| \leq 5^\circ$), using the AKARI all-sky survey data in the mid-IR wavelengths (central wavelengths $9\ \mu\text{m}$ and $18\ \mu\text{m}$; Onaka et al. 2007; Ishihara et al. in preparation). In this paper, we identify IR bubbles as objects which apparently possess shell-like structures in the AKARI $9\ \mu\text{m}$ band images. Figure 1 shows examples of the $9\ \mu\text{m}$ band images of the IR bubbles newly found in this study. Since the resolution of the AKARI $9\ \mu\text{m}$ band image is $4''.68$, which is lower than that of the Spitzer $8\ \mu\text{m}$ band image ($1''.2$; Benjamin et al. 2003), we limit our study on large bubbles with angular radii, r , of $> 1'$ to reliably identify and characterize them. We also reject some objects which are too large ($r > 20'$) or very faint for IR bubbles, such as those with the averaged shell brightnesses lower than the sky background levels. As a result, we newly found 179 IR bubbles which consist of 141 objects in the outer Galactic regions and 38 objects in the high-latitude inner Galactic regions. We also derived the central position and r of each IR bubble, following the same procedure as in Hattori et al. (2016).

We characterize the morphologies of 319 IR bubbles including the objects investigated in Hattori et al. (2016) by the covering fraction (CF), rather than classify it into only two types (i.e., broken or closed) as performed in the previous studies. First, we applied smoothing for the $9\ \mu\text{m}$ images with a Gaussian kernel of 3 pixels to improve the accuracy in determining the shell morphology. Then, in order to estimate the CF, we divided the shell region (defined as an annular region from $0.8r$ to $1.2r$ as shown in figure 1) into 12 sectors. The number of the sectors for each shell is determined so that one sector has more than 30 pixels regardless of the angular sizes of the shells.

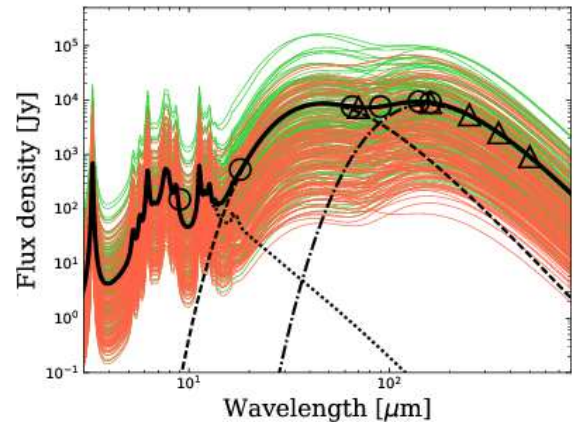
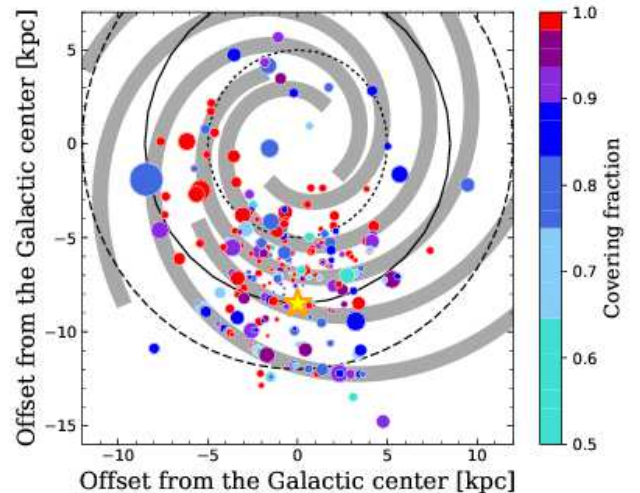
Table 1. Correction factors of the AKARI far-IR bands for the aperture photometry of the IR bubbles with various radii.

IR bubble radius	65 μm	90 μm	140 and 160 μm
$1' \leq R < 1'25$	1.30	1.44	1.23
$1'25 \leq R < 1'5$	1.19	1.27	1.12
$1'5 \leq R < 1'75$	1.14	1.18	1.07
$1'75 \leq R < 2'$	1.09	1.11	1.04
$2' \leq R < 2'25$	1.06	1.07	1.02
$2'25 \leq R < 2'5$	1.03	1.03	1.01

To judge whether each sector is filled or not, we adopted the condition that 40% of the pixels in the sector should be brighter than a certain brightness threshold. Here, we used two levels for the brightness threshold, 20% and 30% of the brightness averaged over the shell region, as also used in Hattori et al. (2016), and took the average of the two results to facilitate consistency check with the result of Hattori et al. (2016). In this study, we also took into account the dependence of the CF on the phase of the sector division. We shifted the sector-dividing positions by half a sector and re-estimated the CF. Finally, we again took the average of the two CFs before and after changing the dividing positions.

To estimate the IR fluxes, we used the AKARI mid-IR (9 and 18 μm) and far-IR (65, 90, 140 and 160 μm ; Kawada et al. 2007; Doi et al. 2015) all-sky survey data as well as Herschel Hi-GAL data (70, 160, 250, 350 and 500 μm). For the objects in the high-latitude regions ($1^\circ < |b| \leq 5^\circ$), we used only the AKARI data since Herschel Hi-GAL data are not available in those regions. The photometry aperture and the background region are defined by the same procedure as in Hattori et al. (2016), which are a circular region of $< 2r$ and an annular region at from $2r$ to $4r$, respectively. Since the target sizes are not large enough to neglect the aperture corrections in the AKARI far-IR images, we estimated the aperture correction factors for the IR bubbles with various radii, based on the encircled energies of the point spread functions created from point-like galaxies in Kokusho et al. (2017). The aperture correction factors thus obtained are shown in table 1 and we applied them to the AKARI far-IR fluxes. On the other hand, the target sizes are large enough for AKARI in the mid-IR and Herschel, and therefore aperture corrections for those images are negligible ($< 1\%$) and not applied. Here, we considered random and systematic errors as flux uncertainties; we calculated the random errors from the background fluctuation, while we adopted the systematic errors of 10% for the AKARI mid-IR and Herschel data (Ishihara et al. in preparation; Molinari et al. 2016) and 15% for the AKARI far-IR data (Takita et al. 2015).

We created the spectral energy distributions (SEDs) of the IR bubbles from the photometry fluxes, and fitted the SEDs with a dust model which includes PAHs, warm dust and cold

**Fig. 2.** Result of the SED fitting. The black circles and triangles are the AKARI and Herschel data points, respectively, which are averaged for all IR bubbles. The black solid line shows the best-fit model, while the dotted, dashed and dash-dotted lines show PAH, warm dust and cold dust components, respectively. The green and red solid lines correspond to the best-fit spectral models of the other IR bubbles in the inner and outer Galactic regions, respectively.**Fig. 3.** Distribution of the IR bubbles plotted on the pattern of the Galactic spiral arms modeled by Nakanishi and Sofue (2016). The colors correspond to the CF. The size of the symbol is proportional to the absolute shell radius of each IR bubble from 0.3 pc to 50 pc. The dotted, solid and dashed lines correspond to the distances of 5, 8.5 and 12 kpc from the Galactic center, respectively. The star symbol indicates the position of the Sun.

dust components. We adopted the PAH model by Draine and Li (2007) and assumed the dust components as modified blackbody. The emissivity power-law indices of the modified blackbody dust components are assumed to be 2 and the dust temperatures are allowed to vary for both warm and cold dust components (Anderson et al. 2012). However, when we fit the SEDs of the IR bubbles in the high-latitude inner Galactic regions ($1^\circ < |b| \leq 5^\circ$) where we have no Herschel data, we fixed the dust temperature of the cold dust at 18 K, which is a typical value of the IR bubbles analyzed in this study, due to the lack of the data points to be fitted. Figure 2 shows the results

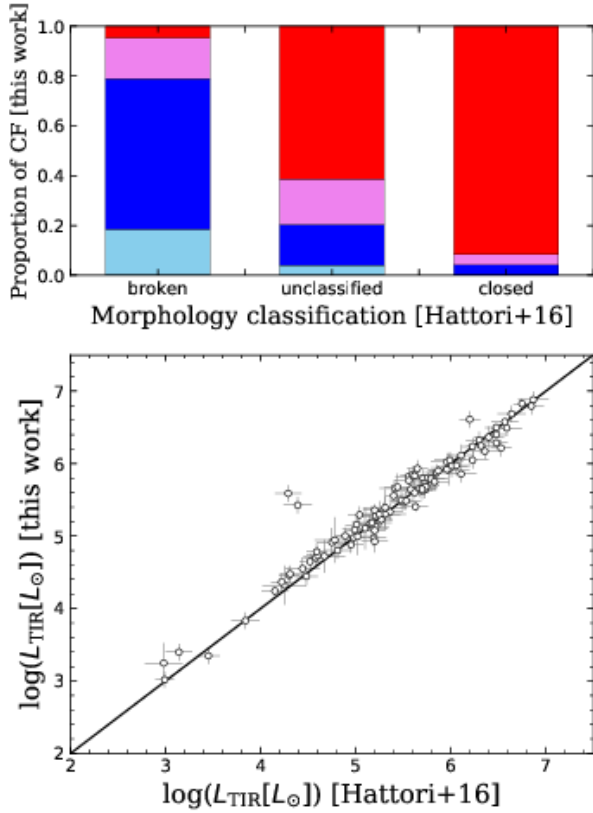


Fig. 4. Comparison between the results of this work and Hattori et al. (2016). The upper panel shows the proportion of the CF. The red, violet, blue and cyan areas correspond to $CF=1.0$, $0.9 \leq CF < 1.0$, $0.75 \leq CF < 0.9$ and $0.5 \leq CF < 0.75$, respectively. The lower panel shows comparison of L_{TIR} . The black line corresponds to $y = x$.

of the SED fitting. Based on the reduced χ^2 values, about 90% of our samples are accepted with a 90% confidence level. From this figure, we can recognize that the fluxes of the IR bubbles in inner Galactic regions are systematically higher than those in outer Galactic regions.

Among the IR bubbles newly found in this study, we cross-identified 60 IR bubbles in the catalog of H II regions in Milky Way (Hou & Han 2014) to estimate their distances. Figure 3 shows the distribution of the IR bubbles with the known distance on the Galactic disk, from which we confirm that most of them are located on or near the Galactic spiral arms (Nakanishi & Sofue 2016). Hence, we assume that, for the IR bubbles with their distances unknown, 32 IR bubbles are located on the Perseus arm in outer Galactic regions ($90^\circ < l < 225^\circ$) and 30 IR bubbles are located on the Orion and Sagittarius arms in inner Galactic regions at $|b| > 2^\circ$, toward which there is only a single arm along the line of sight. For the 259 bubbles whose distances were thus determined, we obtained the luminosities of the SED components, L_{PAH} , L_{warm} , L_{cold} and L_{TIR} ($= L_{\text{PAH}} + L_{\text{warm}} + L_{\text{cold}}$) as well as the absolute shell radii, R . In figure 4, we check the consistency of our result with the

result of Hattori et al. (2016), regarding the classification of the bubble morphology and estimation of L_{TIR} . From the figure, we confirm that there is a global consistency between the two results. For a few IR bubbles which show considerably higher L_{TIR} than those in Hattori et al. (2016), their distances were ambiguous (Deharveng et al. 2010; Watson et al. 2010; Kuchar & Bania 1994), and changed from Hattori et al. (2016) to those estimated in the catalog of H II regions (Hou & Han 2014).

The properties of all the IR bubbles detected in this study, including those in the previous studies with $r > 1'$, are summarized in Appendix. Note that the central positions of the IR bubbles are not necessarily close to the true positions of massive stars. For example, massive stars are expected to lie outside bubbles, when the bubbles are part of a large irregular cavity created by the massive star. Such cases are, “ES6”, “E58”, “E97” and “E109” (Deharveng et al. 2012; Dubner et al. 1992; Bassino et al. 1982). Also note that objects such as planetary nebulae (PNe), luminous blue variables (LBVs) and supernova remnants (SNRs) can be picked up as IR bubbles mistakenly. We have confirmed that “E12” and “E43” belong to LBVs and SNRs, respectively (Kraemer et al. 2010; Acero et al. 2016), which are removed from our sample, while PNe are not included in our sample based on the PNe catalogs (Parker et al. 2006; Miszalski et al. 2008). Furthermore, when H II regions have bipolar morphology, they can also be mistaken as two independent bubbles (e.g., Deharveng et al. 2015; Samal et al. 2018). We have confirmed that 10 bubbles belong to 5 bipolar H II regions (“S18” and “S20”; Samal et al. 2018, “S97”; Deharveng et al. 2015, “S109”, “S110” and “S111”; Dalglish et al. 2018, “CN107” and “CN109”; Bally et al. 1983; Dewangan et al. 2016, “EN13” and “EN14”; Mallick et al. 2013), which are also removed from our sample. As a result, 247 IR bubbles remain in our final sample. We have confirmed that 241 out of the 247 IR bubbles show the significant presence of diffuse emission at $18 \mu\text{m}$ within the shell boundaries. Deharveng et al. (2010), in their study of Galactic bubbles, find that extended $24 \mu\text{m}$ emission often lies close to the exciting star or cluster of the bubbles. Therefore, almost all the IR bubbles in our sample are likely to be indeed associated with massive stars.

3 Result

Figure 5 shows the relation between L_{TIR} and R . From the figure, we confirm that the result of our analysis for the IR bubbles treated in the previous study (open symbols) is consistent with the best-fit result of Hattori et al. (2016) with $L_{\text{TIR}} = aR^3$. Here, Hattori et al. (2016) assumed that L_{TIR} is proportional to Q , the total number rate of ionizing photons from central stars, and Q is described as the following equation (Strömgren 1939):

$$Q = \frac{4\pi}{3} R_S^3 n_e n_p \alpha_B(T_e), \quad (1)$$

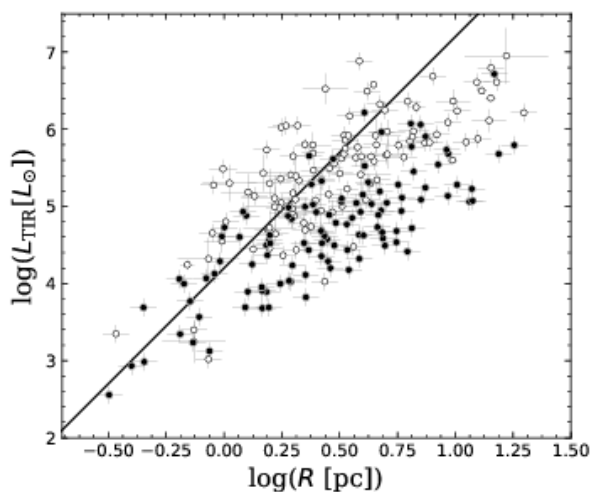


Fig. 5. Relation between L_{TIR} and the shell radius of each bubble. The filled symbols correspond to the IR bubbles newly found in this study, while the open symbols correspond to those investigated in Hattori et al. (2016). The black line corresponds to the best-fit result of Hattori et al. (2016) with $L_{\text{TIR}} = aR^3$.

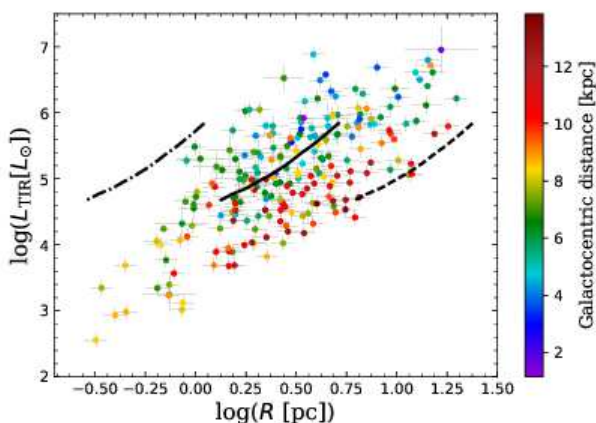


Fig. 6. Same as figure 5, but the data points are color-coded according to the Galactocentric distance. The black dash-dotted, solid and dashed lines show the relations calculated for O3V–O9V stars (Martins et al. 2005) in H II regions with the electron densities of 1000, 100 and 10 cm^{-3} , respectively, for the temperature of 10^4 K .

where R_S , n_e , n_p , T_e and α_B are the Strömgen sphere radius, electron density, proton density, electron temperature and “case-B” recombination coefficient (Osterbrock 1989), respectively. Hence, the IR bubbles in the previous study follow the conventional picture of the Strömgen sphere. However, we find a systematic difference between the IR bubbles newly found in this study (filled symbols) and those investigated in the previous study; the former shows L_{TIR} significantly lower than the latter, while both show no systematic difference in the range of R . Moreover, the former IR bubbles do not apparently follow the picture of the Strömgen sphere (i.e., $L_{\text{TIR}} \propto R^3$).

Most of the IR bubbles newly found in this study are located in outer Galactic regions, while all the previous samples are in

inner Galactic regions. Therefore, the systematic difference in figure 5 is likely to be caused by the dependence of L_{TIR} on the Galactocentric distance. In figure 6, we color-coded the data points of the $L_{\text{TIR}}-R$ relation, based on the Galactocentric distance. The figure indeed shows the $L_{\text{TIR}}-R$ relation depends on the Galactocentric distance and their correlation becomes tighter for a limited range of the distance. Furthermore, the upper panel of figure 7 shows that L_{TIR} monotonically decreases with the Galactocentric distance, except for the local minimum in the solar neighborhood ($\sim 8 \text{ kpc}$) where relatively faint IR bubbles are detected because of their proximity. Considering that L_{TIR} is roughly approximated by the bolometric luminosities of the massive stars associated with the IR bubbles, this result indicates that the central stars tend to be of earlier spectral types in inner Galactic regions. Martins, Schaerer and Hillier (2005) showed that $\log(L_{\text{TIR}}/L_\odot)$ of a star of spectral type O9V–O3V ranges from 4.77 to 5.84. The L_{TIR} values in figure 7 suggest that almost all the IR bubbles in inner Galactic regions ($\lesssim 7 \text{ kpc}$) contain an O-type star and some of them may have tens of O-type stars, whereas a significant fraction of the IR bubbles in outer Galactic regions ($\gtrsim 9 \text{ kpc}$) are not IR luminous enough to have a single O-type star. Indeed, the distribution of the star forming rate is known to steadily decrease outward from a peak at $\sim 5 \text{ kpc}$ from the Galactic center (e.g., Guesten & Mezger 1982; Misiriotis et al. 2006; Kennicutt & Evans 2012).

The middle panel in figure 7 shows that R does not clearly depend on the Galactocentric distance, except for the local minimum in the solar neighborhood where relatively small IR bubbles satisfy our size limit, $r > 1'$. Although L_{TIR} decreases monotonically, R does not with the Galactocentric distance, which is consistent with the result in figure 6. Moreover, the lower panel in figure 7 indicates that the proportion of the IR bubbles with relatively low CFs increases with the Galactocentric distance, i.e., the IR bubbles tend to be observed as broken bubbles in outer Galactic regions.

Figure 8 shows the fractional PAH luminosities ($L_{\text{PAH}}/L_{\text{TIR}}$) of the IR bubbles plotted against L_{TIR} , color-coded according to the Galactocentric distance. The figure clearly exhibits a negative correlation between $L_{\text{PAH}}/L_{\text{TIR}}$ and L_{TIR} . As suggested by Hattori et al. (2016), this trend can be interpreted in such a way that intense UV fluxes from central stars increase L_{TIR} , which accelerate photodissociation of PAHs, thus lowering $L_{\text{PAH}}/L_{\text{TIR}}$. Our new finding is that the $L_{\text{PAH}}/L_{\text{TIR}}$ values of the IR bubbles in outer Galactic regions are systematically higher than those in inner Galactic regions; the relation of the IR bubbles in outer Galactic regions appears to follow a trend similar to that in inner Galactic regions. Moreover, a significant fraction of the IR bubbles in outer Galactic regions shows $L_{\text{PAH}}/L_{\text{TIR}}$ as high as 30–40%, which is unusually high as compared to 10–20% typically observed

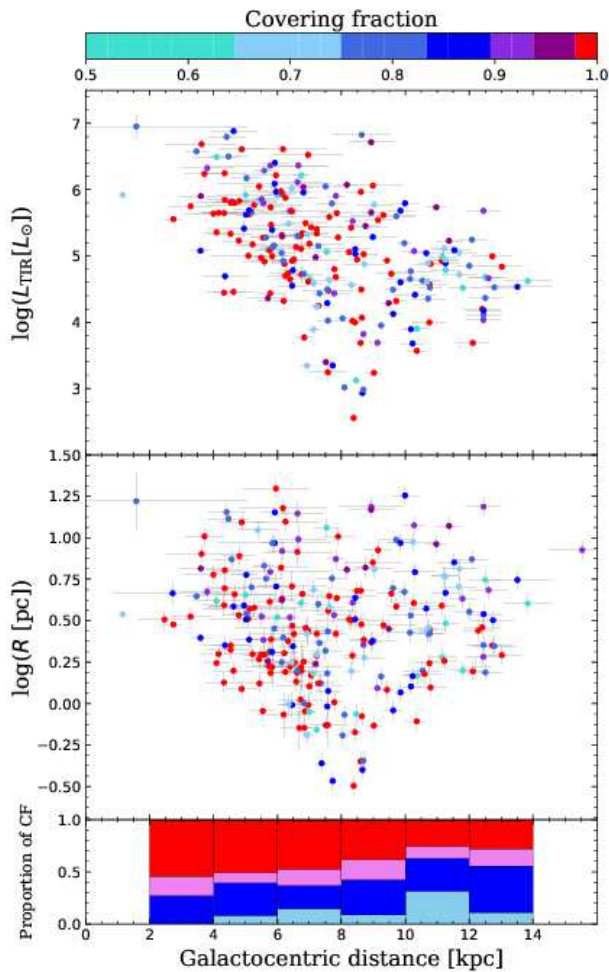


Fig. 7. Upper and middle panels show the distributions of L_{TIR} and R , respectively, as a function of the Galactocentric distance, color-coded according to the CF. The lower panel shows the proportion of the CF every 2 kpc bin. The red, violet, blue and cyan areas correspond to $\text{CF}=1.0$, $0.9 \leq \text{CF} < 1.0$, $0.75 \leq \text{CF} < 0.9$ and $0.5 \leq \text{CF} < 0.75$, respectively.

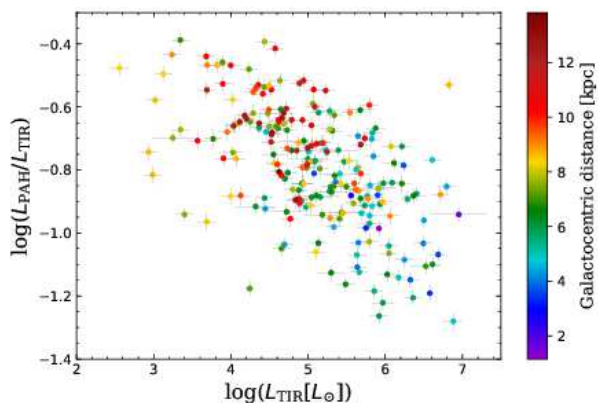


Fig. 8. Relation between $L_{\text{PAH}}/L_{\text{TIR}}$ and L_{TIR} . The data points are color-coded according to the Galactocentric distance.

for star-forming galaxies (e.g., Smith et al. 2007; Stierwalt et al. 2014) as well as star-forming regions and diffuse interstellar regions in our Galaxy (e.g., Onaka et al. 1996; Arendt et al. 1998; Draine 2011; Kaneda et al. 2013). On the other hand, the ratio of the sum of L_{PAH} to the sum of L_{TIR} for all the IR bubbles along the whole Galactic plane (i.e., $\Sigma L_{\text{PAH}}/\Sigma L_{\text{TIR}}$) is 14% as a whole, which is usual as typically observed values.

4 Discussion

4.1 Dependence of the IR bubble properties on the Galactocentric distance

We discuss the $L_{\text{TIR}}-R$ relation of the IR bubbles which shows a systematic difference between inner and outer Galactic regions. In order to interpret the result in light of the Strömgen sphere picture, in figure 6 we overplot the relation between the bolometric luminosity and the radius expected for a set of O3V–O9V stars with different electron densities (Martins et al. 2005). We find that the $L_{\text{TIR}}-R$ relation at ~ 3 kpc corresponds to the density of $\sim 200 \text{ cm}^{-3}$ while that at ~ 11 kpc corresponds to $\sim 30 \text{ cm}^{-3}$, and thus the required density is likely to decrease monotonically with the Galactocentric distance. Those trends suggest that the shell may be expanded more easily in outer Galactic regions, which can explain the result that the observed range of R is similar between inner and outer Galactic regions even though L_{TIR} is systematically lower in outer Galactic regions. Considering the pressure balance between the inside and the outside of the shells, this may be related to the decline in the interstellar energy density, which is dominated by the cosmic ray and magnetic energy in the local ISM (Mathis et al. 1983; Webber & Yushak 1983; Arendt et al. 1998; Heiles & Crutcher 2005; Draine 2011). Indeed, the cosmic ray sources, which contain SNRs, pulsars and OB stars, and magnetic field strength decrease roughly by a factor of 2 from 3 kpc to 10 kpc, which is consistent with the change of the electron density and the gas pressure assuming a constant gas temperature (e.g., Case & Bhattacharya 1998; Bronfman et al. 2000; Han et al. 2006; Lorimer et al. 2006; Ackermann et al. 2012). This can also explain the trend of the CF decreasing with the Galactocentric distance (figure 7), since the IR bubbles are expected to break more easily in the ISM of lower gas densities.

4.2 Fractional PAH luminosities of the IR bubbles

We discuss the variation of the fractional PAH luminosities of the IR bubbles and its implications for the interstellar environments. Figure 8 shows a global trend of $L_{\text{PAH}}/L_{\text{TIR}}$ decreasing with L_{TIR} . However, as far as the IR bubbles in outer ($\gtrsim 8$ kpc) Galactic regions are concerned, dependence of $L_{\text{PAH}}/L_{\text{TIR}}$ on L_{TIR} is not significant. In figure 9, we plot $L_{\text{PAH}}/L_{\text{TIR}}$ against $L_{\text{warm}}/L_{\text{cold}}$ instead of L_{TIR} . The figure shows the dependence

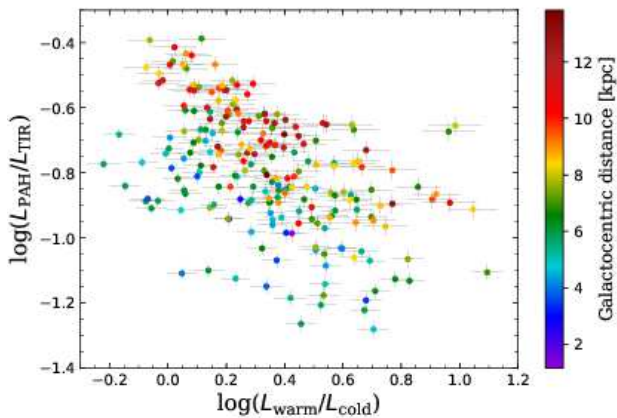


Fig. 9. Relation between $L_{\text{PAH}}/L_{\text{TIR}}$ and $L_{\text{warm}}/L_{\text{cold}}$. The data points are color-coded according to the Galactocentric distance.

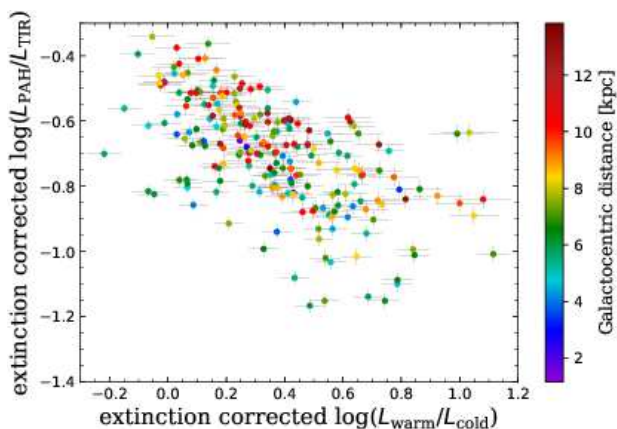


Fig. 10. Same as figure 9, but modified considering the effect of the interstellar extinction for $L_{\text{PAH}}/L_{\text{TIR}}$ and $L_{\text{warm}}/L_{\text{cold}}$.

of $L_{\text{PAH}}/L_{\text{TIR}}$ on $L_{\text{warm}}/L_{\text{cold}}$ more clearly than on L_{TIR} for both inner and outer Galactic regions. This is probably because $L_{\text{warm}}/L_{\text{cold}}$ (i.e., dust color temperature) indicates the strength of the UV radiation exposed to the PAHs more directly than L_{TIR} (e.g., Tielens 2008). Therefore, the negative correlation between $L_{\text{PAH}}/L_{\text{TIR}}$ and $L_{\text{warm}}/L_{\text{cold}}$ in figure 9 is likely to be caused by photodestruction of PAHs.

More importantly, figure 9 clearly shows a systematic difference in $L_{\text{PAH}}/L_{\text{TIR}}$ between inner and outer Galactic regions. Under the assumption that the relative abundance of PAHs to total dust is constant along the Galactic plane, there are mainly two causes to systematically change $L_{\text{PAH}}/L_{\text{TIR}}$; the cold dust component in outer Galactic regions may be too cold to fully contribute to L_{TIR} , or the interstellar extinction may lower the observed L_{PAH} more in inner Galactic regions. The former possibility calls for denser cold gas surrounding the IR bubbles in outer Galactic regions, which is rather unlikely considering that the IR bubbles tend to be more easily expanded and observed as broken bubbles in outer Galactic regions. We evaluated the effects of the interstellar extinction on L_{PAH} (and also L_{warm}) as

follows: first, we derive the optical depth, τ , to each IR bubble. τ is described as:

$$\tau = C_{\text{ext}}(\lambda)n_{\text{H}}D, \quad (2)$$

where $C_{\text{ext}}(\lambda)$, n_{H} and D are the dust extinction cross section as a function of wavelength, the hydrogen density and the distance to each IR bubble, respectively. We adopted $C_{\text{ext}}(\lambda)$ given in Draine (2003) and calculated the effective values of $C_{\text{ext}}(\lambda)$ for the AKARI 9 μm and 18 μm bands to be $1.77 \times 10^{-23} \text{ cm}^2$ and $1.04 \times 10^{-23} \text{ cm}^2$, respectively, considering their band response curves. We took the sum of the hydrogen atomic and molecular gas densities (i.e., $n_{\text{H}} = n_{\text{H1}} + 2n_{\text{H2}}$) in the calculation where the n_{H1} distribution on the Galactic plane is taken from Wolfire et al. (2003) while the n_{H2} distribution from that estimated by Nakanishi and Sofue (2006) with the ^{12}CO ($J = 1 - 0$) survey data. We then modified the 9 μm and 18 μm fluxes with τ , and fitted the SEDs again to re-estimate L_{PAH} and L_{warm} . Figure 10 shows the result thus modified for the interstellar extinction. This result still shows the systematic difference persistently, although the difference between inner and outer Galactic regions is reduced. Therefore, the interstellar extinction is not a dominant factor to cause the systematic difference in $L_{\text{PAH}}/L_{\text{TIR}}$ between inner and outer Galactic regions.

It is likely that the relative abundance of PAHs to the total dust is not constant along the Galactic plane. Mass losses from asymptotic giant branch (AGB) stars are believed to make a significant contribution to the formation of dust in the ISM (e.g., Matsuura et al. 2009). Among them, carbon-rich (C-rich) AGB stars are considered as suppliers of carbonaceous dust including PAHs, while oxygen-rich (O-rich) AGB stars as suppliers of silicate dust (Latter 1991; Tielens 2008). Ishihara et al. (2011) investigated the distributions of C-rich and O-rich AGB stars in our Galaxy and obtained that the C-rich AGB stars are uniformly distributed within the Galactic disk, while the O-rich AGB stars are concentrated toward the Galactic center. Therefore, the relative contribution of the C-rich stars to the formation of dust in the ISM is higher in outer Galactic regions, which can explain the systematically higher $L_{\text{PAH}}/L_{\text{TIR}}$ for IR bubbles in outer Galactic regions. Figure 10 also suggests that the environments in the solar neighborhood belong to those relatively rich in PAHs in outer Galactic regions.

4.3 Properties of the IR bubbles in light of CCC

In the previous study, Hattori et al. (2016) suggested that many of the large broken bubbles might have been formed by the CCC mechanism, based on the observational facts that large broken bubbles tend to have higher L_{TIR} and lower $L_{\text{PAH}}/L_{\text{TIR}}$. Here we also discuss this possibility, investigating the dependence of L_{TIR} and $L_{\text{PAH}}/L_{\text{TIR}}$ on the CF. To remove the dependence on the Galactocentric distance as much as possible, we treat the IR

bubbles in inner (≤ 7 kpc) and outer (> 7 kpc) Galactic regions, separately.

In figure 11, we plotted the $L_{\text{TIR}}-R$ and $L_{\text{PAH}}/L_{\text{TIR}}-L_{\text{warm}}/L_{\text{cold}}$ relations color-coded according to the CF. In each panel, the black line corresponds to the best-fit relation for the closed (i.e., $\text{CF}=1$) bubble only. The figure does not clearly show any systematic difference between the broken and closed bubbles, except for the $L_{\text{TIR}}-R$ relation in outer Galactic regions. The $L_{\text{TIR}}-R$ relation of the broken bubbles is significantly deviated from that of the closed bubbles toward larger R in outer Galactic regions. This can be explained by considering that the IR bubbles of lower gas densities are more deviated from the $L_{\text{TIR}}-R$ relation for the other IR bubbles and expected to break more easily as mentioned above. On the other hand, there is no systematic difference in the $L_{\text{TIR}}-R$ relation between the closed and broken bubbles in inner Galactic regions, which implies that the morphology of the IR bubbles is likely to be less affected by the ambient interstellar environments in inner Galactic regions.

In order to clearly visualize trends, if any, on the right-hand side of each panel in figure 11, the proportions of the CF are shown for L_{TIR} and $L_{\text{PAH}}/L_{\text{TIR}}$ averaged every 15 objects. From this figure, we can confirm the trends pointed out by Hattori et al. (2016) for the bubbles in inner Galactic regions, i.e., the IR bubbles with higher L_{TIR} and lower $L_{\text{PAH}}/L_{\text{TIR}}$ tend to have lower CFs. On the other hand, we find that there is no such a trend in outer Galactic regions, and thus the trends are not universal for the bubbles along the whole Galactic plane.

Recently, Whitworth et al. (2018) developed a model for the formation of bipolar H II regions and suggested that bipolar bubbles can be formed by CCC. As far as our bipolar bubbles (they were removed from our sample) are concerned, however, they are not necessarily attributed to CCC; the massive star associated with the bipolar H II region composed of “EN13” and “EN14” is formed by merging of multiple filaments (Mallick et al. 2013), while the massive stars associated with other two are formed by gravitational collapse of the massive clumps (“S109”, “S110” and “S111”; Dalglish et al. 2018, “CN107” and “CN109”; Dewangan et al. 2016). In figure 11, we also show their locations, from which we find that the bipolar bubbles have relatively small radii for L_{TIR} and high $L_{\text{warm}}/L_{\text{cold}}$ but not low $L_{\text{PAH}}/L_{\text{TIR}}$. Hence those bubbles, even if included, are unlikely to contribute to the CCC trends suggested by Hattori et al. (2016).

As another possible formation mechanism of broken morphology, we consider the champagne flow model (Tenorio-Tagle 1979). Since a massive star forms near the edge of a cloud in this model, we expect that $L_{\text{warm}}/L_{\text{cold}}$ of the broken bubbles would differ systematically from that of the closed bubbles, when most of the broken bubbles are of champagne flow origin. We performed a two sample Kolmogorov-Smirnov (K-

S) test with respect to the distribution of $L_{\text{warm}}/L_{\text{cold}}$ between the broken ($\text{CF}<0.9$) and closed ($\text{CF}=1$) bubbles. The result of the K-S test shows that the distributions are not significantly different ($p>0.20$), thus not calling for the necessity of the champagne flow model to explain the broken bubbles. To verify the possibility that the morphology and the IR properties of the bubbles may be related with the CCC mechanism, we will investigate the spatial distributions of the bubbles in the PAH and dust emissions and compare them with the CO position-velocity maps, the results of which will be reported in a separate paper.

5 Summary

Using AKARI and Herschel data, we obtained R , L_{TIR} and CF of 247 IR bubbles with $r>1'$ along the whole Galactic plane ($0^\circ \leq l < 360^\circ$, $|b| \leq 5^\circ$). As a result, we find that there are systematic differences in the properties of the IR bubbles between the inner and outer Galactic regions; L_{TIR} and CF are systematically lower while $L_{\text{PAH}}/L_{\text{TIR}}$ is higher in outer Galactic regions. Investigating the dependence of those properties on the Galactocentric distance, we suggest that the results are explained by the changes in the properties of the massive stars and the interstellar environments associated with the Galactic IR bubbles from inner to outer Galactic regions; (1) the central massive stars are likely to be of later spectral types, (2) the IR bubbles may be more easily expanded and broken due to lower ambient interstellar pressure and (3) the higher ratios of C-rich AGBs to O-rich AGBs may cause the shells of the IR bubbles to be richer in PAH in outer Galactic regions. Finally, the IR bubbles in outer Galactic regions do not show evidence for the possibility that large broken IR bubbles may be caused by CCC, although the IR bubbles in inner Galactic regions show results consistent with those in Hattori et al. (2016) which are indicative of CCC for large broken IR bubbles.

Acknowledgments

We thank the referee for carefully reading our manuscript and giving us helpful comments. This research is based on observations with AKARI, a JAXA project with the participation of ESA. Herschel is an ESA space observatory with science instruments provided by European-led Principal Investigator consortia and with important participation from NASA. We thank all the members of the AKARI and Herschel projects, particularly the all-sky survey and Hi-GAL data reduction teams.

Appendix. Data set of the IR bubbles discussed in this study.

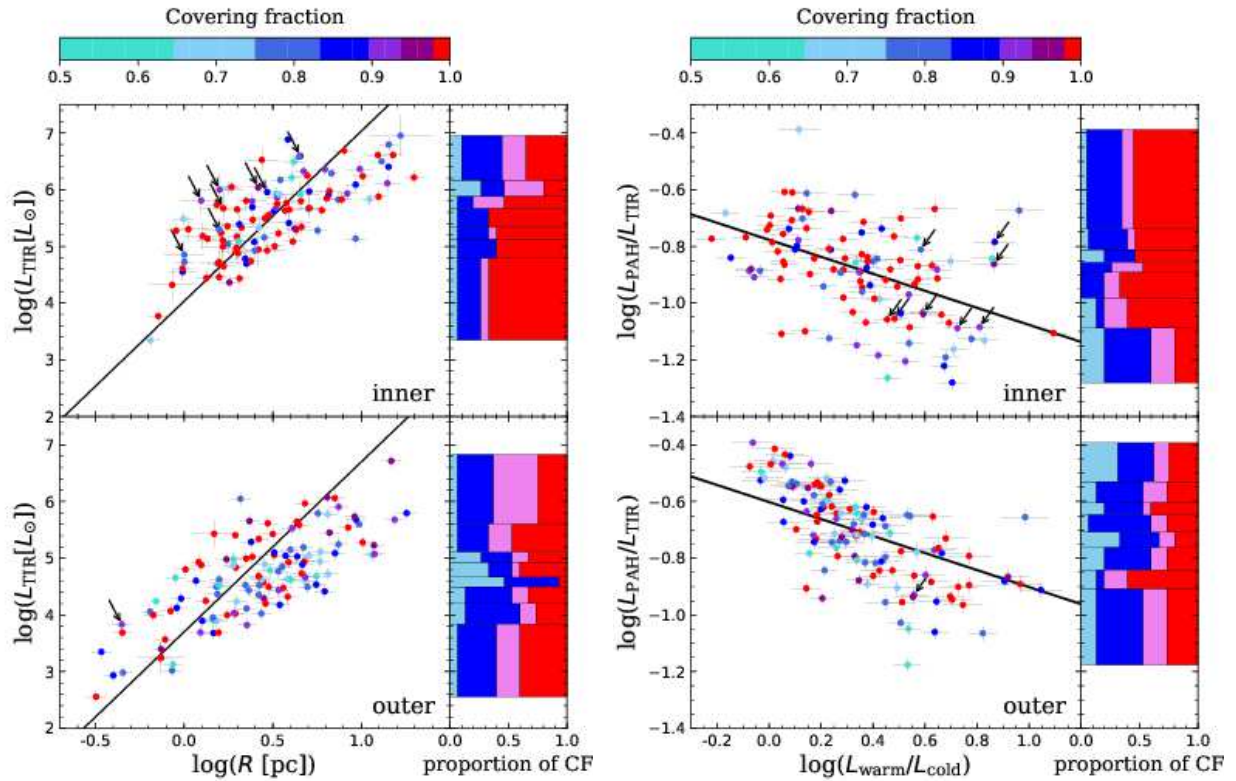


Fig. 11. Same relations as (left) figure 5 and (right) figure 8, but color-coded with the CF, and shown separately for the IR bubbles in inner (≤ 7 kpc) and outer (> 7 kpc) Galactic regions in the upper and lower panels, respectively. In each panel, the black line corresponds to the best-fit power-law relation to the data points of the IR bubbles with the CF of unity, where the power-law indices are fixed at 3 for the left panels while they are allowed to vary for the right panels. The right-hand side of each panel shows the proportion of the CF for L_{TIR} and $L_{\text{PAH}}/L_{\text{TIR}}$ averaged every 15 objects. The red, violet, blue and cyan areas correspond to $\text{CF}=1.0$, $0.9 \leq \text{CF} < 1.0$, $0.75 \leq \text{CF} < 0.9$ and $0.5 \leq \text{CF} < 0.75$, respectively. Only in this figure, we plot the data points of the bubbles originating from bipolar H II regions, which are denoted by arrows.

Table 2. Summary of the central positions, radii, distances and covering fractions of the IR bubbles.

Name	l [°]	b [°]	r [']	D [kpc]	Distance ref.†	$D_{\text{Gal.}}$ [kpc]	R [pc]	CF
N2	10.749	-0.468	6.81	8.4±3.5	Churchwell+06	1.6±3.5	16.63	0.75
N4	11.892	0.750	2.01	3.4±0.4	Watson+10	5.2±0.4	1.99	1.00
N5	12.478	-1.140	3.63	3.7±1.1	Beaumont+10	5.0±1.1	3.90	0.83
N6	12.522	-0.625	6.18	4.1±0.5§	Deharveng+10	4.6±0.5	7.40	0.75
N10	13.188	0.040	1.49	4.6±0.6	Deharveng+10	4.2±0.6	1.99	1.00
N11	13.225	0.085	1.11	3.8±0.5	Watson+10	4.9±0.5	1.23	1.00
N12	13.724	-0.018	4.98	4.4±0.6§	Deharveng+10	4.4±0.6	6.37	1.00
N14	14.004	-0.142	1.00	3.1±0.4	Watson+10	5.5±0.4	0.90	1.00
N15	15.009	-0.599	1.29	1.9±0.6	Beaumont+10	6.7±0.6	0.71	1.00
N16	15.009	0.053	2.33	13.7±1.8	Deharveng+10	5.9±1.8	9.29	0.83
N18	16.684	-0.356	6.67	4.0±0.5	Hou&Han+14	4.8±0.5	7.76	1.00
N20	17.919	-0.686	1.14	—	—	—	—	1.00
N24	18.933	-0.307	10.67	4.6±0.6	Deharveng+10	4.4±0.6	14.27	0.79
N29	23.050	0.559	2.76	2.2±0.3	Deharveng+10	6.5±0.3	1.76	1.00
N30	23.116	0.564	1.13	2.6±0.8§	Beaumont+10	6.2±0.8	0.86	1.00
N34	24.295	-0.170	1.11	11.7±1.5	Deharveng+10	5.3±1.5	3.78	1.00
N35	24.496	0.221	3.19	8.6±1.1	Deharveng+10	3.6±1.1	7.99	1.00
N36	24.837	0.096	2.54	6.4±0.8	Deharveng+10	3.8±0.8	4.72	0.92
N37	25.282	0.292	2.12	3.3±0.4	Watson+10	5.7±0.4	2.04	0.63
N39	25.362	-0.149	2.47	5.8±0.8	Watson+10	4.1±0.8	4.16	0.63
N40	25.367	-0.364	1.13	11.3±1.5	Deharveng+10	5.1±1.5	3.72	1.00
N44	26.822	0.382	1.08	5.0±0.7§	Deharveng+10	4.6±0.7	1.58	1.00
N45	26.993	-0.053	1.54	10.2±1.3	Deharveng+10	4.7±1.3	4.56	1.00
N46	27.310	-0.109	1.38	5.6±0.7	Deharveng+10	4.4±0.7	2.25	0.83
N47	28.030	-0.044	2.82	7.3±0.9	Watson+10	4.0±0.9	5.99	1.00
N49	28.828	-0.230	1.32	5.5±0.7	Deharveng+10	4.5±0.7	2.11	1.00
N50	29.000	0.093	1.63	10.6±1.4	Deharveng+10	5.2±1.4	5.03	0.75
N51	29.154	-0.263	2.08	3.4±0.4	Watson+10	5.8±0.4	2.05	1.00
N52	30.736	-0.018	2.32	5.7±0.7	Watson+10	4.6±0.7	3.85	0.83
N54	31.164	0.295	2.03	3.0±0.4	Watson+10	6.1±0.4	1.77	0.75
N56	32.579	0.001	1.19	9.4±1.2	Deharveng+10	5.1±1.2	3.24	1.00
N59	33.093	-0.068	7.62	5.6±0.7	Deharveng+10	4.9±0.7	12.40	1.00
N61	34.160	0.137	3.35	3.4±0.4	Deharveng+10	6.0±0.4	3.31	0.63
N62	34.336	0.218	1.49	3.9±0.5	Watson+10	5.7±0.5	1.69	1.00
N64	34.755	-0.669	4.61	3.2±0.4	Deharveng+10	6.1±0.4	4.29	1.00
N65	35.001	0.332	2.24	3.1±0.4	Watson+10	6.2±0.4	2.02	1.00
N68	35.650	-0.058	4.90	10.6±1.4	Deharveng+10	6.2±1.4	15.09	1.00
N69	36.240	0.660	7.81	4.9±0.6	Deharveng+10	5.4±0.6	11.13	0.71
N71	38.290	-0.008	8.18	3.5±0.5§	Rahman+10	6.1±0.5	8.32	0.92
N72	38.353	-0.132	1.00	1.5±0.2	Watson+10	7.4±0.2	0.44	0.88
N73	38.738	-0.141	1.06	9.2±1.2	Deharveng+10	5.9±1.2	2.84	0.79
N74	38.906	-0.439	1.34	2.3±0.3	Watson+10	6.9±0.3	0.90	1.00
N77	40.422	-0.055	1.24	5.0±0.7	Watson+10	5.7±0.7	1.80	0.96
N79	41.514	0.029	1.33	11.5±1.5	Hou&Han+14	7.6±1.5	4.45	1.00
N80	41.932	0.037	1.82	1.4±0.2	Watson+10	7.5±0.2	0.74	0.96
N81	41.994	-0.518	8.41	8.1±1.1	Deharveng+10	6.0±1.1	19.81	1.00
N82	42.103	-0.623	1.61	5.2±0.7	Watson+10	5.8±0.7	2.44	1.00
N84	42.833	-0.157	1.07	1.1±0.1	Watson+10	7.7±0.1	0.34	0.83
N90	43.775	0.058	1.71	3.1±0.4	Watson+10	6.6±0.4	1.54	1.00

Table 2. (Continued)

Name	l [°]	b [°]	r [']	D [kpc]	Distance ref.†	$D_{\text{Gal.}}$ [kpc]	R [pc]	CF
N91	44.215	0.041	5.31	8.1±1.1	Deharveng+10	6.2±1.1	12.51	1.00
N92	44.336	-0.829	1.55	3.7±0.5	Watson+10	6.4±0.5	1.67	1.00
N95	45.377	-0.716	1.21	4.4±0.6	Watson+10	6.2±0.6	1.55	1.00
N98	47.032	0.227	1.78	4.6±0.6	Watson+10	6.3±0.6	2.38	1.00
N101	49.195	-0.359	1.19	5.1±0.7	Watson+10	6.4±0.7	1.77	0.71
N107	50.949	0.112	10.25	4.7±0.8§	Churchwell+06	6.6±0.8	14.01	0.92
N109	52.007	0.547	16.61	10.7±0.9	Rodríguez+12	8.6±0.9	51.67	0.79
N114	52.250	0.704	1.60	9.3±0.5	Hou&Gao+14	7.9±0.5	4.33	1.00
N115	53.551	-0.009	3.36	2.7±0.4	Watson+10	7.2±0.4	2.64	1.00
N117	54.107	-0.068	1.93	5.1±0.7	Watson+10	6.9±0.7	2.86	1.00
N120	55.268	0.250	1.34	1.9±0.6§	Beaumont+10	7.6±0.6	0.74	1.00
N123	57.534	-0.281	1.24	8.8±1.1	Hou&Han+14	8.3±1.1	3.17	1.00
N124	58.607	0.632	1.43	3.2±0.4	Watson+10	7.4±0.4	1.33	0.79
N126	59.601	0.319	1.98	6.3±0.8	Watson+10	7.6±0.8	3.63	1.00
N127	60.649	-0.061	3.27	0.9±0.1	Watson+10	8.1±0.1	0.86	0.79
N128	61.669	0.946	3.35	2.8±0.4	Watson+10	7.6±0.4	2.73	0.79
N130	62.376	-0.543	1.37	3.0±0.4	Watson+10	7.6±0.4	1.19	0.88
N131	63.084	-0.410	6.16	8.6±1.0	Zhang+13	8.9±1.0	15.39	0.92
N133	63.159	0.449	1.67	2.1±0.3	Watson+10	7.8±0.3	1.02	1.00
S1	349.814	-0.605	4.33	3.6±0.9§	Churchwell+06	5.0±0.9	4.53	0.54
S7	348.259	0.483	4.45	1.3±0.2	Deharveng+09	7.2±0.2	1.73	0.96
S8	347.397	0.261	1.64	6.3±0.3	Churchwell+06	2.7±0.3	3.00	1.00
S11	345.482	0.400	2.33	2.0±0.3	Watson+10	6.6±0.3	1.36	1.00
S13	345.041	-0.737	8.76	1.8±0.2	Watson+10	6.8±0.2	4.58	1.00
S14	344.761	-0.551	4.88	2.9±0.4	Watson+10	5.8±0.4	4.11	1.00
S15	343.916	-0.647	2.18	3.1±0.7§	Churchwell+06	5.6±0.7	1.97	1.00
S17	343.480	-0.048	1.81	2.9±0.4	Watson+10	5.8±0.4	1.53	1.00
S18	342.075	0.433	1.34	4.2±0.3	Hou&Gao+14	4.7±0.3	1.62	1.00
S20	342.045	0.386	1.53	1.0±0.1§	Churchwell+06	7.6±0.1	0.45	0.92
S23	341.280	-0.346	2.06	3.3±0.4	Watson+10	5.5±0.4	1.97	1.00
S27	340.040	-0.147	1.70	12.1±0.3	Hou&Gao+14	5.0±0.3	5.98	0.83
S29	338.906	0.612	2.52	3.3±0.6§	Churchwell+06	5.6±0.6	2.42	0.92
S36	337.965	-0.469	3.00	4.0±0.5§	Churchwell+06	5.0±0.5	3.49	0.75
S37	337.688	-0.343	1.30	3.5±0.5	Rahman+10	5.4±0.5	1.32	1.00
S41	336.484	-0.216	3.35	5.1±0.7	Watson+10	4.3±0.7	4.96	1.00
S44	334.520	0.818	2.55	4.6±0.5§	Churchwell+06	4.8±0.5	3.41	1.00
S51	332.666	-0.615	1.68	3.8±0.5	Hou&Gao+14	5.4±0.5	1.85	1.00
S54	332.314	-0.565	1.08	—	—	—	—	1.00
S62	331.318	-0.356	1.90	4.4±0.5§	Churchwell+06	5.1±0.5	2.43	0.88
S64	331.005	-0.148	3.03	3.8±0.5§	Churchwell+06	5.5±0.5	3.35	0.92
S66	330.784	-0.414	6.31	3.7±0.3	Hou&Gao+14	5.6±0.3	6.78	0.79
S70	329.275	0.112	1.13	9.8±0.3	Hou&Gao+14	5.0±0.3	3.22	0.83
S71	327.986	-0.109	1.07	7.2±0.6	Churchwell+06	4.5±0.6	2.24	1.00
S73	327.547	-0.814	3.88	2.6±0.5	Hou&Gao+14	6.5±0.5	2.94	1.00
S74	327.527	-0.848	1.29	2.6±0.5	Hou&Gao+14	6.5±0.5	0.98	0.88
S76	326.927	-0.021	5.14	3.4±0.6§	Churchwell+06	6.0±0.6	5.08	0.88
S79	326.698	0.515	2.79	1.8±0.5	Hou&Gao+14	7.1±0.5	1.48	1.00
S91	320.868	-0.417	2.56	3.0±0.4	Hou&Gao+14	6.5±0.4	2.21	0.88
S92	320.595	0.163	5.49	8.9±0.5	Hou&Gao+14	5.9±0.5	14.23	0.88

Table 2. (Continued)

Name	l [°]	b [°]	r [']	D [kpc]	Distance ref.†	$D_{\text{Gal.}}$ [kpc]	R [pc]	CF
S96	320.164	0.795	1.40	2.6±0.7§	Churchwell+06	6.7±0.7	1.06	1.00
S97	319.886	0.770	1.28	2.7±0.7	Churchwell+06	6.7±0.7	1.00	0.79
S104	317.995	-0.750	2.01	2.7±0.7§	Churchwell+06	6.7±0.7	1.58	1.00
S109	316.818	-0.101	1.59	3.6±1.1	Hou&Gao+14	6.4±1.1	1.66	1.00
S110	316.806	-0.032	1.59	2.7±0.7	Churchwell+06	6.8±0.7	1.25	0.92
S111	316.772	-0.075	1.52	3.6±1.1	Hou&Gao+14	6.4±1.1	1.59	0.92
S116	314.237	0.477	3.85	5.9±0.9	Churchwell+06	6.1±0.9	6.60	1.00
S123	312.976	-0.436	2.32	3.9±1.4§	Churchwell+06	6.5±1.4	2.63	1.00
S133	311.487	0.398	2.03	5.6±0.3	Churchwell+06	6.4±0.3	3.31	0.92
S137	310.981	0.410	3.43	5.1±1.1§	Churchwell+06	6.5±1.1	5.09	1.00
S141	309.552	-0.721	1.46	3.9±1.3§	Churchwell+06	6.7±1.3	1.66	1.00
S143	309.050	0.157	5.34	5.3±1.1	Churchwell+06	6.6±1.1	8.22	1.00
S145	308.701	0.641	6.36	5.3±0.9	Churchwell+06	6.7±0.9	9.80	0.92
S150	305.534	0.357	1.10	4.0±1.1	Hou&Gao+14	7.0±1.1	1.27	1.00
S156	305.261	0.215	1.93	4.9±1.1	Churchwell+06	7.0±1.1	2.75	1.00
S163	303.893	-0.704	2.94	11.4±0.6	Hou&Gao+14	9.7±0.6	9.72	0.75
S181	298.218	-0.315	1.79	4.0±0.5	Churchwell+06	7.5±0.5	2.08	0.75
S186	295.177	-0.661	5.43	3.6±0.5	Churchwell+06	7.7±0.5	5.68	0.79
CN24	1.150	-0.091	1.42	11.2±1.9	Hou&Gao+14	2.7±1.9	4.63	0.88
CN60	4.421	0.089	1.51	14.2±1.9	Hou&Gao+14	5.8±1.9	6.23	0.92
CN63	4.563	-0.126	1.87	12.0±0.7	Hou&Gao+14	3.6±0.7	6.53	0.96
CN71	5.883	-0.472	5.23	1.3±0.1	Hou&Gao+14	7.2±0.1	1.95	1.00
CN73	6.060	-0.130	1.87	1.3±0.1	Hou&Gao+14	7.2±0.1	0.69	0.58
CN88	7.001	-0.294	2.61	2.7±0.8	Hou&Gao+14	5.8±0.8	2.05	0.88
CN90	7.021	-0.193	2.11	2.7±0.8	Hou&Gao+14	5.8±0.8	1.66	1.00
CN99	7.411	0.689	3.51	12.8±0.6	Hou&Gao+14	4.5±0.6	13.02	0.79
CN107	8.114	0.231	1.20	13.0±0.7	Hou&Gao+14	4.7±0.7	4.53	0.96
CN108	8.128	-0.483	7.15	4.9±0.6	Watson+09	3.7±0.6	10.19	1.00
CN109	8.150	0.243	1.27	13.0±0.7	Hou&Gao+14	4.7±0.7	4.79	0.92
CN111	8.314	-0.084	1.70	5.0±0.3	Hou&Gao+14	3.6±0.3	2.49	0.88
CN114	8.361	-0.296	1.34	4.5±0.4	Hou&Gao+14	4.1±0.4	1.76	1.00
CN138	9.834	-0.709	1.07	4.3±0.6	Watson+09	4.3±0.6	1.34	1.00
CN139	9.937	-0.746	3.14	4.3±0.7	Churchwell+07	4.3±0.7	3.93	1.00
CN148	10.316	-0.140	1.55	2.2±0.3	Dewangan+15	6.3±0.3	0.99	0.67
CS2	359.742	-0.412	2.05	1.5±0.2	Hou&Gao+14	7.0±0.2	0.89	0.63
CS33	356.235	0.677	1.25	9.5±0.1	Hou&Gao+14	1.2±0.1	3.45	0.71
CS39	354.977	-0.531	1.43	—	—	—	—	1.00
CS51	354.184	-0.050	2.17	5.3±0.7	Churchwell+07	3.3±0.7	3.35	1.00
CS57	353.354	-0.140	1.78	6.2±0.8	Watson+09	2.5±0.8	3.21	1.00
CS62	353.096	0.330	2.85	1.9±0.4	Hou&Gao+14	6.6±0.4	1.58	0.75
CS79	351.675	0.522	3.62	1.7±0.3	Hou&Gao+14	6.8±0.3	1.79	1.00
CS81	351.646	0.165	1.31	11.6±0.3	Hou&Gao+14	3.5±0.3	4.44	0.79
EN1	6.132	-1.436	10.04	—	—	—	—	1.00
EN2	6.929	-2.298	2.17	1.6±0.2	Sagittarius	7.0±0.2	0.98	1.00
EN3	7.213	-2.166	5.52	0.9±0.1	Hou&Han+14	7.6±0.1	1.52	0.79
EN4	7.306	-2.015	3.48	0.9±0.1	Hou&Han+14	7.6±0.1	0.96	0.83
EN5	11.451	-1.525	3.65	1.3±0.2	Hou&Han+14	7.3±0.2	1.33	1.00
EN6	12.472	-1.139	3.59	2.4±0.3	Hou&Han+14	6.2±0.3	2.51	0.75
EN7	14.408	3.949	1.36	1.6±0.2	Sagittarius	6.9±0.2	0.65	0.71

Table 2. (Continued)

Name	l [°]	b [°]	r [']	D [kpc]	Distance ref.†	$D_{\text{Gal.}}$ [kpc]	R [pc]	CF
EN8	14.637	1.514	1.29	—	—	—	—	1.00
EN9	15.172	3.366	11.40	2.8±0.4	Hou&Han+14	5.8±0.4	9.28	0.75
EN10	18.969	2.199	7.39	—	—	—	—	0.79
EN11	26.730	3.541	1.28	1.9±0.3	Sagittarius	6.8±0.3	0.71	1.00
EN12	26.822	3.493	1.78	1.9±0.3	Sagittarius	6.8±0.3	1.00	0.79
EN13	28.743	3.392	5.05	2.0±0.3	Sagittarius	6.8±0.3	2.94	0.88
EN14	28.851	3.526	4.49	2.0±0.3	Sagittarius	6.8±0.3	2.62	0.96
EN15	31.801	1.460	2.46	—	—	—	—	0.83
EN16	31.915	1.446	5.13	3.8±0.5	Hou&Han+14	5.6±0.5	5.66	0.75
EN17	35.391	-1.859	4.42	3.3±0.4	Hou&Han+14	6.1±0.4	4.21	0.96
EN18	36.436	-1.653	9.30	1.8±0.2	Hou&Han+14	7.1±0.2	4.86	0.71
EN19	37.365	1.532	2.57	—	—	—	—	0.79
EN20	38.221	1.565	2.90	—	—	—	—	0.83
EN21	40.139	1.574	4.84	1.6±0.2	Hou&Han+14	7.3±0.2	2.32	0.79
EN22	40.500	2.412	7.96	1.7±0.2	Hou&Han+14	7.3±0.2	3.98	0.79
ES1	295.155	-1.805	11.64	2.2±0.3	Hou&Han+14	7.8±0.3	7.44	0.92
ES2	296.474	-2.715	3.70	3.6±0.5	Sagittarius	7.6±0.5	3.83	0.71
ES3	298.495	2.295	12.63	3.1±0.4	Sagittarius	7.5±0.4	11.51	0.58
ES4	305.672	1.612	1.83	5.0±0.6	Hou&Han+14	6.9±0.6	2.64	0.71
ES5	318.502	-4.303	3.71	1.8±0.2	Sagittarius	7.2±0.2	1.98	0.67
ES6	320.401	-1.905	2.43	—	—	—	—	1.00
ES7	320.476	-1.976	5.83	—	—	—	—	0.79
ES8	326.908	-1.099	1.53	—	—	—	—	0.58
ES9	335.761	2.592	3.41	1.5±0.2	Sagittarius	7.1±0.2	1.53	0.71
ES10	336.533	-1.793	3.40	—	—	—	—	0.79
ES11	337.475	-1.043	1.29	—	—	—	—	0.71
ES12	341.032	-2.168	19.40	—	—	—	—	0.92
ES13	351.528	-1.362	1.74	—	—	—	—	1.00
ES14	351.547	-1.294	1.74	—	—	—	—	1.00
ES15	351.640	-1.361	1.77	—	—	—	—	1.00
ES16	353.285	1.016	7.82	1.8±0.2	Hou&Han+14	6.7±0.2	4.05	0.50
E1	65.909	-2.687	2.94	4.0±0.5	Orion	7.8±0.5	3.41	0.92
E2	66.946	-1.302	1.50	1.5±0.2	Hou&Han+14	8.0±0.2	0.64	0.75
E3	68.154	1.054	9.72	3.6±0.5	Hou&Han+14	7.9±0.5	10.17	1.00
E4	69.857	1.721	1.80	—	—	—	—	0.75
E5	70.203	1.693	3.48	7.0±0.9	Hou&Han+14	9.0±0.9	7.09	1.00
E6	72.177	0.885	1.02	—	—	—	—	1.00
E7	74.764	0.627	3.57	3.1±0.4	Hou&Han+14	8.2±0.4	3.22	1.00
E8	78.112	3.689	2.73	2.0±0.3	Orion	8.3±0.3	1.57	0.67
E9	78.769	1.058	6.05	—	—	—	—	0.79
E10	78.985	4.196	3.57	1.9±0.2	Orion	8.3±0.2	1.95	1.00
E11	79.256	2.476	7.54	1.9±0.2	Orion	8.4±0.2	4.06	0.92
E12	79.284	0.461	1.46	—	—	—	—	0.96
E13	80.916	-0.189	5.03	3.3±0.4	Hou&Han+14	8.6±0.4	4.80	1.00
E14	81.415	0.613	7.33	—	—	—	—	0.75
E15	81.644	0.225	6.55	—	—	—	—	0.83
E16	81.654	1.524	4.86	—	—	—	—	1.00
E17	81.693	1.509	1.91	—	—	—	—	0.67
E18	82.037	2.292	1.46	1.6±0.2	Orion	8.4±0.2	0.67	1.00

Table 2. (Continued)

Name	l [°]	b [°]	r [']	D [kpc]	Distance ref.†	$D_{\text{Gal.}}$ [kpc]	R [pc]	CF
E19	82.047	2.350	2.46	3.4±0.4	Hou&Han+14	8.7±0.4	2.43	1.00
E20	82.501	2.942	9.61	1.6±0.2	Orion	8.4±0.2	4.35	0.83
E21	82.539	0.375	5.11	4.4±0.6	Hou&Han+14	9.0±0.6	6.47	0.71
E22	83.462	0.151	1.32	—	—	—	—	0.67
E23	84.600	0.990	1.96	—	—	—	—	0.96
E24	84.897	3.833	7.58	3.0±0.4	Hou&Han+14	8.8±0.4	6.61	0.96
E25	85.168	3.880	12.15	1.4±0.2	Orion	8.5±0.2	4.78	1.00
E26	86.153	-0.544	3.08	—	—	—	—	0.83
E27	90.241	1.752	1.67	5.5±0.7	Perseus	10.1±0.7	2.68	0.79
E28	90.941	1.506	2.14	5.5±0.7	Perseus	10.2±0.7	3.40	0.75
E29	93.142	2.824	1.64	0.9±0.1	Orion	8.6±0.1	0.45	1.00
E30	93.328	1.757	6.16	5.3±0.7	Perseus	10.2±0.7	9.42	0.71
E31	93.939	1.579	2.66	5.2±0.7	Perseus	10.3±0.7	4.04	1.00
E32	94.493	-1.493	4.19	3.8±0.5	Hou&Han+14	9.6±0.5	4.61	1.00
E33	95.150	-0.748	4.17	5.1±0.7	Perseus	10.3±0.7	6.21	0.88
E34	99.998	4.181	1.85	0.7±0.1	Orion	8.7±0.1	0.40	0.83
E35	102.881	-0.703	9.32	3.4±0.4	Hou&Han+14	9.9±0.4	9.32	0.88
E36	103.665	2.151	1.19	4.6±0.6	Perseus	10.5±0.6	1.58	0.79
E37	104.710	2.838	2.38	0.7±0.1	Orion	8.7±0.1	0.45	0.75
E38	105.320	3.265	12.19	0.6±0.1	Orion	8.7±0.1	2.26	0.92
E39	106.252	0.960	1.18	4.4±0.6	Perseus	10.6±0.6	1.51	1.00
E40	106.807	3.314	2.29	8.3±1.1	Hou&Han+14	13.5±1.1	5.56	0.83
E41	108.298	-1.069	2.99	4.3±0.6	Perseus	10.7±0.6	3.74	0.88
E42	110.880	-0.947	2.18	4.2±0.5	Perseus	10.7±0.5	2.64	0.79
E43	111.737	-2.132	1.62	4.1±0.5	Perseus	10.7±0.5	1.94	1.00
E44	112.718	-1.671	1.47	4.1±0.5	Perseus	10.8±0.5	1.75	1.00
E45	112.757	-1.792	2.35	4.1±0.5	Perseus	10.8±0.5	2.80	1.00
E46	114.522	-0.539	1.07	4.0±0.5	Perseus	10.8±0.5	1.25	1.00
E47	114.613	0.216	4.95	2.0±0.3	Hou&Han+14	9.5±0.3	2.82	0.96
E48	114.606	-0.804	5.60	2.4±0.3	Hou&Han+14	9.7±0.3	3.84	1.00
E49	115.794	-1.565	1.46	2.1±0.3	Hou&Han+14	9.6±0.3	0.91	0.83
E50	118.276	2.492	1.60	3.1±0.4	Sagittarius	10.4±0.4	1.47	0.58
E51	119.475	-0.917	13.82	3.0±0.4	Hou&Han+14	10.3±0.4	11.90	0.92
E52	120.637	3.563	1.78	2.8±0.4	Sagittarius	10.2±0.4	1.47	0.88
E53	121.753	4.017	1.61	2.7±0.4	Sagittarius	10.2±0.4	1.27	0.83
E54	126.665	-0.796	2.89	1.4±0.2	Hou&Han+14	9.4±0.2	1.21	1.00
E55	133.422	0.085	3.89	3.4±0.4	Perseus	11.1±0.4	3.89	1.00
E56	134.185	0.808	1.91	3.4±0.4	Perseus	11.2±0.4	1.90	0.50
E57	136.121	2.062	1.12	2.4±0.3	Hou&Han+14	10.4±0.3	0.78	1.00
E58	138.239	1.658	6.05	3.3±0.4	Perseus	11.2±0.4	5.89	0.71
E59	138.451	1.687	1.86	3.3±0.4	Perseus	11.2±0.4	1.81	1.00
E60	140.761	-0.853	4.83	3.3±0.4	Perseus	11.3±0.4	4.65	0.88
E61	140.774	-0.700	6.07	3.3±0.4	Perseus	11.3±0.4	5.85	0.71
E62	141.052	-1.114	3.16	3.3±0.4	Perseus	11.3±0.4	3.05	0.63
E63	148.074	-0.355	12.54	3.2±0.4	Perseus	11.4±0.4	11.79	0.96
E64	151.185	2.129	2.32	4.3±0.6	Hou&Han+14	12.4±0.6	2.88	1.00
E65	155.345	2.618	1.40	4.8±0.6	Hou&Han+14	13.0±0.6	1.96	1.00
E66	159.145	3.329	4.58	4.2±0.5	Hou&Han+14	12.5±0.5	5.57	0.54
E67	159.356	2.590	1.27	4.2±0.5	Hou&Han+14	12.5±0.5	1.54	0.75

Table 2. (Continued)

Name	l [°]	b [°]	r [']	D [kpc]	Distance ref.†	$D_{\text{Gal.}}$ [kpc]	R [pc]	CF
E68	173.448	2.607	10.97	1.5±0.2	Sagittarius	10.0±0.2	4.72	0.79
E69	173.578	2.817	2.95	1.4±0.2	Hou&Han+14	9.9±0.2	1.17	0.83
E70	176.788	0.141	4.48	3.3±0.4	Perseus	11.8±0.4	4.29	0.92
E71	177.695	-0.321	1.65	3.3±0.4	Perseus	11.8±0.4	1.58	0.54
E72	182.351	0.176	4.28	2.2±0.3	Hou&Han+14	10.7±0.3	2.72	0.71
E73	182.482	0.248	2.49	—	—	—	—	1.00
E74	188.938	0.792	4.40	2.2±0.3	Hou&Han+14	10.7±0.3	2.85	0.67
E75	190.082	0.787	3.48	3.5±0.5	Perseus	12.0±0.5	3.58	0.75
E76	190.057	0.483	12.61	2.5±0.3	Hou&Han+14	11.0±0.3	9.17	0.96
E77	196.219	-1.204	2.43	3.9±0.5	Hou&Han+14	12.3±0.5	2.75	1.00
E78	201.595	1.628	6.78	3.8±0.5	Hou&Han+14	12.1±0.5	7.43	0.75
E79	211.143	-1.004	1.34	4.0±0.5	Hou&Han+14	12.1±0.5	1.56	1.00
E80	211.873	-1.338	1.50	4.4±0.6	Perseus	12.4±0.6	1.91	0.92
E81	211.992	-1.070	1.76	4.4±0.6	Perseus	12.4±0.6	2.25	0.79
E82	212.031	-1.244	12.06	4.4±0.6	Perseus	12.4±0.6	15.40	0.92
E83	212.052	-0.745	2.35	5.9±0.8	Hou&Han+14	13.8±0.8	4.01	0.58
E84	212.397	-1.152	2.70	4.4±0.6	Perseus	12.5±0.6	3.46	0.88
E85	217.296	-1.404	3.68	7.9±1.0	Hou&Han+14	15.5±1.0	8.44	0.92
E86	218.198	-0.326	3.48	4.8±0.6	Perseus	12.6±0.6	4.83	0.92
E87	220.907	-2.482	3.26	2.8±0.4	Sagittarius	10.8±0.4	2.65	0.79
E88	221.858	-2.014	1.52	5.1±0.7	Perseus	12.7±0.7	2.24	1.00
E89	222.660	-1.601	2.14	5.1±0.7	Perseus	12.7±0.7	3.18	0.88
E90	224.162	1.247	1.46	5.2±0.7	Perseus	12.8±0.7	2.22	0.75
E91	224.410	-2.756	5.01	1.0±0.1	Hou&Han+14	9.2±0.1	1.46	0.79
E92	231.131	1.483	5.20	4.3±0.6	Hou&Han+14	11.7±0.6	6.49	0.71
E93	231.472	-4.410	4.05	4.3±0.6	Hou&Han+14	11.7±0.6	5.06	0.67
E94	232.549	0.861	10.17	1.7±0.2	Hou&Han+14	9.6±0.2	4.97	0.79
E95	234.786	-0.217	5.68	4.3±0.6	Hou&Han+14	11.5±0.6	7.11	0.83
E96	243.067	0.517	1.18	—	—	—	—	0.79
E97	253.511	-0.380	8.12	—	—	—	—	0.75
E98	253.779	-0.350	18.34	3.4±0.4	Hou&Han+14	10.0±0.4	18.00	0.88
E99	258.102	-4.132	2.13	2.0±0.3	Orion	9.1±0.3	1.24	0.92
E100	259.333	0.814	7.39	—	—	—	—	1.00
E101	259.610	-2.963	1.38	1.8±0.2	Orion	9.0±0.2	0.74	1.00
E102	261.602	0.952	15.41	0.7±0.1	Hou&Han+14	8.6±0.1	3.00	1.00
E103	263.613	-0.494	1.80	—	—	—	—	0.75
E104	263.836	0.126	1.82	—	—	—	—	0.96
E105	264.345	1.466	3.17	0.9±0.1	Hou&Han+14	8.6±0.1	0.84	1.00
E106	264.680	0.234	4.99	—	—	—	—	0.71
E107	265.027	1.379	3.80	—	—	—	—	0.83
E108	269.071	-1.895	19.08	—	—	—	—	0.79
E109	269.120	-1.414	1.32	—	—	—	—	1.00
E110	269.173	-1.436	3.09	2.6±0.3	Hou&Han+14	8.9±0.3	2.34	0.96
E111	269.712	0.992	5.50	—	—	—	—	1.00
E112	270.137	-1.610	2.71	—	—	—	—	1.00
E113	270.296	0.810	8.52	3.4±0.4	Hou&Han+14	9.1±0.4	8.42	1.00
E114	273.996	0.313	1.76	—	—	—	—	1.00
E115	275.694	-2.247	3.43	0.9±0.1	Orion	8.5±0.1	0.86	0.58
E116	277.725	0.658	9.72	—	—	—	—	0.92

Table 2. (Continued)

Name	l [°]	b [°]	r [']	D [kpc]	Distance ref.†	$D_{\text{Gal.}}$ [kpc]	R [pc]	CF
E117	279.424	-1.713	2.72	—	—	—	—	1.00
E118	279.424	-0.949	2.04	—	—	—	—	1.00
E119	280.437	-1.767	3.76	—	—	—	—	1.00
E120	281.917	-2.717	1.54	0.7±0.1	Orion	8.4±0.1	0.32	1.00
E121	282.127	-0.957	6.67	—	—	—	—	0.83
E122	282.259	-1.092	3.48	3.2±0.4	Hou&Han+14	8.4±0.4	3.23	0.83
E123	282.315	-1.811	2.91	—	—	—	—	0.54
E124	283.879	-0.910	9.38	5.4±0.7	Hou&Han+14	8.9±0.7	14.76	0.96
E125	284.638	-0.495	1.30	5.0±0.7	Hou&Han+14	8.7±0.7	1.89	0.67
E126	284.708	0.332	1.43	5.7±0.7	Hou&Han+14	9.0±0.7	2.39	0.83
E127	286.275	-0.155	8.50	2.6±0.3	Hou&Han+14	8.2±0.3	6.42	0.96
E128	286.436	-0.143	1.39	—	—	—	—	0.83
E129	288.744	0.908	2.46	—	—	—	—	0.88
E130	290.348	1.709	2.84	—	—	—	—	0.92
E131	290.495	-0.735	1.90	—	—	—	—	1.00
E132	290.668	-0.138	1.46	—	—	—	—	0.88
E133	291.038	-2.080	1.49	—	—	—	—	0.83
E134	291.068	-0.767	1.29	7.9±1.0	Hou&Han+14	9.3±1.0	2.97	1.00
E135	291.168	-0.226	1.55	—	—	—	—	1.00
E136	291.755	-1.012	1.22	—	—	—	—	1.00
E137	292.414	-1.006	1.72	—	—	—	—	0.88
E138	293.757	-1.046	1.53	—	—	—	—	0.83
E139	294.122	-2.278	3.62	2.5±0.3	Hou&Han+14	7.8±0.3	2.63	1.00
E140	294.220	-0.496	3.69	—	—	—	—	0.79
E141	294.400	-1.616	5.43	—	—	—	—	0.75

†References: Beaumont+10, Beaumont and Williams (2010); Churchwell+06, Churchwell et al. (2006); Churchwell+07, Churchwell et al. (2007); Deharveng+09, Deharveng et al. (2009); Deharveng+10, Deharveng et al. (2010); Dewangan+15, Dewangan et al. (2015); Gennaro+12, Gennaro et al. (2012); Hou&Gao+14, Hou and Gao (2014); Hou&Han+14, Hou and Han (2014); Pavel+12, Pavel and Clemens (2012); Rahman+10, Rahman and Murray (2010); Rodríguez+12, Rodríguez-Esnard, Trinidad and Migenes (2012); Watson+09, Watson et al. (2009); Watson+10, Watson, Hanspal and Mengistu (2010); Zhang+13, Zhang, Wang and Xu (2013); Orion, Perseus, Sagittarius, the distance is estimated by assuming the IR bubble is located on each Galactic spiral arm.

§ The nearer kinematic distance is adopted.

ble 3. Summary of the aperture-corrected flux densities of the IR bubbles obtained by the aperture photometry.

Name	Flux 9 μm [Jy] (AKARI IRC)	Flux 18 μm [Jy] (AKARI IRC)	Flux 65 μm [Jy] (AKARI FIS)	Flux 90 μm [Jy] (AKARI FIS)	Flux 140 μm [Jy] (AKARI FIS)	Flux 160 μm [Jy] (AKARI FIS)	Flux 70 μm [Jy] (Herschel PACS)	Flux 160 μm [Jy] (Herschel PACS)	Flux 250 μm [Jy] (Herschel SPIRE)	Flux 350 μm [Jy] (Herschel SPIRE)	Flux 500 μm [Jy] (Herschel SPIRE)	Notes†
N2	$(8.6\pm 0.9)\times 10^2$	$(1.2\pm 0.1)\times 10^3$	$(3.0\pm 0.4)\times 10^4$	$(4.0\pm 0.6)\times 10^4$	$(5.3\pm 0.8)\times 10^4$	$(7.0\pm 1.0)\times 10^4$	$(3.5\pm 0.4)\times 10^4$	$(7.1\pm 0.7)\times 10^4$	$(3.9\pm 0.4)\times 10^4$	$(1.5\pm 0.2)\times 10^4$	$(5.7\pm 0.6)\times 10^3$	—
N4	$(1.5\pm 0.1)\times 10^2$	$(1.6\pm 0.2)\times 10^2$	$(3.2\pm 0.5)\times 10^3$	$(3.6\pm 0.5)\times 10^3$	$(3.8\pm 0.6)\times 10^3$	$(5.0\pm 0.8)\times 10^3$	$(3.3\pm 0.3)\times 10^3$	$(4.7\pm 0.5)\times 10^3$	$(2.3\pm 0.2)\times 10^3$	$(8.6\pm 0.9)\times 10^2$	$(3.1\pm 0.3)\times 10^2$	—
N5	$(1.7\pm 0.2)\times 10^2$	$(2.3\pm 0.2)\times 10^2$	$(3.8\pm 0.6)\times 10^3$	$(5.5\pm 0.8)\times 10^3$	$(9.0\pm 1.0)\times 10^3$	$(9.0\pm 1.0)\times 10^3$	—	—	—	—	—	—
N6	$(4.6\pm 0.5)\times 10^2$	$(4.6\pm 0.5)\times 10^2$	$(8.0\pm 1.0)\times 10^3$	$(1.1\pm 0.2)\times 10^4$	$(1.9\pm 0.3)\times 10^4$	$(2.1\pm 0.3)\times 10^4$	$(8.6\pm 0.9)\times 10^3$	$(2.0\pm 0.2)\times 10^4$	$(1.2\pm 0.1)\times 10^4$	$(4.8\pm 0.5)\times 10^3$	$(1.9\pm 0.2)\times 10^3$	—
N10	$(1.2\pm 0.1)\times 10^2$	$(3.4\pm 0.3)\times 10^2$	$(6.5\pm 1.0)\times 10^3$	$(5.2\pm 0.8)\times 10^3$	$(7.0\pm 1.0)\times 10^3$	$(8.0\pm 1.0)\times 10^3$	$(5.0\pm 0.5)\times 10^3$	$(5.9\pm 0.6)\times 10^3$	$(3.5\pm 0.3)\times 10^3$	$(1.5\pm 0.2)\times 10^3$	$(6.1\pm 0.6)\times 10^2$	—
N11	$(4.5\pm 0.5)\times 10^1$	$(5.3\pm 0.5)\times 10^1$	$(1.9\pm 0.3)\times 10^3$	$(2.0\pm 0.3)\times 10^3$	$(2.6\pm 0.4)\times 10^3$	$(3.1\pm 0.5)\times 10^3$	$(1.2\pm 0.1)\times 10^3$	$(1.3\pm 0.1)\times 10^3$	$(6.0\pm 0.6)\times 10^2$	$(2.6\pm 0.3)\times 10^2$	$(9.0\pm 1.0)\times 10^1$	—
N12	$(3.7\pm 0.4)\times 10^2$	$(4.3\pm 0.4)\times 10^2$	$(8.0\pm 1.0)\times 10^3$	$(1.2\pm 0.2)\times 10^4$	$(2.1\pm 0.3)\times 10^4$	$(2.1\pm 0.3)\times 10^4$	$(9.4\pm 0.9)\times 10^3$	$(1.8\pm 0.2)\times 10^4$	$(9.6\pm 1.0)\times 10^3$	$(3.5\pm 0.4)\times 10^3$	$(1.3\pm 0.1)\times 10^3$	—
N14	$(1.6\pm 0.2)\times 10^2$	$(3.2\pm 0.3)\times 10^2$	$(6.3\pm 0.9)\times 10^3$	$(4.3\pm 0.7)\times 10^3$	$(5.2\pm 0.8)\times 10^3$	$(5.5\pm 0.8)\times 10^3$	$(4.8\pm 0.5)\times 10^3$	$(4.7\pm 0.5)\times 10^3$	$(2.4\pm 0.2)\times 10^3$	$(9.5\pm 1.0)\times 10^2$	$(3.5\pm 0.3)\times 10^2$	—
N15	$(2.0\pm 0.2)\times 10^2$	$(9.0\pm 0.9)\times 10^2$	$(2.8\pm 0.4)\times 10^4$	$(2.0\pm 0.3)\times 10^4$	$(2.0\pm 0.3)\times 10^4$	$(2.0\pm 0.3)\times 10^4$	$(1.4\pm 0.1)\times 10^4$	$(1.5\pm 0.2)\times 10^4$	$(7.2\pm 0.7)\times 10^3$	$(2.7\pm 0.3)\times 10^3$	$(1.1\pm 0.1)\times 10^3$	—
N16	$(5.6\pm 0.6)\times 10^1$	$(5.1\pm 0.5)\times 10^1$	$(10.0\pm 2.0)\times 10^2$	$(2.3\pm 0.3)\times 10^3$	$(4.6\pm 0.7)\times 10^3$	$(4.4\pm 0.7)\times 10^3$	$(1.5\pm 0.2)\times 10^3$	$(4.7\pm 0.5)\times 10^3$	$(3.2\pm 0.3)\times 10^3$	$(1.4\pm 0.1)\times 10^3$	$(5.3\pm 0.5)\times 10^2$	—
N18	$(3.0\pm 0.3)\times 10^2$	$(6.5\pm 0.7)\times 10^2$	$(7.0\pm 1.0)\times 10^3$	$(1.1\pm 0.2)\times 10^4$	$(2.7\pm 0.4)\times 10^4$	$(3.0\pm 0.4)\times 10^4$	$(8.2\pm 0.8)\times 10^3$	$(2.7\pm 0.3)\times 10^4$	$(1.8\pm 0.2)\times 10^4$	$(7.7\pm 0.8)\times 10^3$	$(3.0\pm 0.3)\times 10^3$	—
N20	$(1.8\pm 0.2)\times 10^1$	$(1.8\pm 0.2)\times 10^1$	$(2.5\pm 0.4)\times 10^2$	$(3.5\pm 0.5)\times 10^2$	$(5.2\pm 0.8)\times 10^2$	$(5.5\pm 0.9)\times 10^2$	$(3.3\pm 0.3)\times 10^2$	$(6.4\pm 0.7)\times 10^2$	$(4.2\pm 0.4)\times 10^2$	$(1.9\pm 0.2)\times 10^2$	$(6.8\pm 0.7)\times 10^1$	—
N24	$(2.4\pm 0.2)\times 10^3$	$(3.9\pm 0.4)\times 10^3$	$(8.0\pm 1.0)\times 10^4$	$(9.0\pm 1.0)\times 10^4$	$(1.1\pm 0.2)\times 10^5$	$(1.1\pm 0.2)\times 10^5$	$(8.3\pm 0.8)\times 10^4$	$(8.8\pm 0.9)\times 10^4$	$(4.5\pm 0.5)\times 10^4$	$(1.6\pm 0.2)\times 10^4$	$(6.8\pm 0.7)\times 10^3$	—
N29	$(1.3\pm 0.2)\times 10^2$	$(1.8\pm 0.2)\times 10^2$	$(2.4\pm 0.4)\times 10^3$	$(3.5\pm 0.5)\times 10^3$	$(3.5\pm 0.5)\times 10^3$	$(5.4\pm 0.8)\times 10^3$	$(3.1\pm 0.3)\times 10^3$	$(7.0\pm 0.7)\times 10^3$	$(4.0\pm 0.4)\times 10^3$	$(1.5\pm 0.2)\times 10^3$	$(5.5\pm 0.6)\times 10^2$	—
N30	$(2.2\pm 0.2)\times 10^1$	$(5.8\pm 0.6)\times 10^1$	$(8.0\pm 1.0)\times 10^2$	$(8.0\pm 1.0)\times 10^2$	$(7.0\pm 1.0)\times 10^2$	$(8.0\pm 1.0)\times 10^2$	$(7.3\pm 0.7)\times 10^2$	$(8.4\pm 0.8)\times 10^2$	$(4.5\pm 0.5)\times 10^2$	$(1.8\pm 0.2)\times 10^2$	$(6.8\pm 0.7)\times 10^1$	sc
N34	$(3.3\pm 0.3)\times 10^1$	$(4.9\pm 0.5)\times 10^1$	$(1.1\pm 0.2)\times 10^3$	$(1.3\pm 0.2)\times 10^3$	$(1.8\pm 0.3)\times 10^3$	$(2.0\pm 0.3)\times 10^3$	$(1.3\pm 0.1)\times 10^3$	$(1.7\pm 0.2)\times 10^3$	$(7.8\pm 0.8)\times 10^2$	$(2.9\pm 0.3)\times 10^2$	$(1.1\pm 0.1)\times 10^2$	sc
N35	$(3.3\pm 0.3)\times 10^2$	$(8.6\pm 0.9)\times 10^2$	$(1.9\pm 0.3)\times 10^4$	$(1.9\pm 0.3)\times 10^4$	$(2.5\pm 0.4)\times 10^4$	$(2.3\pm 0.3)\times 10^4$	$(1.8\pm 0.2)\times 10^4$	$(2.6\pm 0.3)\times 10^4$	$(1.4\pm 0.1)\times 10^4$	$(5.2\pm 0.5)\times 10^3$	$(1.9\pm 0.2)\times 10^3$	—
N36	$(2.2\pm 0.2)\times 10^2$	$(8.4\pm 0.8)\times 10^2$	$(1.3\pm 0.2)\times 10^4$	$(1.6\pm 0.2)\times 10^4$	$(2.0\pm 0.3)\times 10^4$	$(2.8\pm 0.4)\times 10^4$	$(1.6\pm 0.2)\times 10^4$	$(1.9\pm 0.2)\times 10^4$	$(8.6\pm 0.9)\times 10^3$	$(3.5\pm 0.3)\times 10^3$	$(1.3\pm 0.1)\times 10^3$	—
N37	$(1.1\pm 0.1)\times 10^2$	$(3.3\pm 0.3)\times 10^2$	$(1.9\pm 0.3)\times 10^3$	$(2.7\pm 0.4)\times 10^3$	$(2.1\pm 0.3)\times 10^3$	$(2.8\pm 0.4)\times 10^3$	$(2.8\pm 0.3)\times 10^3$	$(2.5\pm 0.2)\times 10^3$	$(1.2\pm 0.1)\times 10^3$	$(4.3\pm 0.4)\times 10^2$	$(1.6\pm 0.2)\times 10^2$	—
N39	$(5.1\pm 0.5)\times 10^2$	$(2.4\pm 0.2)\times 10^3$	$(3.0\pm 0.4)\times 10^4$	$(2.3\pm 0.3)\times 10^4$	$(2.3\pm 0.3)\times 10^4$	$(2.3\pm 0.3)\times 10^4$	$(2.1\pm 0.2)\times 10^4$	$(2.0\pm 0.2)\times 10^4$	$(8.9\pm 0.9)\times 10^3$	$(3.2\pm 0.3)\times 10^3$	$(1.2\pm 0.1)\times 10^3$	—
N40	$(1.7\pm 0.2)\times 10^1$	$(5.4\pm 0.5)\times 10^1$	$(9.0\pm 1.0)\times 10^2$	$(10.0\pm 2.0)\times 10^2$	$(7.0\pm 1.0)\times 10^2$	$(1.2\pm 0.2)\times 10^3$	$(8.4\pm 0.8)\times 10^2$	$(8.4\pm 0.9)\times 10^2$	$(4.6\pm 0.5)\times 10^2$	$(1.9\pm 0.2)\times 10^2$	$(7.5\pm 0.8)\times 10^1$	—
N44	$(1.4\pm 0.1)\times 10^1$	$(1.3\pm 0.1)\times 10^1$	$(2.7\pm 0.4)\times 10^2$	$(3.2\pm 0.5)\times 10^2$	$(8.0\pm 1.0)\times 10^2$	$(8.0\pm 1.0)\times 10^2$	$(2.9\pm 0.3)\times 10^2$	$(5.0\pm 0.5)\times 10^2$	$(2.6\pm 0.3)\times 10^2$	$(10.0\pm 1.0)\times 10^1$	$(3.9\pm 0.4)\times 10^1$	—
N45	$(4.1\pm 0.4)\times 10^1$	$(7.9\pm 0.8)\times 10^1$	$(1.6\pm 0.2)\times 10^3$	$(1.8\pm 0.3)\times 10^3$	$(2.5\pm 0.4)\times 10^3$	$(2.0\pm 0.3)\times 10^3$	$(1.7\pm 0.2)\times 10^3$	$(2.1\pm 0.2)\times 10^3$	$(10.0\pm 1.0)\times 10^2$	$(4.0\pm 0.4)\times 10^2$	$(1.6\pm 0.2)\times 10^2$	sc
N46	$(8.5\pm 1.0)\times 10^0$	$(2.2\pm 0.2)\times 10^1$	$(4.6\pm 0.7)\times 10^2$	$(5.5\pm 0.9)\times 10^2$	$(4.9\pm 0.8)\times 10^2$	$(5.3\pm 0.8)\times 10^2$	$(4.1\pm 0.4)\times 10^2$	$(4.6\pm 0.5)\times 10^2$	$(2.4\pm 0.3)\times 10^2$	$(10.0\pm 1.0)\times 10^1$	$(4.2\pm 0.5)\times 10^1$	—
N47	$(3.7\pm 0.4)\times 10^1$	$(8.3\pm 0.8)\times 10^1$	$(1.5\pm 0.2)\times 10^3$	$(2.5\pm 0.4)\times 10^3$	$(6.2\pm 1.0)\times 10^3$	$(7.0\pm 1.0)\times 10^3$	$(2.1\pm 0.2)\times 10^3$	$(5.1\pm 0.5)\times 10^3$	$(3.5\pm 0.4)\times 10^3$	$(1.5\pm 0.2)\times 10^3$	$(6.2\pm 0.6)\times 10^2$	—
N49	$(4.4\pm 0.4)\times 10^1$	$(10.0\pm 1.0)\times 10^1$	$(2.2\pm 0.3)\times 10^3$	$(2.5\pm 0.4)\times 10^3$	$(3.6\pm 0.5)\times 10^3$	$(3.1\pm 0.5)\times 10^3$	$(1.7\pm 0.2)\times 10^3$	$(2.7\pm 0.3)\times 10^3$	$(1.5\pm 0.2)\times 10^3$	$(6.2\pm 0.6)\times 10^2$	$(2.5\pm 0.3)\times 10^2$	—
N50	$(1.8\pm 0.2)\times 10^1$	$(3.0\pm 0.3)\times 10^1$	$(1.1\pm 0.2)\times 10^3$	$(1.5\pm 0.2)\times 10^3$	$(2.2\pm 0.3)\times 10^3$	$(2.3\pm 0.3)\times 10^3$	$(1.1\pm 0.1)\times 10^3$	$(2.1\pm 0.2)\times 10^3$	$(1.4\pm 0.1)\times 10^3$	$(6.3\pm 0.6)\times 10^2$	$(2.5\pm 0.3)\times 10^2$	—
N51	$(1.8\pm 0.3)\times 10^1$	$(1.7\pm 0.3)\times 10^1$	$(6.3\pm 1.0)\times 10^2$	$(8.0\pm 1.0)\times 10^2$	$(8.0\pm 1.0)\times 10^2$	$(1.1\pm 0.2)\times 10^3$	$(7.3\pm 0.7)\times 10^2$	$(1.1\pm 0.1)\times 10^3$	$(5.6\pm 0.6)\times 10^2$	$(2.3\pm 0.2)\times 10^2$	$(9.6\pm 1.0)\times 10^1$	—
N52	$(7.3\pm 0.7)\times 10^2$	$(4.4\pm 0.4)\times 10^3$	$(8.0\pm 1.0)\times 10^4$	$(4.7\pm 0.7)\times 10^4$	$(6.0\pm 0.9)\times 10^4$	$(7.0\pm 1.0)\times 10^4$	$(6.3\pm 0.6)\times 10^4$	$(5.9\pm 0.6)\times 10^4$	$(2.9\pm 0.3)\times 10^4$	$(1.1\pm 0.1)\times 10^4$	$(4.0\pm 0.4)\times 10^3$	—
N54	$(9.5\pm 1.0)\times 10^1$	$(1.1\pm 0.1)\times 10^2$	$(2.8\pm 0.4)\times 10^3$	$(4.5\pm 0.7)\times 10^3$	$(9.0\pm 1.0)\times 10^3$	$(8.0\pm 1.0)\times 10^3$	$(3.3\pm 0.3)\times 10^3$	$(7.9\pm 0.8)\times 10^3$	$(4.6\pm 0.5)\times 10^3$	$(1.7\pm 0.2)\times 10^3$	$(6.3\pm 0.6)\times 10^2$	sc
N56	$(1.2\pm 0.1)\times 10^1$	$(10.0\pm 1.0)\times 10^0$	$(1.8\pm 0.3)\times 10^2$	$(3.2\pm 0.5)\times 10^2$	$(7.0\pm 1.0)\times 10^2$	$(9.0\pm 1.0)\times 10^2$	$(2.5\pm 0.2)\times 10^2$	$(7.0\pm 0.7)\times 10^2$	$(5.0\pm 0.5)\times 10^2$	$(2.2\pm 0.2)\times 10^2$	$(9.0\pm 1.0)\times 10^1$	—
N59	$(1.3\pm 0.1)\times 10^3$	$(1.3\pm 0.1)\times 10^3$	$(2.1\pm 0.3)\times 10^4$	$(3.9\pm 0.6)\times 10^4$	$(8.0\pm 1.0)\times 10^4$	$(8.0\pm 1.0)\times 10^4$	$(2.8\pm 0.3)\times 10^4$	$(9.2\pm 0.9)\times 10^4$	$(6.0\pm 0.6)\times 10^4$	$(2.5\pm 0.2)\times 10^4$	$(9.4\pm 0.9)\times 10^3$	—
N61	$(2.3\pm 0.2)\times 10^2$	$(7.6\pm 0.8)\times 10^2$	$(2.3\pm 0.4)\times 10^4$	$(1.8\pm 0.3)\times 10^4$	$(2.9\pm 0.4)\times 10^4$	$(3.7\pm 0.6)\times 10^4$	$(2.1\pm 0.2)\times 10^4$	$(3.1\pm 0.3)\times 10^4$	$(1.6\pm 0.2)\times 10^4$	$(6.9\pm 0.7)\times 10^3$	$(2.8\pm 0.3)\times 10^3$	—
N62	$(2.8\pm 0.3)\times 10^1$	$(3.8\pm 0.4)\times 10^1$	$(10.0\pm 2.0)\times 10^2$	$(1.5\pm 0.2)\times 10^3$	$(1.6\pm 0.2)\times 10^3$	$(1.9\pm 0.3)\times 10^3$	$(7.3\pm 0.7)\times 10^2$	$(2.6\pm 0.3)\times 10^3$	$(1.9\pm 0.2)\times 10^3$	$(8.3\pm 0.8)\times 10^2$	$(3.4\pm 0.3)\times 10^2$	—
N64	$(1.6\pm 0.2)\times 10^2$	$(1.7\pm 0.2)\times 10^2$	$(3.2\pm 0.5)\times 10^3$	$(5.6\pm 0.8)\times 10^3$	$(1.1\pm 0.2)\times 10^4$	$(1.2\pm 0.2)\times 10^4$	$(4.3\pm 0.4)\times 10^3$	$(1.2\pm 0.1)\times 10^4$	$(8.7\pm 0.9)\times 10^3$	$(4.2\pm 0.4)\times 10^3$	$(1.9\pm 0.2)\times 10^3$	—
N65	$(6.4\pm 0.6)\times 10^1$	$(5.8\pm 0.6)\times 10^1$	$(2.2\pm 0.3)\times 10^3$	$(3.0\pm 0.5)\times 10^3$	$(4.8\pm 0.7)\times 10^3$	$(4.2\pm 0.6)\times 10^3$	$(2.1\pm 0.2)\times 10^3$	$(4.2\pm 0.4)\times 10^3$	$(2.4\pm 0.2)\times 10^3$	$(9.6\pm 1.0)\times 10^2$	$(3.7\pm 0.4)\times 10^2$	—
N68	$(1.7\pm 0.3)\times 10^2$	$(2.3\pm 0.4)\times 10^2$	$(1.1\pm 0.2)\times 10^4$	$(1.5\pm 0.2)\times 10^4$	$(2.0\pm 0.3)\times 10^4$	$(1.7\pm 0.3)\times 10^4$	$(1.2\pm 0.1)\times 10^4$	$(1.8\pm 0.2)\times 10^4$	$(9.7\pm 1.0)\times 10^3$	$(3.8\pm 0.4)\times 10^3$	$(1.5\pm 0.2)\times 10^3$	—
N69	$(3.5\pm 0.4)\times 10^2$	$(3.2\pm 0.3)\times 10^2$	$(3.5\pm 0.5)\times 10^3$	$(8.0\pm 1.0)\times 10^3$	$(1.9\pm 0.3)\times 10^4$	$(2.0\pm 0.3)\times 10^4$	$(5.5\pm 0.6)\times 10^3$	$(2.1\pm 0.2)\times 10^4$	$(1.4\pm 0.1)\times 10^4$	$(5.8\pm 0.6)\times 10^3$	$(2.3\pm 0.2)\times 10^3$	—
N71	$(5.1\pm 0.5)\times 10^2$	$(5.3\pm 0.5)\times 10^2$	$(1.3\pm 0.2)\times 10^4$	$(2.4\pm 0.4)\times 10^4$	$(4.3\pm 0.7)\times 10^4$	$(4.9\pm 0.7)\times 10^4$	$(1.7\pm 0.2)\times 10^4$	$(5.3\pm 0.5)\times 10^4$	$(3.1\pm 0.3)\times 10^4$	$(1.3\pm 0.1)\times 10^4$	$(5.3\pm 0.5)\times 10^3$	—
N72	$(8.9\pm 0.9)\times 10^0$	$(6.7\pm 0.7)\times 10^0$	$(1.2\pm 0.2)\times 10^2$	$(3.1\pm 0.5)\times 10^2$	$(4.6\pm 0.7)\times 10^2$	$(6.0\pm 0.9)\times 10^2$	$(2.1\pm 0.2)\times 10^2$	$(7.5\pm 0.8)\times 10^2$	$(5.5\pm 0.5)\times 10^2$	$(2.3\pm 0.2)\times 10^2$	$(9.0\pm 0.9)\times 10^1$	sc

ble 3. (Continued)

Name	Flux 9 μm [Jy] (AKARI IRC)	Flux 18 μm [Jy] (AKARI IRC)	Flux 65 μm [Jy] (AKARI FIS)	Flux 90 μm [Jy] (AKARI FIS)	Flux 140 μm [Jy] (AKARI FIS)	Flux 160 μm [Jy] (AKARI FIS)	Flux 70 μm [Jy] (Herschel PACS)	Flux 160 μm [Jy] (Herschel PACS)	Flux 250 μm [Jy] (Herschel SPIRE)	Flux 350 μm [Jy] (Herschel SPIRE)	Flux 500 μm [Jy] (Herschel SPIRE)	Notes†
N73	$(1.3 \pm 0.1) \times 10^{-1}$	$(1.1 \pm 0.1) \times 10^{-1}$	$(4.1 \pm 0.6) \times 10^{-2}$	$(6.5 \pm 1.0) \times 10^{-2}$	$(1.1 \pm 0.2) \times 10^{-3}$	$(1.1 \pm 0.2) \times 10^{-3}$	$(5.1 \pm 0.5) \times 10^{-2}$	$(10.0 \pm 1.0) \times 10^{-2}$	$(5.8 \pm 0.6) \times 10^{-2}$	$(2.2 \pm 0.2) \times 10^{-2}$	$(8.0 \pm 0.8) \times 10^{-1}$	sc
N74	$(4.2 \pm 0.4) \times 10^{-1}$	$(3.0 \pm 0.3) \times 10^{-1}$	$(4.1 \pm 0.6) \times 10^{-2}$	$(10.0 \pm 2.0) \times 10^{-2}$	$(1.8 \pm 0.3) \times 10^{-3}$	$(1.9 \pm 0.3) \times 10^{-3}$	$(8.4 \pm 0.8) \times 10^{-2}$	$(1.8 \pm 0.2) \times 10^{-3}$	$(1.1 \pm 0.1) \times 10^{-3}$	$(4.8 \pm 0.5) \times 10^{-2}$	$(1.8 \pm 0.2) \times 10^{-2}$	—
N77	$(1.2 \pm 0.1) \times 10^{-1}$	$(9.4 \pm 1.0) \times 10^0$	$(1.7 \pm 0.3) \times 10^{-2}$	$(2.7 \pm 0.4) \times 10^{-2}$	$(4.2 \pm 0.6) \times 10^{-2}$	$(4.3 \pm 0.7) \times 10^{-2}$	$(2.1 \pm 0.2) \times 10^{-2}$	$(4.9 \pm 0.5) \times 10^{-2}$	$(3.0 \pm 0.3) \times 10^{-2}$	$(1.3 \pm 0.1) \times 10^{-2}$	$(4.8 \pm 0.5) \times 10^{-1}$	—
N79	$(2.1 \pm 0.2) \times 10^{-1}$	$(3.4 \pm 0.3) \times 10^{-1}$	$(8.0 \pm 1.0) \times 10^{-2}$	$(1.1 \pm 0.2) \times 10^{-3}$	$(1.3 \pm 0.2) \times 10^{-3}$	$(1.1 \pm 0.2) \times 10^{-3}$	$(9.8 \pm 1.0) \times 10^{-2}$	$(1.2 \pm 0.1) \times 10^{-3}$	$(5.3 \pm 0.5) \times 10^{-2}$	$(1.9 \pm 0.2) \times 10^{-2}$	$(6.7 \pm 0.7) \times 10^{-1}$	sc
N80	$(9.0 \pm 1.0) \times 10^0$	$(1.1 \pm 0.1) \times 10^{-1}$	$(3.0 \pm 0.4) \times 10^{-2}$	$(3.3 \pm 0.5) \times 10^{-2}$	$(7.0 \pm 1.0) \times 10^{-2}$	$(7.0 \pm 1.0) \times 10^{-2}$	$(3.3 \pm 0.3) \times 10^{-2}$	$(7.4 \pm 0.7) \times 10^{-2}$	$(4.6 \pm 0.5) \times 10^{-2}$	$(2.0 \pm 0.2) \times 10^{-2}$	$(7.8 \pm 0.8) \times 10^{-1}$	—
N81	$(2.8 \pm 0.3) \times 10^{-2}$	$(3.1 \pm 0.3) \times 10^{-2}$	$(3.6 \pm 0.5) \times 10^{-3}$	$(6.2 \pm 0.9) \times 10^{-3}$	$(1.4 \pm 0.2) \times 10^{-4}$	$(1.5 \pm 0.2) \times 10^{-4}$	$(4.9 \pm 0.5) \times 10^{-3}$	$(1.7 \pm 0.2) \times 10^{-4}$	$(1.1 \pm 0.1) \times 10^{-4}$	$(4.8 \pm 0.5) \times 10^{-3}$	$(1.9 \pm 0.2) \times 10^{-3}$	—
N82	$(1.1 \pm 0.1) \times 10^{-2}$	$(1.6 \pm 0.2) \times 10^{-2}$	$(3.1 \pm 0.5) \times 10^{-3}$	$(3.6 \pm 0.5) \times 10^{-3}$	$(3.2 \pm 0.5) \times 10^{-3}$	$(2.5 \pm 0.4) \times 10^{-3}$	$(3.2 \pm 0.3) \times 10^{-3}$	$(3.2 \pm 0.3) \times 10^{-3}$	$(1.4 \pm 0.1) \times 10^{-3}$	$(4.7 \pm 0.5) \times 10^{-2}$	$(1.7 \pm 0.2) \times 10^{-2}$	—
N84	$(2.3 \pm 0.2) \times 10^{-1}$	$(2.0 \pm 0.2) \times 10^{-1}$	$(5.8 \pm 0.9) \times 10^{-2}$	$(7.0 \pm 1.0) \times 10^{-2}$	$(7.0 \pm 1.0) \times 10^{-2}$	$(7.0 \pm 1.0) \times 10^{-2}$	$(5.4 \pm 0.5) \times 10^{-2}$	$(6.5 \pm 0.7) \times 10^{-2}$	$(3.0 \pm 0.3) \times 10^{-2}$	$(10.0 \pm 1.0) \times 10^{-1}$	$(3.4 \pm 0.4) \times 10^{-1}$	—
N90	$(1.2 \pm 0.2) \times 10^{-1}$	$(1.4 \pm 0.2) \times 10^{-1}$	$(2.7 \pm 0.4) \times 10^{-2}$	$(4.1 \pm 0.6) \times 10^{-2}$	$(4.4 \pm 0.7) \times 10^{-2}$	$(4.7 \pm 0.7) \times 10^{-2}$	$(4.3 \pm 0.4) \times 10^{-2}$	$(5.7 \pm 0.6) \times 10^{-2}$	$(2.3 \pm 0.2) \times 10^{-2}$	$(7.7 \pm 0.8) \times 10^{-1}$	$(2.6 \pm 0.3) \times 10^{-1}$	—
N91	$(1.5 \pm 0.1) \times 10^{-2}$	$(1.5 \pm 0.1) \times 10^{-2}$	$(1.8 \pm 0.3) \times 10^{-3}$	$(3.0 \pm 0.4) \times 10^{-3}$	$(5.0 \pm 0.8) \times 10^{-3}$	$(4.3 \pm 0.7) \times 10^{-3}$	$(2.9 \pm 0.3) \times 10^{-3}$	$(5.9 \pm 0.6) \times 10^{-3}$	$(3.6 \pm 0.4) \times 10^{-3}$	$(1.5 \pm 0.1) \times 10^{-3}$	$(5.4 \pm 0.5) \times 10^{-2}$	—
N92	$(4.7 \pm 0.5) \times 10^{-1}$	$(3.4 \pm 0.3) \times 10^{-1}$	$(5.7 \pm 0.9) \times 10^{-2}$	$(10.0 \pm 1.0) \times 10^{-2}$	$(1.4 \pm 0.2) \times 10^{-3}$	$(1.4 \pm 0.2) \times 10^{-3}$	$(9.1 \pm 0.9) \times 10^{-2}$	$(1.6 \pm 0.2) \times 10^{-3}$	$(8.3 \pm 0.8) \times 10^{-2}$	$(3.2 \pm 0.3) \times 10^{-2}$	$(1.2 \pm 0.1) \times 10^{-2}$	—
N95	$(2.3 \pm 0.2) \times 10^{-1}$	$(3.7 \pm 0.4) \times 10^{-1}$	$(5.1 \pm 0.8) \times 10^{-2}$	$(7.0 \pm 1.0) \times 10^{-2}$	$(9.0 \pm 1.0) \times 10^{-2}$	$(8.0 \pm 1.0) \times 10^{-2}$	$(7.2 \pm 0.7) \times 10^{-2}$	$(9.9 \pm 1.0) \times 10^{-2}$	$(5.6 \pm 0.6) \times 10^{-2}$	$(2.3 \pm 0.2) \times 10^{-2}$	$(8.7 \pm 0.9) \times 10^{-1}$	—
N98	$(2.4 \pm 0.3) \times 10^{-1}$	$(2.8 \pm 0.3) \times 10^{-1}$	$(4.6 \pm 0.7) \times 10^{-2}$	$(7.0 \pm 1.0) \times 10^{-2}$	$(10.0 \pm 1.0) \times 10^{-2}$	$(10.0 \pm 2.0) \times 10^{-2}$	$(6.4 \pm 0.6) \times 10^{-2}$	$(1.4 \pm 0.1) \times 10^{-3}$	$(9.5 \pm 0.9) \times 10^{-2}$	$(4.3 \pm 0.4) \times 10^{-2}$	$(1.7 \pm 0.2) \times 10^{-2}$	—
N101	$(1.8 \pm 0.2) \times 10^{-2}$	$(7.0 \pm 0.7) \times 10^{-2}$	$(1.6 \pm 0.2) \times 10^{-4}$	$(10.0 \pm 2.0) \times 10^{-3}$	$(6.5 \pm 1.0) \times 10^{-3}$	$(7.0 \pm 1.0) \times 10^{-3}$	$(1.1 \pm 0.1) \times 10^{-4}$	$(7.7 \pm 0.8) \times 10^{-3}$	$(3.3 \pm 0.3) \times 10^{-3}$	$(1.2 \pm 0.1) \times 10^{-3}$	$(4.2 \pm 0.4) \times 10^{-2}$	—
N107	$(5.8 \pm 0.6) \times 10^{-2}$	$(6.8 \pm 0.7) \times 10^{-2}$	$(1.1 \pm 0.2) \times 10^{-4}$	$(1.7 \pm 0.3) \times 10^{-4}$	$(2.8 \pm 0.4) \times 10^{-4}$	$(2.9 \pm 0.4) \times 10^{-4}$	$(1.5 \pm 0.2) \times 10^{-4}$	$(3.3 \pm 0.3) \times 10^{-4}$	$(1.9 \pm 0.2) \times 10^{-4}$	$(7.6 \pm 0.8) \times 10^{-3}$	$(3.0 \pm 0.3) \times 10^{-3}$	—
N109	$(10.0 \pm 1.0) \times 10^{-2}$	$(8.7 \pm 0.9) \times 10^{-2}$	$(10.0 \pm 2.0) \times 10^{-3}$	$(1.5 \pm 0.2) \times 10^{-4}$	$(2.7 \pm 0.4) \times 10^{-4}$	$(2.4 \pm 0.4) \times 10^{-4}$	$(1.4 \pm 0.1) \times 10^{-4}$	$(2.4 \pm 0.2) \times 10^{-4}$	$(1.2 \pm 0.1) \times 10^{-4}$	$(4.4 \pm 0.4) \times 10^{-3}$	$(1.6 \pm 0.2) \times 10^{-3}$	—
N114	$(4.9 \pm 0.5) \times 10^{-1}$	$(6.9 \pm 0.7) \times 10^{-1}$	$(1.1 \pm 0.2) \times 10^{-3}$	$(1.5 \pm 0.2) \times 10^{-3}$	$(1.8 \pm 0.3) \times 10^{-3}$	$(1.9 \pm 0.3) \times 10^{-3}$	$(1.4 \pm 0.1) \times 10^{-3}$	$(2.1 \pm 0.2) \times 10^{-3}$	$(1.1 \pm 0.1) \times 10^{-3}$	$(3.8 \pm 0.4) \times 10^{-2}$	$(1.4 \pm 0.1) \times 10^{-2}$	—
N115	$(4.2 \pm 0.4) \times 10^{-2}$	$(3.4 \pm 0.3) \times 10^{-2}$	$(6.2 \pm 0.9) \times 10^{-3}$	$(8.0 \pm 1.0) \times 10^{-3}$	$(9.0 \pm 1.0) \times 10^{-3}$	$(8.0 \pm 1.0) \times 10^{-3}$	$(7.6 \pm 0.8) \times 10^{-3}$	$(1.2 \pm 0.1) \times 10^{-4}$	$(5.9 \pm 0.6) \times 10^{-3}$	$(2.3 \pm 0.2) \times 10^{-3}$	$(9.0 \pm 0.9) \times 10^{-2}$	—
N117	$(9.9 \pm 1.0) \times 10^{-1}$	$(1.5 \pm 0.1) \times 10^{-2}$	$(2.9 \pm 0.4) \times 10^{-3}$	$(3.7 \pm 0.6) \times 10^{-3}$	$(4.0 \pm 0.6) \times 10^{-3}$	$(3.2 \pm 0.5) \times 10^{-3}$	$(3.2 \pm 0.3) \times 10^{-3}$	$(4.6 \pm 0.5) \times 10^{-3}$	$(2.4 \pm 0.2) \times 10^{-3}$	$(9.8 \pm 1.0) \times 10^{-2}$	$(3.9 \pm 0.4) \times 10^{-2}$	—
N120	$(5.8 \pm 0.6) \times 10^0$	$(5.8 \pm 0.6) \times 10^0$	$(8.0 \pm 1.0) \times 10^{-1}$	$(1.1 \pm 0.2) \times 10^{-2}$	$(2.4 \pm 0.4) \times 10^{-2}$	$(2.1 \pm 0.3) \times 10^{-2}$	$(9.3 \pm 0.9) \times 10^{-1}$	$(3.1 \pm 0.3) \times 10^{-2}$	$(2.0 \pm 0.2) \times 10^{-2}$	$(8.7 \pm 0.9) \times 10^{-1}$	$(3.7 \pm 0.4) \times 10^{-1}$	—
N123	$(2.9 \pm 0.3) \times 10^{-1}$	$(5.4 \pm 0.5) \times 10^{-1}$	$(10.0 \pm 1.0) \times 10^{-2}$	$(1.1 \pm 0.2) \times 10^{-3}$	$(8.0 \pm 1.0) \times 10^{-2}$	$(7.0 \pm 1.0) \times 10^{-2}$	$(8.8 \pm 0.9) \times 10^{-2}$	$(10.0 \pm 1.0) \times 10^{-2}$	$(4.7 \pm 0.5) \times 10^{-2}$	$(1.8 \pm 0.2) \times 10^{-2}$	$(6.3 \pm 0.6) \times 10^{-1}$	—
N124	$(1.1 \pm 0.1) \times 10^{-1}$	$(9.1 \pm 0.9) \times 10^0$	$(10.0 \pm 2.0) \times 10^{-1}$	$(1.9 \pm 0.3) \times 10^{-2}$	$(3.7 \pm 0.6) \times 10^{-2}$	$(3.4 \pm 0.5) \times 10^{-2}$	$(1.7 \pm 0.2) \times 10^{-2}$	$(4.1 \pm 0.4) \times 10^{-2}$	$(2.3 \pm 0.2) \times 10^{-2}$	$(8.9 \pm 0.9) \times 10^{-1}$	$(3.2 \pm 0.4) \times 10^{-1}$	—
N126	$(1.1 \pm 0.1) \times 10^{-1}$	$(1.1 \pm 0.1) \times 10^{-1}$	$(1.1 \pm 0.2) \times 10^{-2}$	$(2.0 \pm 0.3) \times 10^{-2}$	$(2.7 \pm 0.4) \times 10^{-2}$	$(3.3 \pm 0.5) \times 10^{-2}$	$(1.5 \pm 0.1) \times 10^{-2}$	$(3.6 \pm 0.4) \times 10^{-2}$	$(2.4 \pm 0.2) \times 10^{-2}$	$(1.1 \pm 0.1) \times 10^{-2}$	$(4.5 \pm 0.5) \times 10^{-1}$	—
N127	$(2.0 \pm 0.2) \times 10^{-1}$	$(2.3 \pm 0.2) \times 10^{-1}$	$(1.6 \pm 0.2) \times 10^{-2}$	$(2.3 \pm 0.3) \times 10^{-2}$	$(4.9 \pm 0.7) \times 10^{-2}$	$(4.8 \pm 0.7) \times 10^{-2}$	$(2.0 \pm 0.2) \times 10^{-2}$	$(7.2 \pm 0.7) \times 10^{-2}$	$(5.0 \pm 0.5) \times 10^{-2}$	$(2.1 \pm 0.2) \times 10^{-2}$	$(8.4 \pm 0.9) \times 10^{-1}$	—
N128	$(1.4 \pm 0.1) \times 10^{-1}$	$(1.6 \pm 0.2) \times 10^{-1}$	$(2.3 \pm 0.3) \times 10^{-2}$	$(3.6 \pm 0.5) \times 10^{-2}$	$(5.8 \pm 0.9) \times 10^{-2}$	$(5.8 \pm 0.9) \times 10^{-2}$	$(3.0 \pm 0.3) \times 10^{-2}$	$(6.4 \pm 0.6) \times 10^{-2}$	$(4.3 \pm 0.4) \times 10^{-2}$	$(2.1 \pm 0.2) \times 10^{-2}$	$(9.3 \pm 0.9) \times 10^{-1}$	—
N130	$(4.7 \pm 0.5) \times 10^0$	$(4.5 \pm 0.5) \times 10^0$	$(3.9 \pm 0.6) \times 10^{-1}$	$(5.6 \pm 0.8) \times 10^{-1}$	$(1.3 \pm 0.2) \times 10^{-2}$	$(1.4 \pm 0.2) \times 10^{-2}$	$(5.6 \pm 0.6) \times 10^{-1}$	$(1.9 \pm 0.2) \times 10^{-2}$	$(1.3 \pm 0.1) \times 10^{-2}$	$(5.1 \pm 0.5) \times 10^{-1}$	$(2.0 \pm 0.2) \times 10^{-1}$	sc
N131	$(6.4 \pm 0.6) \times 10^{-1}$	$(7.2 \pm 0.7) \times 10^{-1}$	$(7.0 \pm 1.0) \times 10^{-2}$	$(10.0 \pm 2.0) \times 10^{-2}$	$(1.8 \pm 0.3) \times 10^{-3}$	$(1.8 \pm 0.3) \times 10^{-3}$	$(1.1 \pm 0.1) \times 10^{-3}$	$(2.3 \pm 0.2) \times 10^{-3}$	$(1.4 \pm 0.1) \times 10^{-3}$	$(6.1 \pm 0.6) \times 10^{-2}$	$(2.5 \pm 0.2) \times 10^{-2}$	—
N133	$(1.2 \pm 0.1) \times 10^{-2}$	$(2.6 \pm 0.3) \times 10^{-2}$	$(4.0 \pm 0.6) \times 10^{-3}$	$(4.0 \pm 0.6) \times 10^{-3}$	$(3.2 \pm 0.5) \times 10^{-3}$	$(2.6 \pm 0.4) \times 10^{-3}$	$(3.5 \pm 0.3) \times 10^{-3}$	$(3.8 \pm 0.4) \times 10^{-3}$	$(1.7 \pm 0.2) \times 10^{-3}$	$(6.5 \pm 0.7) \times 10^{-2}$	$(2.5 \pm 0.3) \times 10^{-2}$	—
S1	$(5.2 \pm 0.5) \times 10^{-2}$	$(1.3 \pm 0.1) \times 10^{-3}$	$(1.8 \pm 0.3) \times 10^{-4}$	$(1.9 \pm 0.3) \times 10^{-4}$	$(2.0 \pm 0.3) \times 10^{-4}$	$(1.8 \pm 0.3) \times 10^{-4}$	$(1.8 \pm 0.2) \times 10^{-4}$	$(1.7 \pm 0.2) \times 10^{-4}$	$(7.3 \pm 0.7) \times 10^{-3}$	$(2.5 \pm 0.2) \times 10^{-3}$	$(8.7 \pm 0.9) \times 10^{-2}$	—
S7	$(5.1 \pm 0.5) \times 10^{-2}$	$(7.2 \pm 0.7) \times 10^{-2}$	$(1.1 \pm 0.2) \times 10^{-4}$	$(1.5 \pm 0.2) \times 10^{-4}$	$(2.1 \pm 0.3) \times 10^{-4}$	$(2.2 \pm 0.3) \times 10^{-4}$	$(1.2 \pm 0.1) \times 10^{-4}$	$(2.1 \pm 0.2) \times 10^{-4}$	$(1.2 \pm 0.1) \times 10^{-4}$	$(5.4 \pm 0.5) \times 10^{-3}$	$(2.2 \pm 0.2) \times 10^{-3}$	—
S8	$(7.0 \pm 0.7) \times 10^{-1}$	$(8.0 \pm 0.8) \times 10^{-1}$	$(2.5 \pm 0.4) \times 10^{-3}$	$(2.9 \pm 0.4) \times 10^{-3}$	$(3.4 \pm 0.5) \times 10^{-3}$	$(4.0 \pm 0.6) \times 10^{-3}$	$(3.0 \pm 0.3) \times 10^{-3}$	$(4.1 \pm 0.4) \times 10^{-3}$	$(1.9 \pm 0.2) \times 10^{-3}$	$(6.9 \pm 0.7) \times 10^{-2}$	$(2.4 \pm 0.2) \times 10^{-2}$	sc
S11	$(1.9 \pm 0.2) \times 10^{-2}$	$(3.2 \pm 0.3) \times 10^{-2}$	$(1.2 \pm 0.2) \times 10^{-4}$	$(1.2 \pm 0.2) \times 10^{-4}$	$(1.9 \pm 0.3) \times 10^{-4}$	$(2.1 \pm 0.3) \times 10^{-4}$	$(9.0 \pm 0.9) \times 10^{-3}$	$(1.3 \pm 0.1) \times 10^{-4}$	$(7.1 \pm 0.7) \times 10^{-3}$	$(3.1 \pm 0.3) \times 10^{-3}$	$(1.3 \pm 0.1) \times 10^{-3}$	—
S13	$(6.1 \pm 0.6) \times 10^{-2}$	$(8.2 \pm 0.8) \times 10^{-2}$	$(1.2 \pm 0.2) \times 10^{-4}$	$(1.9 \pm 0.3) \times 10^{-4}$	$(4.2 \pm 0.6) \times 10^{-4}$	$(3.6 \pm 0.5) \times 10^{-4}$	$(1.7 \pm 0.2) \times 10^{-4}$	$(4.2 \pm 0.4) \times 10^{-4}$	$(2.5 \pm 0.2) \times 10^{-4}$	$(10.0 \pm 1.0) \times 10^{-3}$	$(3.8 \pm 0.4) \times 10^{-3}$	—
S14	$(1.4 \pm 0.1) \times 10^{-2}$	$(8.0 \pm 1.0) \times 10^{-1}$	$(2.4 \pm 0.4) \times 10^{-3}$	$(5.3 \pm 0.8) \times 10^{-3}$	$(9.0 \pm 1.0) \times 10^{-3}$	$(7.0 \pm 1.0) \times 10^{-3}$	$(3.2 \pm 0.3) \times 10^{-3}$	$(1.2 \pm 0.1) \times 10^{-4}$	$(8.3 \pm 0.8) \times 10^{-3}$	$(3.4 \pm 0.3) \times 10^{-3}$	$(1.3 \pm 0.1) \times 10^{-3}$	—
S15	$(6.4 \pm 0.6) \times 10^{-1}$	$(6.4 \pm 0.6) \times 10^{-1}$	$(1.7 \pm 0.3) \times 10^{-3}$	$(2.5 \pm 0.4) \times 10^{-3}$	$(4.0 \pm 0.6) \times 10^{-3}$	$(4.5 \pm 0.7) \times 10^{-3}$	$(2.0 \pm 0.2) \times 10^{-3}$	$(5.4 \pm 0.5) \times 10^{-3}$	$(3.9 \pm 0.4) \times 10^{-3}$	$(1.9 \pm 0.2) \times 10^{-3}$	$(7.5 \pm 0.8) \times 10^{-2}$	sc
S17	$(4.6 \pm 0.5) \times 10^{-2}$	$(1.4 \pm 0.1) \times 10^{-3}$	$(1.9 \pm 0.3) \times 10^{-4}$	$(1.3 \pm 0.2) \times 10^{-4}$	$(1.4 \pm 0.2) \times 10^{-4}$	$(1.6 \pm 0.2) \times 10^{-4}$	$(1.7 \pm 0.2) \times 10^{-4}$	$(1.4 \pm 0.1) \times 10^{-4}$	$(5.8 \pm 0.6) \times 10^{-3}$	$(2.0 \pm 0.2) \times 10^{-3}$	$(6.6 \pm 0.7) \times 10^{-2}$	—
S18	$(5.1 \pm 0.5) \times 10^{-1}$	$(1.4 \pm 0.1) \times 10^{-2}$	$(3.1 \pm 0.5) \times 10^{-3}$	$(3.2 \pm 0.5) \times 10^{-3}$	$(3.9 \pm 0.6) \times 10^{-3}$	$(3.9 \pm 0.6) \times 10^{-3}$	$(2.4 \pm 0.2) \times 10^{-3}$	$(3.0 \pm 0.3) \times 10^{-3}$	$(1.8 \pm 0.2) \times 10^{-3}$	$(7.8 \pm 0.8) \times 10^{-2}$	$(3.2 \pm 0.3) \times 10^{-2}$	sc
S20	$(4.7 \pm 0.5) \times 10^{-1}$	$(1.2 \pm 0.1) \times 10^{-2}$	$(1.6 \pm 0.2) \times 10^{-3}$	$(1.5 \pm 0.2) \times 10^{-3}$	$(1.7 \pm 0.2) \times 10^{-3}$	$(1.4 \pm 0.2) \times 10^{-3}$	$(1.8 \pm 0.2) \times 10^{-3}$	$(2.2 \pm 0.2) \times 10^{-3}$	$(1.1 \pm 0.1) \times 10^{-3}$	$(4.1 \pm 0.4) \times 10^{-2}$	$(1.4 \pm 0.2) \times 10^{-2}$	—
S23	$(6.2 \pm 0.6) \times 10^{-1}$	$(10.0 \pm 1.0) \times 10^{-1}$	$(2.1 \pm 0.3) \times 10^{-3}$	$(2.3 \pm 0.4) \times 10^{-3}$	$(2.7 \pm 0.4) \times 10^{-3}$	$(3.5 \pm 0.6) \times 10^{-3}$	$(2.4 \pm 0.2) \times 10^{-3}$	$(3.4 \pm 0.3) \times 10^{-3}$	$(1.9 \pm 0.2) \times 10^{-3}$	$($		

ble 3. (Continued)

Name	Flux 9 μm [Jy] (AKARI IRC)	Flux 18 μm [Jy] (AKARI IRC)	Flux 65 μm [Jy] (AKARI FIS)	Flux 90 μm [Jy] (AKARI FIS)	Flux 140 μm [Jy] (AKARI FIS)	Flux 160 μm [Jy] (AKARI FIS)	Flux 70 μm [Jy] (Herschel PACS)	Flux 160 μm [Jy] (Herschel PACS)	Flux 250 μm [Jy] (Herschel SPIRE)	Flux 350 μm [Jy] (Herschel SPIRE)	Flux 500 μm [Jy] (Herschel SPIRE)	Notes†
S29	$(3.6\pm 0.4)\times 10^2$	$(1.1\pm 0.1)\times 10^3$	$(1.2\pm 0.2)\times 10^4$	$(1.6\pm 0.2)\times 10^4$	$(1.5\pm 0.2)\times 10^4$	$(1.6\pm 0.2)\times 10^4$	$(1.5\pm 0.2)\times 10^4$	$(1.7\pm 0.2)\times 10^4$	$(8.7\pm 0.9)\times 10^3$	$(3.9\pm 0.4)\times 10^3$	$(1.5\pm 0.2)\times 10^3$	sc
S36	$(4.0\pm 0.4)\times 10^2$	$(1.7\pm 0.2)\times 10^3$	$(3.3\pm 0.5)\times 10^4$	$(2.6\pm 0.4)\times 10^4$	$(3.5\pm 0.5)\times 10^4$	$(3.5\pm 0.5)\times 10^4$	$(2.3\pm 0.2)\times 10^4$	$(2.4\pm 0.2)\times 10^4$	$(1.2\pm 0.1)\times 10^4$	$(4.8\pm 0.5)\times 10^3$	$(1.8\pm 0.2)\times 10^3$	—
S37	$(10.0\pm 1.0)\times 10^1$	$(1.3\pm 0.1)\times 10^2$	$(3.7\pm 0.6)\times 10^3$	$(3.4\pm 0.5)\times 10^3$	$(3.5\pm 0.5)\times 10^3$	$(4.2\pm 0.6)\times 10^3$	$(3.2\pm 0.3)\times 10^3$	$(3.3\pm 0.3)\times 10^3$	$(1.3\pm 0.1)\times 10^3$	$(4.0\pm 0.4)\times 10^2$	$(1.2\pm 0.2)\times 10^2$	sc
S41	$(3.3\pm 0.3)\times 10^2$	$(9.8\pm 1.0)\times 10^2$	$(2.3\pm 0.3)\times 10^4$	$(2.0\pm 0.3)\times 10^4$	$(1.9\pm 0.3)\times 10^4$	$(2.5\pm 0.4)\times 10^4$	$(1.9\pm 0.2)\times 10^4$	$(1.8\pm 0.2)\times 10^4$	$(8.5\pm 0.9)\times 10^3$	$(3.2\pm 0.3)\times 10^3$	$(1.2\pm 0.1)\times 10^3$	—
S44	$(8.7\pm 0.9)\times 10^1$	$(1.3\pm 0.1)\times 10^2$	$(2.0\pm 0.3)\times 10^3$	$(2.4\pm 0.4)\times 10^3$	$(3.4\pm 0.5)\times 10^3$	$(3.4\pm 0.5)\times 10^3$	$(2.4\pm 0.2)\times 10^3$	$(3.0\pm 0.3)\times 10^3$	$(1.3\pm 0.1)\times 10^3$	$(4.4\pm 0.4)\times 10^2$	$(1.5\pm 0.2)\times 10^2$	—
S51	$(4.1\pm 0.4)\times 10^2$	$(1.6\pm 0.2)\times 10^3$	$(2.8\pm 0.4)\times 10^4$	$(1.8\pm 0.3)\times 10^4$	$(1.9\pm 0.3)\times 10^4$	$(2.1\pm 0.3)\times 10^4$	$(1.9\pm 0.2)\times 10^4$	$(1.6\pm 0.2)\times 10^4$	$(7.7\pm 0.8)\times 10^3$	$(2.9\pm 0.3)\times 10^3$	$(1.1\pm 0.1)\times 10^3$	sc
S54	$(6.7\pm 0.7)\times 10^1$	$(6.4\pm 0.6)\times 10^1$	$(1.5\pm 0.2)\times 10^3$	$(2.1\pm 0.3)\times 10^3$	$(2.2\pm 0.3)\times 10^3$	$(2.2\pm 0.3)\times 10^3$	$(1.4\pm 0.1)\times 10^3$	$(2.1\pm 0.2)\times 10^3$	$(1.1\pm 0.1)\times 10^3$	$(4.6\pm 0.5)\times 10^2$	$(1.7\pm 0.2)\times 10^2$	sc
S62	$(1.7\pm 0.2)\times 10^2$	$(5.2\pm 0.5)\times 10^2$	$(7.0\pm 1.0)\times 10^3$	$(7.0\pm 1.0)\times 10^3$	$(8.0\pm 1.0)\times 10^3$	$(5.7\pm 0.9)\times 10^3$	$(7.0\pm 0.7)\times 10^3$	$(6.7\pm 0.7)\times 10^3$	$(2.9\pm 0.3)\times 10^3$	$(10.0\pm 1.0)\times 10^2$	$(3.7\pm 0.4)\times 10^2$	—
S64	$(1.9\pm 0.2)\times 10^2$	$(5.7\pm 0.6)\times 10^2$	$(2.0\pm 0.3)\times 10^4$	$(1.6\pm 0.2)\times 10^4$	$(1.9\pm 0.3)\times 10^4$	$(2.1\pm 0.3)\times 10^4$	$(1.5\pm 0.1)\times 10^4$	$(1.7\pm 0.2)\times 10^4$	$(7.4\pm 0.7)\times 10^3$	$(2.9\pm 0.3)\times 10^3$	$(1.1\pm 0.1)\times 10^3$	—
S66	$(1.1\pm 0.1)\times 10^3$	$(1.9\pm 0.2)\times 10^3$	$(3.7\pm 0.6)\times 10^4$	$(4.2\pm 0.6)\times 10^4$	$(5.4\pm 0.8)\times 10^4$	$(4.7\pm 0.7)\times 10^4$	$(3.7\pm 0.4)\times 10^4$	$(6.1\pm 0.6)\times 10^4$	$(3.1\pm 0.3)\times 10^4$	$(1.2\pm 0.1)\times 10^4$	$(4.0\pm 0.4)\times 10^3$	—
S70	$(4.1\pm 0.4)\times 10^1$	$(5.2\pm 0.5)\times 10^1$	$(1.7\pm 0.3)\times 10^3$	$(1.9\pm 0.3)\times 10^3$	$(1.8\pm 0.3)\times 10^3$	$(2.1\pm 0.3)\times 10^3$	$(1.3\pm 0.1)\times 10^3$	$(1.5\pm 0.2)\times 10^3$	$(6.4\pm 0.6)\times 10^2$	$(2.3\pm 0.2)\times 10^2$	$(8.1\pm 0.8)\times 10^1$	—
S71	$(10.0\pm 1.0)\times 10^1$	$(2.1\pm 0.2)\times 10^2$	$(3.8\pm 0.6)\times 10^3$	$(3.4\pm 0.5)\times 10^3$	$(2.7\pm 0.4)\times 10^3$	$(2.5\pm 0.4)\times 10^3$	$(3.4\pm 0.3)\times 10^3$	$(2.9\pm 0.3)\times 10^3$	$(1.1\pm 0.1)\times 10^3$	$(3.6\pm 0.4)\times 10^2$	$(1.1\pm 0.1)\times 10^2$	—
S73	$(1.1\pm 0.4)\times 10^2$	$(9.0\pm 3.0)\times 10^1$	$(3.3\pm 0.5)\times 10^3$	$(4.7\pm 0.7)\times 10^3$	$(4.7\pm 0.7)\times 10^3$	$(5.4\pm 0.8)\times 10^3$	$(4.3\pm 0.4)\times 10^3$	$(6.1\pm 0.6)\times 10^3$	$(2.6\pm 0.3)\times 10^3$	$(9.6\pm 1.0)\times 10^2$	$(3.5\pm 0.4)\times 10^2$	—
S74	$(5.5\pm 0.5)\times 10^1$	$(8.5\pm 0.9)\times 10^1$	$(1.5\pm 0.2)\times 10^3$	$(1.8\pm 0.3)\times 10^3$	$(1.5\pm 0.2)\times 10^3$	$(1.6\pm 0.2)\times 10^3$	$(1.3\pm 0.1)\times 10^3$	$(1.4\pm 0.1)\times 10^3$	$(6.6\pm 0.7)\times 10^2$	$(2.4\pm 0.2)\times 10^2$	$(8.8\pm 0.9)\times 10^1$	—
S76	$(2.9\pm 0.3)\times 10^2$	$(1.3\pm 0.1)\times 10^3$	$(2.1\pm 0.3)\times 10^4$	$(2.2\pm 0.3)\times 10^4$	$(1.9\pm 0.3)\times 10^4$	$(2.0\pm 0.3)\times 10^4$	$(2.2\pm 0.2)\times 10^4$	$(2.2\pm 0.2)\times 10^4$	$(1.1\pm 0.1)\times 10^4$	$(4.7\pm 0.5)\times 10^3$	$(1.9\pm 0.2)\times 10^3$	—
S79	$(5.6\pm 0.6)\times 10^2$	$(2.1\pm 0.2)\times 10^3$	$(2.0\pm 0.3)\times 10^4$	$(1.6\pm 0.2)\times 10^4$	$(1.4\pm 0.2)\times 10^4$	$(1.4\pm 0.2)\times 10^4$	$(2.2\pm 0.2)\times 10^4$	$(1.5\pm 0.1)\times 10^4$	$(5.3\pm 0.6)\times 10^3$	$(1.8\pm 0.2)\times 10^3$	$(5.4\pm 0.7)\times 10^2$	—
S91	$(7.4\pm 0.7)\times 10^1$	$(6.5\pm 0.7)\times 10^1$	$(1.3\pm 0.2)\times 10^3$	$(2.0\pm 0.3)\times 10^3$	$(4.2\pm 0.6)\times 10^3$	$(4.8\pm 0.7)\times 10^3$	$(1.6\pm 0.2)\times 10^3$	$(3.8\pm 0.4)\times 10^3$	$(2.5\pm 0.3)\times 10^3$	$(1.1\pm 0.1)\times 10^3$	$(4.3\pm 0.4)\times 10^2$	—
S92	$(2.5\pm 0.3)\times 10^2$	$(4.4\pm 0.4)\times 10^2$	$(7.0\pm 1.0)\times 10^3$	$(10.0\pm 1.0)\times 10^3$	$(10.0\pm 2.0)\times 10^3$	$(10.0\pm 1.0)\times 10^3$	$(8.6\pm 0.9)\times 10^3$	$(1.2\pm 0.1)\times 10^4$	$(6.0\pm 0.6)\times 10^3$	$(2.4\pm 0.2)\times 10^3$	$(9.2\pm 0.9)\times 10^2$	—
S96	$(2.4\pm 0.2)\times 10^2$	$(5.5\pm 0.5)\times 10^2$	$(9.0\pm 1.0)\times 10^3$	$(7.0\pm 1.0)\times 10^3$	$(7.0\pm 1.0)\times 10^3$	$(6.2\pm 0.9)\times 10^3$	$(7.3\pm 0.7)\times 10^3$	$(7.3\pm 0.7)\times 10^3$	$(3.4\pm 0.3)\times 10^3$	$(1.2\pm 0.1)\times 10^3$	$(4.5\pm 0.5)\times 10^2$	—
S97	$(8.9\pm 0.9)\times 10^1$	$(1.3\pm 0.1)\times 10^2$	$(2.5\pm 0.4)\times 10^3$	$(2.4\pm 0.4)\times 10^3$	$(2.3\pm 0.3)\times 10^3$	$(2.2\pm 0.3)\times 10^3$	$(2.7\pm 0.3)\times 10^3$	$(2.7\pm 0.3)\times 10^3$	$(1.3\pm 0.1)\times 10^3$	$(5.2\pm 0.5)\times 10^2$	$(1.9\pm 0.2)\times 10^2$	—
S104	$(5.0\pm 0.5)\times 10^1$	$(1.3\pm 0.1)\times 10^2$	$(2.1\pm 0.3)\times 10^3$	$(2.2\pm 0.3)\times 10^3$	$(1.5\pm 0.2)\times 10^3$	$(1.3\pm 0.2)\times 10^3$	$(2.1\pm 0.2)\times 10^3$	$(1.5\pm 0.2)\times 10^3$	$(5.7\pm 0.6)\times 10^2$	$(1.9\pm 0.2)\times 10^2$	$(6.9\pm 0.7)\times 10^1$	—
S109	$(1.9\pm 0.2)\times 10^2$	$(7.0\pm 0.7)\times 10^2$	$(10.0\pm 2.0)\times 10^3$	$(9.0\pm 1.0)\times 10^3$	$(1.1\pm 0.2)\times 10^4$	$(1.1\pm 0.2)\times 10^4$	$(10.0\pm 1.0)\times 10^3$	$(9.9\pm 1.0)\times 10^3$	$(4.4\pm 0.4)\times 10^3$	$(1.6\pm 0.2)\times 10^3$	$(5.1\pm 0.5)\times 10^2$	—
S110	$(4.2\pm 0.4)\times 10^2$	$(2.4\pm 0.2)\times 10^3$	$(2.7\pm 0.4)\times 10^4$	$(1.9\pm 0.3)\times 10^4$	$(1.9\pm 0.3)\times 10^4$	$(2.2\pm 0.3)\times 10^4$	$(1.9\pm 0.2)\times 10^4$	$(1.7\pm 0.2)\times 10^4$	$(8.5\pm 0.8)\times 10^3$	$(3.4\pm 0.3)\times 10^3$	$(1.2\pm 0.1)\times 10^3$	—
S111	$(3.7\pm 0.4)\times 10^2$	$(2.0\pm 0.2)\times 10^3$	$(2.3\pm 0.3)\times 10^4$	$(1.4\pm 0.2)\times 10^4$	$(1.6\pm 0.2)\times 10^4$	$(1.9\pm 0.3)\times 10^4$	$(1.8\pm 0.2)\times 10^4$	$(1.4\pm 0.1)\times 10^4$	$(6.6\pm 0.7)\times 10^3$	$(2.4\pm 0.2)\times 10^3$	$(9.2\pm 0.9)\times 10^2$	—
S116	$(2.3\pm 0.2)\times 10^2$	$(4.4\pm 0.4)\times 10^2$	$(7.0\pm 1.0)\times 10^3$	$(8.0\pm 1.0)\times 10^3$	$(9.0\pm 1.0)\times 10^3$	$(9.0\pm 1.0)\times 10^3$	$(7.5\pm 0.7)\times 10^3$	$(9.5\pm 1.0)\times 10^3$	$(4.2\pm 0.4)\times 10^3$	$(1.5\pm 0.2)\times 10^3$	$(5.7\pm 0.6)\times 10^2$	—
S123	$(6.7\pm 0.7)\times 10^1$	$(6.1\pm 0.6)\times 10^1$	$(1.1\pm 0.2)\times 10^3$	$(1.8\pm 0.3)\times 10^3$	$(2.7\pm 0.4)\times 10^3$	$(2.5\pm 0.4)\times 10^3$	$(1.4\pm 0.1)\times 10^3$	$(3.1\pm 0.3)\times 10^3$	$(1.8\pm 0.2)\times 10^3$	$(7.2\pm 0.7)\times 10^2$	$(2.8\pm 0.3)\times 10^2$	—
S133	$(1.2\pm 0.1)\times 10^2$	$(2.0\pm 0.2)\times 10^2$	$(5.1\pm 0.8)\times 10^3$	$(5.1\pm 0.8)\times 10^3$	$(4.8\pm 0.7)\times 10^3$	$(4.7\pm 0.7)\times 10^3$	$(4.6\pm 0.5)\times 10^3$	$(4.5\pm 0.4)\times 10^3$	$(1.8\pm 0.2)\times 10^3$	$(6.5\pm 0.7)\times 10^2$	$(2.4\pm 0.3)\times 10^2$	—
S137	$(2.6\pm 0.3)\times 10^2$	$(2.0\pm 0.2)\times 10^2$	$(3.4\pm 0.5)\times 10^3$	$(5.0\pm 0.8)\times 10^3$	$(9.0\pm 1.0)\times 10^3$	$(1.1\pm 0.2)\times 10^4$	$(4.3\pm 0.4)\times 10^3$	$(8.9\pm 0.9)\times 10^3$	$(5.0\pm 0.5)\times 10^3$	$(2.0\pm 0.2)\times 10^3$	$(7.3\pm 0.7)\times 10^2$	sc
S141	$(6.5\pm 0.7)\times 10^1$	$(1.3\pm 0.1)\times 10^2$	$(2.1\pm 0.3)\times 10^3$	$(2.9\pm 0.4)\times 10^3$	$(2.4\pm 0.4)\times 10^3$	$(2.4\pm 0.4)\times 10^3$	$(2.2\pm 0.2)\times 10^3$	$(2.4\pm 0.2)\times 10^3$	$(1.2\pm 0.1)\times 10^3$	$(4.7\pm 0.5)\times 10^2$	$(1.9\pm 0.2)\times 10^2$	sc
S143	$(5.5\pm 0.5)\times 10^2$	$(6.9\pm 0.7)\times 10^2$	$(10.0\pm 1.0)\times 10^3$	$(1.3\pm 0.2)\times 10^4$	$(1.9\pm 0.3)\times 10^4$	$(1.8\pm 0.3)\times 10^4$	$(1.2\pm 0.1)\times 10^4$	$(1.3\pm 0.1)\times 10^4$	$(1.3\pm 0.1)\times 10^4$	$(5.2\pm 0.5)\times 10^3$	$(2.0\pm 0.2)\times 10^3$	—
S145	$(6.4\pm 0.6)\times 10^2$	$(1.7\pm 0.2)\times 10^3$	$(2.0\pm 0.3)\times 10^4$	$(2.3\pm 0.3)\times 10^4$	$(2.0\pm 0.3)\times 10^4$	$(1.6\pm 0.2)\times 10^4$	$(2.2\pm 0.2)\times 10^4$	$(1.4\pm 0.1)\times 10^4$	$(7.8\pm 0.8)\times 10^3$	$(2.7\pm 0.3)\times 10^3$	$(9.6\pm 1.0)\times 10^2$	—
S150	$(6.5\pm 0.7)\times 10^1$	$(1.6\pm 0.2)\times 10^2$	$(2.9\pm 0.4)\times 10^3$	$(2.8\pm 0.4)\times 10^3$	$(2.9\pm 0.4)\times 10^3$	$(3.5\pm 0.5)\times 10^3$	$(2.4\pm 0.2)\times 10^3$	$(2.7\pm 0.3)\times 10^3$	$(1.4\pm 0.1)\times 10^3$	$(5.6\pm 0.6)\times 10^2$	$(2.1\pm 0.2)\times 10^2$	—
S156	$(6.4\pm 0.6)\times 10^2$	$(3.8\pm 0.4)\times 10^3$	$(4.0\pm 0.6)\times 10^4$	$(2.3\pm 0.3)\times 10^4$	$(1.6\pm 0.3)\times 10^4$	$(10.0\pm 2.0)\times 10^3$	$(3.3\pm 0.3)\times 10^4$	$(1.5\pm 0.1)\times 10^4$	$(4.6\pm 0.5)\times 10^3$	$(1.5\pm 0.2)\times 10^3$	$(4.6\pm 0.5)\times 10^2$	—
S163	$(2.6\pm 0.3)\times 10^1$	$(3.2\pm 0.3)\times 10^1$	$(5.6\pm 0.8)\times 10^2$	$(8.0\pm 1.0)\times 10^2$	$(1.4\pm 0.2)\times 10^3$	$(1.4\pm 0.2)\times 10^3$	$(8.7\pm 0.9)\times 10^2$	$(1.6\pm 0.2)\times 10^3$	$(9.4\pm 0.9)\times 10^2$	$(4.3\pm 0.4)\times 10^2$	$(1.9\pm 0.2)\times 10^2$	—
S181	$(3.6\pm 0.4)\times 10^2$	$(2.3\pm 0.2)\times 10^3$	$(2.2\pm 0.3)\times 10^4$	$(1.6\pm 0.2)\times 10^4$	$(1.1\pm 0.2)\times 10^4$	$(9.0\pm 1.0)\times 10^3$	$(1.5\pm 0.1)\times 10^4$	$(8.9\pm 0.9)\times 10^3$	$(3.4\pm 0.3)\times 10^3$	$(1.2\pm 0.1)\times 10^3$	$(4.4\pm 0.4)\times 10^2$	—
S186	$(2.6\pm 0.3)\times 10^2$	$(8.8\pm 0.9)\times 10^2$	$(1.1\pm 0.2)\times 10^4$	$(1.3\pm 0.2)\times 10^4$	$(1.4\pm 0.2)\times 10^4$	$(1.4\pm 0.2)\times 10^4$	$(1.2\pm 0.1)\times 10^4$	$(1.5\pm 0.2)\times 10^4$	$(8.1\pm 0.8)\times 10^3$	$(3.5\pm 0.3)\times 10^3$	$(1.5\pm 0.1)\times 10^3$	—
CN24	$(10.0\pm 1.0)\times 10^1$	$(4.1\pm 0.4)\times 10^2$	$(8.0\pm 1.0)\times 10^3$	$(6.0\pm 0.9)\times 10^3$	$(9.0\pm 1.0)\times 10^3$	$(1.1\pm 0.2)\times 10^4$	$(4.9\pm 0.5)\times 10^3$	$(5.9\pm 0.6)\times 10^3$	$(3.8\pm 0.4)\times 10^3$	$(1.8\pm 0.2)\times 10^3$	$(6.4\pm 0.7)\times 10^2$	—
CN60	$(4.2\pm 0.4)\times 10^1$	$(1.8\pm 0.2)\times 10^2$	$(3.0\pm 0.5)\times 10^3$	$(2.9\pm 0.4)\times 10^3$	$(3.5\pm 0.5)\times 10^3$	$(3.4\pm 0.5)\times 10^3$	$(3.4\pm 0.3)\times 10^3$	$(3.6\pm 0.4)\times 10^3$	$(1.9\pm 0.2)\times 10^3$	$(7.1\pm 0.7)\times 10^2$	$(2.5\pm 0.3)\times 10^2$	—
CN63	$(4.3\pm 0.5)\times 10^1$	$(4.9\pm 0.5)\times 10^1$	$(1.7\pm 0.3)\times 10^3$	$(2.3\pm 0.3)\times 10^3$	$(3.5\pm 0.5)\times 10^3$	$(3.2\pm 0.5)\times 10^3$	$(1.7\pm 0.2)\times 10^3$	$(3.0\pm 0.3)\times 10^3$	$(1.5\pm 0.1)\times 10^3$	$(5.1\pm 0.5)\times 10^2$	$(1.7\pm 0.2)\times 10^2$	sc
CN71	$(10.0\pm 1.0)\times 10^2$	$(2.6\pm 0.3)\times 10^3$	$(5.1\pm 0.8)\times 10^4$	$(4.0\pm 0.6)\times 10^4$	$(5.0\pm 0.8)\times 10^4$	$(4.9\pm 0.7)\times 10^4$	$(4.0\pm 0.4)\times 10^4$	$(4.2\pm 0.4)\times 10^4$	$(1.9\pm 0.2)\times 10^4$	$(7.3\pm 0.7)\times 10^3$	$(2.7\pm 0.3)\times 10^3$	—

ble 3. (Continued)

Name	Flux 9 μm [Jy] (AKARI IRC)	Flux 18 μm [Jy] (AKARI IRC)	Flux 65 μm [Jy] (AKARI FIS)	Flux 90 μm [Jy] (AKARI FIS)	Flux 140 μm [Jy] (AKARI FIS)	Flux 160 μm [Jy] (AKARI FIS)	Flux 70 μm [Jy] (Herschel PACS)	Flux 160 μm [Jy] (Herschel PACS)	Flux 250 μm [Jy] (Herschel SPIRE)	Flux 350 μm [Jy] (Herschel SPIRE)	Flux 500 μm [Jy] (Herschel SPIRE)	Notes†	
CN73	$(4.2\pm 0.4)\times 10^{-1}$	$(1.8\pm 0.2)\times 10^{-2}$	$(3.2\pm 0.5)\times 10^{-3}$	$(3.1\pm 0.5)\times 10^{-3}$	$(3.1\pm 0.5)\times 10^{-3}$	$(3.0\pm 0.4)\times 10^{-3}$	$(2.9\pm 0.3)\times 10^{-3}$	$(2.9\pm 0.3)\times 10^{-3}$	$(1.4\pm 0.1)\times 10^{-3}$	$(5.3\pm 0.5)\times 10^{-2}$	$(2.0\pm 0.2)\times 10^{-2}$	sc	
CN88	$(3.7\pm 0.4)\times 10^{-2}$	$(6.3\pm 0.6)\times 10^{-2}$	$(8.0\pm 1.0)\times 10^{-3}$	$(9.0\pm 1.0)\times 10^{-3}$	$(9.0\pm 1.0)\times 10^{-3}$	$(9.0\pm 1.0)\times 10^{-3}$	$(8.4\pm 0.8)\times 10^{-3}$	$(9.5\pm 1.0)\times 10^{-3}$	$(4.3\pm 0.4)\times 10^{-3}$	$(1.5\pm 0.2)\times 10^{-3}$	$(5.7\pm 0.6)\times 10^{-2}$	—	
CN90	$(1.4\pm 0.1)\times 10^{-2}$	$(2.6\pm 0.3)\times 10^{-2}$	$(4.1\pm 0.6)\times 10^{-3}$	$(3.7\pm 0.6)\times 10^{-3}$	$(3.3\pm 0.5)\times 10^{-3}$	$(4.0\pm 0.6)\times 10^{-3}$	$(3.2\pm 0.3)\times 10^{-3}$	$(3.3\pm 0.3)\times 10^{-3}$	$(1.5\pm 0.2)\times 10^{-3}$	$(5.3\pm 0.6)\times 10^{-2}$	$(1.9\pm 0.2)\times 10^{-2}$	—	
CN99	$(1.3\pm 0.1)\times 10^{-2}$	$(3.1\pm 0.3)\times 10^{-2}$	$(4.5\pm 0.7)\times 10^{-3}$	$(5.6\pm 0.8)\times 10^{-3}$	$(6.0\pm 0.9)\times 10^{-3}$	$(6.0\pm 0.9)\times 10^{-3}$	$(6.0\pm 0.9)\times 10^{-3}$	$(5.4\pm 0.5)\times 10^{-3}$	$(8.1\pm 0.8)\times 10^{-3}$	$(4.1\pm 0.4)\times 10^{-3}$	$(1.5\pm 0.1)\times 10^{-3}$	$(5.0\pm 0.5)\times 10^{-2}$	—
CN107	$(1.3\pm 0.1)\times 10^{-2}$	$(4.1\pm 0.4)\times 10^{-2}$	$(10.0\pm 1.0)\times 10^{-3}$	$(6.7\pm 1.0)\times 10^{-3}$	$(6.4\pm 1.0)\times 10^{-3}$	$(6.4\pm 1.0)\times 10^{-3}$	$(8.0\pm 1.0)\times 10^{-3}$	$(5.4\pm 0.5)\times 10^{-3}$	$(5.9\pm 0.6)\times 10^{-3}$	$(3.2\pm 0.3)\times 10^{-3}$	$(1.3\pm 0.1)\times 10^{-3}$	$(4.7\pm 0.5)\times 10^{-2}$	—
CN108	$(7.0\pm 0.7)\times 10^{-2}$	$(6.8\pm 0.7)\times 10^{-2}$	$(1.3\pm 0.2)\times 10^{-4}$	$(2.3\pm 0.3)\times 10^{-4}$	$(3.8\pm 0.6)\times 10^{-4}$	$(4.0\pm 0.6)\times 10^{-4}$	$(1.7\pm 0.2)\times 10^{-4}$	$(4.7\pm 0.5)\times 10^{-4}$	$(2.9\pm 0.3)\times 10^{-4}$	$(1.2\pm 0.1)\times 10^{-4}$	$(4.4\pm 0.4)\times 10^{-3}$	—	
CN109	$(1.2\pm 0.1)\times 10^{-2}$	$(4.2\pm 0.4)\times 10^{-2}$	$(10.0\pm 1.0)\times 10^{-3}$	$(7.0\pm 1.0)\times 10^{-3}$	$(9.0\pm 1.0)\times 10^{-3}$	$(7.0\pm 1.0)\times 10^{-3}$	$(5.2\pm 0.5)\times 10^{-3}$	$(5.6\pm 0.6)\times 10^{-3}$	$(3.1\pm 0.3)\times 10^{-3}$	$(1.3\pm 0.1)\times 10^{-3}$	$(4.7\pm 0.5)\times 10^{-2}$	—	
CN111	$(4.3\pm 0.4)\times 10^{-1}$	$(5.3\pm 0.5)\times 10^{-1}$	$(1.4\pm 0.2)\times 10^{-3}$	$(1.9\pm 0.3)\times 10^{-3}$	$(2.1\pm 0.3)\times 10^{-3}$	$(2.2\pm 0.3)\times 10^{-3}$	$(1.2\pm 0.1)\times 10^{-3}$	$(2.2\pm 0.2)\times 10^{-3}$	$(1.2\pm 0.1)\times 10^{-3}$	$(4.4\pm 0.4)\times 10^{-2}$	$(1.5\pm 0.2)\times 10^{-2}$	sc	
CN114	$(9.6\pm 1.0)\times 10^{-1}$	$(1.2\pm 0.1)\times 10^{-2}$	$(4.0\pm 0.6)\times 10^{-3}$	$(3.9\pm 0.6)\times 10^{-3}$	$(3.8\pm 0.6)\times 10^{-3}$	$(4.3\pm 0.6)\times 10^{-3}$	$(3.0\pm 0.3)\times 10^{-3}$	$(3.6\pm 0.4)\times 10^{-3}$	$(1.8\pm 0.2)\times 10^{-3}$	$(6.6\pm 0.7)\times 10^{-2}$	$(2.5\pm 0.3)\times 10^{-2}$	—	
CN138	$(1.1\pm 0.1)\times 10^{-1}$	$(1.3\pm 0.1)\times 10^{-1}$	$(3.6\pm 0.6)\times 10^{-2}$	$(5.1\pm 0.8)\times 10^{-2}$	$(7.0\pm 1.0)\times 10^{-2}$	$(10.0\pm 2.0)\times 10^{-2}$	$(3.9\pm 0.4)\times 10^{-2}$	$(6.4\pm 0.6)\times 10^{-2}$	$(4.7\pm 0.5)\times 10^{-2}$	$(2.3\pm 0.2)\times 10^{-2}$	$(10.0\pm 1.0)\times 10^{-1}$	—	
CN139	$(2.9\pm 0.3)\times 10^{-2}$	$(4.3\pm 0.4)\times 10^{-2}$	$(7.0\pm 1.0)\times 10^{-3}$	$(8.0\pm 1.0)\times 10^{-3}$	$(1.2\pm 0.2)\times 10^{-4}$	$(1.3\pm 0.2)\times 10^{-4}$	$(6.8\pm 0.7)\times 10^{-3}$	$(9.1\pm 0.9)\times 10^{-3}$	$(4.1\pm 0.4)\times 10^{-3}$	$(1.4\pm 0.1)\times 10^{-3}$	$(4.4\pm 0.5)\times 10^{-2}$	—	
CN148	$(2.6\pm 0.3)\times 10^{-2}$	$(1.5\pm 0.2)\times 10^{-3}$	$(2.5\pm 0.4)\times 10^{-4}$	$(1.4\pm 0.2)\times 10^{-4}$	$(1.5\pm 0.2)\times 10^{-4}$	$(1.9\pm 0.3)\times 10^{-4}$	$(1.4\pm 0.1)\times 10^{-4}$	$(1.4\pm 0.1)\times 10^{-4}$	$(7.3\pm 0.7)\times 10^{-3}$	$(2.9\pm 0.3)\times 10^{-3}$	$(10.0\pm 1.0)\times 10^{-2}$	sc	
CS2	$(1.1\pm 0.1)\times 10^{-2}$	$(2.9\pm 0.3)\times 10^{-2}$	$(7.0\pm 1.0)\times 10^{-3}$	$(5.2\pm 0.8)\times 10^{-3}$	$(6.5\pm 1.0)\times 10^{-3}$	$(8.0\pm 1.0)\times 10^{-3}$	$(5.4\pm 0.5)\times 10^{-3}$	$(5.7\pm 0.6)\times 10^{-3}$	$(2.7\pm 0.3)\times 10^{-3}$	$(1.2\pm 0.1)\times 10^{-3}$	$(3.9\pm 0.4)\times 10^{-2}$	sc	
CS33	$(5.6\pm 0.6)\times 10^{-1}$	$(1.4\pm 0.1)\times 10^{-2}$	$(3.2\pm 0.5)\times 10^{-3}$	$(2.7\pm 0.4)\times 10^{-3}$	$(2.6\pm 0.4)\times 10^{-3}$	$(3.2\pm 0.5)\times 10^{-3}$	$(2.7\pm 0.3)\times 10^{-3}$	$(2.6\pm 0.3)\times 10^{-3}$	$(1.1\pm 0.1)\times 10^{-3}$	$(3.7\pm 0.4)\times 10^{-2}$	$(1.2\pm 0.1)\times 10^{-2}$	—	
CS39	$(4.1\pm 0.4)\times 10^{-1}$	$(3.9\pm 0.4)\times 10^{-1}$	$(5.4\pm 0.8)\times 10^{-2}$	$(8.0\pm 1.0)\times 10^{-2}$	$(1.3\pm 0.2)\times 10^{-3}$	$(1.3\pm 0.2)\times 10^{-3}$	$(7.9\pm 0.8)\times 10^{-2}$	$(1.5\pm 0.1)\times 10^{-3}$	$(8.5\pm 0.9)\times 10^{-2}$	$(3.5\pm 0.3)\times 10^{-2}$	$(1.3\pm 0.1)\times 10^{-2}$	—	
CS51	$(1.2\pm 0.1)\times 10^{-2}$	$(2.8\pm 0.3)\times 10^{-2}$	$(6.4\pm 1.0)\times 10^{-3}$	$(6.4\pm 1.0)\times 10^{-3}$	$(5.9\pm 0.9)\times 10^{-3}$	$(5.7\pm 0.9)\times 10^{-3}$	$(5.6\pm 0.6)\times 10^{-3}$	$(6.5\pm 0.6)\times 10^{-3}$	$(3.0\pm 0.3)\times 10^{-3}$	$(1.1\pm 0.1)\times 10^{-3}$	$(3.7\pm 0.4)\times 10^{-2}$	—	
CS57	$(1.6\pm 0.2)\times 10^{-2}$	$(2.2\pm 0.2)\times 10^{-2}$	$(5.5\pm 0.8)\times 10^{-3}$	$(6.2\pm 0.9)\times 10^{-3}$	$(6.1\pm 0.9)\times 10^{-3}$	$(7.0\pm 1.0)\times 10^{-3}$	$(5.6\pm 0.6)\times 10^{-3}$	$(7.3\pm 0.7)\times 10^{-3}$	$(3.1\pm 0.3)\times 10^{-3}$	$(8.8\pm 0.9)\times 10^{-2}$	$(2.8\pm 0.3)\times 10^{-2}$	—	
CS62	$(2.4\pm 0.2)\times 10^{-2}$	$(1.8\pm 0.2)\times 10^{-3}$	$(1.3\pm 0.2)\times 10^{-4}$	$(1.2\pm 0.2)\times 10^{-4}$	$(9.0\pm 1.0)\times 10^{-3}$	$(9.0\pm 1.0)\times 10^{-3}$	$(1.2\pm 0.1)\times 10^{-4}$	$(9.4\pm 0.9)\times 10^{-3}$	$(4.4\pm 0.4)\times 10^{-3}$	$(1.6\pm 0.2)\times 10^{-3}$	$(5.7\pm 0.6)\times 10^{-2}$	—	
CS79	$(2.8\pm 0.3)\times 10^{-2}$	$(3.8\pm 0.4)\times 10^{-2}$	$(8.0\pm 1.0)\times 10^{-3}$	$(8.0\pm 1.0)\times 10^{-3}$	$(8.0\pm 1.0)\times 10^{-3}$	$(7.0\pm 1.0)\times 10^{-3}$	$(10.0\pm 1.0)\times 10^{-3}$	$(5.9\pm 0.6)\times 10^{-3}$	$(1.7\pm 0.2)\times 10^{-3}$	$(6.2\pm 0.6)\times 10^{-2}$	$(2.2\pm 0.2)\times 10^{-2}$	—	
CS81	$(1.1\pm 0.1)\times 10^{-2}$	$(6.2\pm 0.6)\times 10^{-2}$	$(1.1\pm 0.2)\times 10^{-4}$	$(8.0\pm 1.0)\times 10^{-3}$	$(5.7\pm 0.8)\times 10^{-3}$	$(5.8\pm 0.9)\times 10^{-3}$	$(7.0\pm 0.7)\times 10^{-3}$	$(5.2\pm 0.5)\times 10^{-3}$	$(2.3\pm 0.2)\times 10^{-3}$	$(8.2\pm 0.8)\times 10^{-2}$	$(2.9\pm 0.3)\times 10^{-2}$	—	
EN1	$(3.6\pm 0.4)\times 10^{-3}$	$(1.4\pm 0.1)\times 10^{-4}$	$(10.0\pm 2.0)\times 10^{-4}$	$(1.1\pm 0.2)\times 10^{-5}$	$(9.0\pm 1.0)\times 10^{-4}$	$(8.0\pm 1.0)\times 10^{-4}$	—	—	—	—	—	—	
EN2	$(2.2\pm 0.2)\times 10^{-2}$	$(1.4\pm 0.1)\times 10^{-2}$	$(4.4\pm 0.7)\times 10^{-3}$	$(4.9\pm 0.7)\times 10^{-3}$	$(4.7\pm 0.7)\times 10^{-3}$	$(4.0\pm 0.6)\times 10^{-3}$	—	—	—	—	—	—	
EN3	$(4.5\pm 0.4)\times 10^{-2}$	$(4.1\pm 0.4)\times 10^{-2}$	$(7.0\pm 1.0)\times 10^{-3}$	$(9.0\pm 1.0)\times 10^{-3}$	$(1.3\pm 0.2)\times 10^{-4}$	$(1.3\pm 0.2)\times 10^{-4}$	—	—	—	—	—	—	
EN4	$(3.1\pm 0.3)\times 10^{-2}$	$(2.3\pm 0.2)\times 10^{-2}$	$(4.6\pm 0.7)\times 10^{-3}$	$(5.9\pm 0.9)\times 10^{-3}$	$(7.0\pm 1.0)\times 10^{-3}$	$(8.0\pm 1.0)\times 10^{-3}$	—	—	—	—	—	—	
EN5	$(1.5\pm 0.2)\times 10^{-2}$	$(1.2\pm 0.1)\times 10^{-2}$	$(2.2\pm 0.3)\times 10^{-3}$	$(3.0\pm 0.5)\times 10^{-3}$	$(5.0\pm 0.7)\times 10^{-3}$	$(5.7\pm 0.9)\times 10^{-3}$	—	—	—	—	—	—	
EN6	$(1.2\pm 0.1)\times 10^{-2}$	$(1.9\pm 0.2)\times 10^{-2}$	$(3.3\pm 0.5)\times 10^{-3}$	$(4.2\pm 0.6)\times 10^{-3}$	$(5.3\pm 0.8)\times 10^{-3}$	$(5.4\pm 0.8)\times 10^{-3}$	—	—	—	—	—	—	
EN7	$(2.0\pm 0.2)\times 10^{-1}$	$(1.3\pm 0.1)\times 10^{-1}$	$(1.1\pm 0.2)\times 10^{-2}$	$(1.3\pm 0.2)\times 10^{-2}$	$(3.1\pm 0.5)\times 10^{-2}$	$(4.0\pm 0.6)\times 10^{-2}$	—	—	—	—	—	—	
EN8	$(1.8\pm 0.2)\times 10^{-1}$	$(1.6\pm 0.2)\times 10^{-1}$	$(10.0\pm 2.0)\times 10^{-1}$	$(2.1\pm 0.3)\times 10^{-2}$	$(4.3\pm 0.7)\times 10^{-2}$	$(4.7\pm 0.7)\times 10^{-2}$	—	—	—	—	—	sc	
EN9	$(2.5\pm 0.2)\times 10^{-2}$	$(3.3\pm 0.3)\times 10^{-2}$	$(2.8\pm 0.4)\times 10^{-3}$	$(4.5\pm 0.7)\times 10^{-3}$	$(7.0\pm 1.0)\times 10^{-3}$	$(5.9\pm 0.9)\times 10^{-3}$	—	—	—	—	—	—	
EN10	$(7.4\pm 0.7)\times 10^{-2}$	$(10.0\pm 1.0)\times 10^{-2}$	$(1.5\pm 0.2)\times 10^{-4}$	$(2.1\pm 0.3)\times 10^{-4}$	$(2.3\pm 0.4)\times 10^{-4}$	$(2.4\pm 0.4)\times 10^{-4}$	—	—	—	—	—	—	
EN11	$(1.9\pm 0.2)\times 10^{-1}$	$(1.6\pm 0.2)\times 10^{-1}$	$(3.7\pm 0.6)\times 10^{-2}$	$(3.6\pm 0.5)\times 10^{-2}$	$(4.0\pm 0.6)\times 10^{-2}$	$(5.4\pm 0.8)\times 10^{-2}$	—	—	—	—	—	—	
EN12	$(1.8\pm 0.2)\times 10^{-2}$	$(1.7\pm 0.2)\times 10^{-2}$	$(4.8\pm 0.7)\times 10^{-3}$	$(2.3\pm 0.3)\times 10^{-3}$	$(2.2\pm 0.3)\times 10^{-3}$	$(2.2\pm 0.3)\times 10^{-3}$	—	—	—	—	—	—	
EN13	$(2.2\pm 0.2)\times 10^{-3}$	$(3.1\pm 0.3)\times 10^{-3}$	$(5.7\pm 0.9)\times 10^{-4}$	$(5.4\pm 0.8)\times 10^{-4}$	$(4.4\pm 0.7)\times 10^{-4}$	$(3.8\pm 0.6)\times 10^{-4}$	—	—	—	—	—	—	
EN14	$(2.2\pm 0.2)\times 10^{-3}$	$(3.4\pm 0.3)\times 10^{-3}$	$(8.0\pm 1.0)\times 10^{-4}$	$(6.5\pm 1.0)\times 10^{-4}$	$(5.6\pm 0.8)\times 10^{-4}$	$(5.0\pm 0.7)\times 10^{-4}$	—	—	—	—	—	—	
EN15	$(4.6\pm 0.5)\times 10^{-1}$	$(5.2\pm 0.5)\times 10^{-1}$	$(5.8\pm 0.9)\times 10^{-2}$	$(8.0\pm 1.0)\times 10^{-2}$	$(1.3\pm 0.2)\times 10^{-3}$	$(1.3\pm 0.2)\times 10^{-3}$	—	—	—	—	—	sc	
EN16	$(1.9\pm 0.2)\times 10^{-2}$	$(1.5\pm 0.2)\times 10^{-2}$	$(2.4\pm 0.4)\times 10^{-3}$	$(3.3\pm 0.5)\times 10^{-3}$	$(6.1\pm 0.9)\times 10^{-3}$	$(7.0\pm 1.0)\times 10^{-3}$	—	—	—	—	—	—	
EN17	$(2.4\pm 0.2)\times 10^{-2}$	$(2.7\pm 0.3)\times 10^{-2}$	$(3.5\pm 0.5)\times 10^{-3}$	$(5.4\pm 0.8)\times 10^{-3}$	$(8.0\pm 1.0)\times 10^{-3}$	$(8.0\pm 1.0)\times 10^{-3}$	—	—	—	—	—	—	
EN18	$(1.5\pm 0.2)\times 10^{-2}$	$(2.3\pm 0.2)\times 10^{-2}$	$(1.9\pm 0.3)\times 10^{-3}$	$(3.4\pm 0.5)\times 10^{-3}$	$(4.0\pm 0.6)\times 10^{-3}$	$(4.3\pm 0.6)\times 10^{-3}$	—	—	—	—	—	—	
EN19	$(6.0\pm 0.6)\times 10^{-1}$	$(6.0\pm 0.6)\times 10^{-1}$	$(1.2\pm 0.2)\times 10^{-3}$	$(1.8\pm 0.3)\times 10^{-3}$	$(2.8\pm 0.4)\times 10^{-3}$	$(2.8\pm 0.4)\times 10^{-3}$	—	—	—	—	—	—	
EN20	$(2.9\pm 0.3)\times 10^{-1}$	$(4.0\pm 0.4)\times 10^{-1}$	$(3.1\pm 0.5)\times 10^{-2}$	$(5.5\pm 0.8)\times 10^{-2}$	$(1.1\pm 0.2)\times 10^{-3}$	$(1.1\pm 0.2)\times 10^{-3}$	—	—	—	—	—	sc	

ble 3. (Continued)

Name	Flux 9 μm [Jy] (AKARI IRC)	Flux 18 μm [Jy] (AKARI IRC)	Flux 65 μm [Jy] (AKARI FIS)	Flux 90 μm [Jy] (AKARI FIS)	Flux 140 μm [Jy] (AKARI FIS)	Flux 160 μm [Jy] (AKARI FIS)	Flux 70 μm [Jy] (Herschel PACS)	Flux 160 μm [Jy] (Herschel PACS)	Flux 250 μm [Jy] (Herschel SPIRE)	Flux 350 μm [Jy] (Herschel SPIRE)	Flux 500 μm [Jy] (Herschel SPIRE)	Notes†
EN21	$(1.7\pm 0.2)\times 10^2$	$(1.6\pm 0.2)\times 10^2$	$(1.4\pm 0.2)\times 10^3$	$(2.6\pm 0.4)\times 10^3$	$(4.5\pm 0.7)\times 10^3$	$(4.5\pm 0.7)\times 10^3$	—	—	—	—	—	—
EN22	$(4.5\pm 0.5)\times 10^2$	$(7.0\pm 0.7)\times 10^2$	$(10.0\pm 2.0)\times 10^3$	$(1.2\pm 0.2)\times 10^4$	$(1.7\pm 0.3)\times 10^4$	$(1.6\pm 0.2)\times 10^4$	—	—	—	—	—	—
ES1	$(1.4\pm 0.1)\times 10^3$	$(3.1\pm 0.3)\times 10^3$	$(3.5\pm 0.5)\times 10^4$	$(4.3\pm 0.7)\times 10^4$	$(5.0\pm 0.7)\times 10^4$	$(4.2\pm 0.6)\times 10^4$	—	—	—	—	—	—
ES2	$(6.1\pm 0.6)\times 10^1$	$(4.9\pm 0.5)\times 10^1$	$(5.2\pm 0.8)\times 10^2$	$(9.0\pm 1.0)\times 10^2$	$(1.4\pm 0.2)\times 10^3$	$(1.2\pm 0.2)\times 10^3$	—	—	—	—	—	sc
ES3	$(1.8\pm 0.2)\times 10^2$	$(2.1\pm 0.2)\times 10^2$	$(1.9\pm 0.3)\times 10^3$	$(2.5\pm 0.4)\times 10^3$	$(5.0\pm 0.7)\times 10^3$	$(5.0\pm 0.8)\times 10^3$	—	—	—	—	—	—
ES4	$(7.2\pm 0.7)\times 10^1$	$(1.4\pm 0.1)\times 10^2$	$(2.0\pm 0.3)\times 10^3$	$(2.4\pm 0.4)\times 10^3$	$(2.1\pm 0.3)\times 10^3$	$(2.0\pm 0.3)\times 10^3$	—	—	—	—	—	—
ES5	$(10.0\pm 1.0)\times 10^1$	$(7.2\pm 0.7)\times 10^1$	$(7.0\pm 1.0)\times 10^2$	$(1.1\pm 0.2)\times 10^3$	$(2.4\pm 0.4)\times 10^3$	$(2.5\pm 0.4)\times 10^3$	—	—	—	—	—	—
ES6	$(5.7\pm 0.6)\times 10^1$	$(5.1\pm 0.5)\times 10^1$	$(6.0\pm 0.9)\times 10^2$	$(8.0\pm 1.0)\times 10^2$	$(1.1\pm 0.2)\times 10^3$	$(9.0\pm 1.0)\times 10^2$	—	—	—	—	—	—
ES7	$(2.1\pm 0.2)\times 10^2$	$(1.9\pm 0.2)\times 10^2$	$(2.2\pm 0.3)\times 10^3$	$(4.0\pm 0.6)\times 10^3$	$(5.1\pm 0.8)\times 10^3$	$(4.7\pm 0.7)\times 10^3$	—	—	—	—	—	—
ES8	$(6.2\pm 0.6)\times 10^1$	$(5.8\pm 0.6)\times 10^1$	$(9.0\pm 1.0)\times 10^2$	$(1.2\pm 0.2)\times 10^3$	$(1.2\pm 0.2)\times 10^3$	$(1.2\pm 0.2)\times 10^3$	—	—	—	—	—	—
ES9	$(6.8\pm 0.7)\times 10^1$	$(5.0\pm 0.5)\times 10^1$	$(4.2\pm 0.6)\times 10^2$	$(7.0\pm 1.0)\times 10^2$	$(1.8\pm 0.3)\times 10^3$	$(1.5\pm 0.2)\times 10^3$	—	—	—	—	—	—
ES10	$(2.2\pm 0.2)\times 10^2$	$(1.7\pm 0.2)\times 10^2$	$(3.0\pm 0.4)\times 10^3$	$(4.1\pm 0.6)\times 10^3$	$(5.6\pm 0.8)\times 10^3$	$(5.3\pm 0.8)\times 10^3$	—	—	—	—	—	—
ES11	$(2.9\pm 0.3)\times 10^1$	$(2.1\pm 0.2)\times 10^1$	$(4.0\pm 0.6)\times 10^2$	$(5.5\pm 0.8)\times 10^2$	$(6.0\pm 1.0)\times 10^2$	$(8.0\pm 1.0)\times 10^2$	—	—	—	—	—	sc
ES12	$(1.3\pm 0.1)\times 10^3$	$(1.1\pm 0.1)\times 10^3$	$(1.1\pm 0.2)\times 10^4$	$(1.9\pm 0.3)\times 10^4$	$(3.9\pm 0.6)\times 10^4$	$(4.0\pm 0.6)\times 10^4$	—	—	—	—	—	—
ES13	$(6.3\pm 0.6)\times 10^1$	$(4.9\pm 0.5)\times 10^1$	$(10.0\pm 2.0)\times 10^2$	$(1.9\pm 0.3)\times 10^3$	$(3.4\pm 0.5)\times 10^3$	$(3.1\pm 0.5)\times 10^3$	—	—	—	—	—	—
ES14	$(10.0\pm 1.0)\times 10^1$	$(1.4\pm 0.1)\times 10^2$	$(4.3\pm 0.6)\times 10^3$	$(5.1\pm 0.8)\times 10^3$	$(8.0\pm 1.0)\times 10^3$	$(5.7\pm 0.8)\times 10^3$	—	—	—	—	—	—
ES15	$(2.0\pm 0.2)\times 10^2$	$(2.2\pm 0.2)\times 10^2$	$(4.6\pm 0.7)\times 10^3$	$(5.5\pm 0.8)\times 10^3$	$(8.0\pm 1.0)\times 10^3$	$(7.0\pm 1.0)\times 10^3$	—	—	—	—	—	—
ES16	$(4.4\pm 0.4)\times 10^3$	$(8.9\pm 0.9)\times 10^3$	$(1.3\pm 0.2)\times 10^5$	$(1.1\pm 0.2)\times 10^5$	$(10.0\pm 1.0)\times 10^4$	$(9.0\pm 1.0)\times 10^4$	—	—	—	—	—	—
E1	$(4.1\pm 0.4)\times 10^1$	$(2.7\pm 0.3)\times 10^1$	$(1.8\pm 0.3)\times 10^2$	$(3.1\pm 0.5)\times 10^2$	$(8.0\pm 1.0)\times 10^2$	$(9.0\pm 1.0)\times 10^2$	—	—	—	—	—	—
E2	$(6.9\pm 0.7)\times 10^1$	$(5.4\pm 0.5)\times 10^1$	$(1.4\pm 0.2)\times 10^3$	$(1.1\pm 0.2)\times 10^3$	$(8.0\pm 1.0)\times 10^2$	$(8.0\pm 1.0)\times 10^2$	—	—	—	—	—	—
E3	$(1.8\pm 0.2)\times 10^2$	$(2.2\pm 0.2)\times 10^2$	$(2.1\pm 0.3)\times 10^3$	$(2.9\pm 0.4)\times 10^3$	$(7.0\pm 1.0)\times 10^3$	$(6.6\pm 1.0)\times 10^3$	$(3.0\pm 0.3)\times 10^3$	$(8.4\pm 0.8)\times 10^3$	$(4.8\pm 0.5)\times 10^3$	$(2.3\pm 0.2)\times 10^3$	$(9.7\pm 1.0)\times 10^2$	—
E4	$(1.3\pm 0.1)\times 10^1$	$(2.0\pm 0.2)\times 10^1$	$(3.2\pm 0.5)\times 10^2$	$(4.0\pm 0.6)\times 10^2$	$(4.6\pm 0.7)\times 10^2$	$(4.8\pm 0.7)\times 10^2$	$(4.4\pm 0.4)\times 10^2$	$(6.3\pm 0.6)\times 10^2$	$(2.9\pm 0.3)\times 10^2$	$(1.3\pm 0.1)\times 10^2$	$(5.1\pm 0.5)\times 10^1$	—
E5	$(1.6\pm 0.2)\times 10^2$	$(3.3\pm 0.3)\times 10^2$	$(5.9\pm 0.9)\times 10^3$	$(6.5\pm 1.0)\times 10^3$	$(6.4\pm 1.0)\times 10^3$	$(5.3\pm 0.8)\times 10^3$	—	—	—	—	—	—
E6	$(7.3\pm 0.7)\times 10^0$	$(6.1\pm 0.6)\times 10^0$	$(5.0\pm 0.8)\times 10^1$	$(8.0\pm 1.0)\times 10^1$	$(1.4\pm 0.2)\times 10^2$	$(1.5\pm 0.2)\times 10^2$	$(7.1\pm 0.7)\times 10^1$	$(2.2\pm 0.2)\times 10^2$	$(1.2\pm 0.1)\times 10^2$	$(4.6\pm 0.5)\times 10^1$	$(1.7\pm 0.2)\times 10^1$	—
E7	$(1.3\pm 0.1)\times 10^2$	$(2.0\pm 0.2)\times 10^2$	$(2.2\pm 0.3)\times 10^3$	$(3.0\pm 0.5)\times 10^3$	$(3.7\pm 0.6)\times 10^3$	$(3.5\pm 0.5)\times 10^3$	$(3.0\pm 0.3)\times 10^3$	$(4.7\pm 0.5)\times 10^3$	$(2.1\pm 0.2)\times 10^3$	$(9.2\pm 0.9)\times 10^2$	$(3.4\pm 0.3)\times 10^2$	—
E8	$(9.2\pm 0.9)\times 10^1$	$(1.1\pm 0.1)\times 10^2$	$(2.1\pm 0.3)\times 10^3$	$(2.4\pm 0.4)\times 10^3$	$(2.8\pm 0.4)\times 10^3$	$(2.5\pm 0.4)\times 10^3$	—	—	—	—	—	—
E9	$(2.0\pm 0.2)\times 10^2$	$(9.4\pm 0.9)\times 10^2$	$(1.7\pm 0.3)\times 10^4$	$(1.7\pm 0.2)\times 10^4$	$(1.3\pm 0.2)\times 10^4$	$(1.2\pm 0.2)\times 10^4$	$(1.6\pm 0.2)\times 10^4$	$(1.1\pm 0.1)\times 10^4$	$(5.5\pm 0.6)\times 10^3$	$(2.8\pm 0.3)\times 10^3$	$(1.1\pm 0.1)\times 10^3$	—
E10	$(4.7\pm 0.5)\times 10^1$	$(4.9\pm 0.5)\times 10^1$	$(4.8\pm 0.7)\times 10^2$	$(7.0\pm 1.0)\times 10^2$	$(1.2\pm 0.2)\times 10^3$	$(1.2\pm 0.2)\times 10^3$	—	—	—	—	—	sc
E11	$(9.7\pm 1.0)\times 10^2$	$(1.2\pm 0.1)\times 10^3$	$(2.3\pm 0.3)\times 10^4$	$(2.8\pm 0.4)\times 10^4$	$(2.7\pm 0.4)\times 10^4$	$(2.4\pm 0.4)\times 10^4$	—	—	—	—	—	—
E12	$(9.4\pm 0.9)\times 10^0$	$(9.7\pm 1.0)\times 10^1$	$(8.0\pm 1.0)\times 10^2$	$(9.0\pm 1.0)\times 10^2$	$(6.5\pm 1.0)\times 10^2$	$(5.5\pm 0.8)\times 10^2$	—	—	—	—	—	—
E13	$(6.3\pm 0.6)\times 10^2$	$(1.1\pm 0.1)\times 10^3$	$(2.1\pm 0.3)\times 10^4$	$(2.5\pm 0.4)\times 10^4$	$(2.2\pm 0.3)\times 10^4$	$(1.9\pm 0.3)\times 10^4$	—	—	—	—	—	—
E14	$(6.9\pm 0.7)\times 10^2$	$(10.0\pm 1.0)\times 10^2$	$(2.0\pm 0.3)\times 10^4$	$(2.8\pm 0.4)\times 10^4$	$(2.8\pm 0.4)\times 10^4$	$(2.6\pm 0.4)\times 10^4$	$(2.1\pm 0.2)\times 10^4$	$(3.1\pm 0.3)\times 10^4$	$(1.4\pm 0.1)\times 10^4$	$(5.9\pm 0.6)\times 10^3$	$(2.2\pm 0.2)\times 10^3$	—
E15	$(4.8\pm 0.5)\times 10^2$	$(9.1\pm 0.9)\times 10^2$	$(2.0\pm 0.3)\times 10^4$	$(2.3\pm 0.4)\times 10^4$	$(1.9\pm 0.3)\times 10^4$	$(1.8\pm 0.3)\times 10^4$	$(1.9\pm 0.2)\times 10^4$	$(2.2\pm 0.2)\times 10^4$	$(8.4\pm 0.8)\times 10^3$	$(3.6\pm 0.4)\times 10^3$	$(1.4\pm 0.1)\times 10^3$	—
E16	$(2.7\pm 0.3)\times 10^2$	$(2.3\pm 0.2)\times 10^2$	$(3.9\pm 0.6)\times 10^3$	$(5.8\pm 0.9)\times 10^3$	$(8.0\pm 1.0)\times 10^3$	$(7.0\pm 1.0)\times 10^3$	$(4.7\pm 0.5)\times 10^3$	$(8.0\pm 0.8)\times 10^3$	$(3.3\pm 0.3)\times 10^3$	$(1.3\pm 0.1)\times 10^3$	$(4.6\pm 0.5)\times 10^2$	—
E17	$(2.2\pm 0.2)\times 10^1$	$(3.9\pm 0.4)\times 10^1$	$(3.0\pm 0.5)\times 10^2$	$(3.4\pm 0.5)\times 10^2$	$(2.1\pm 0.3)\times 10^2$	$(1.4\pm 0.2)\times 10^2$	$(4.5\pm 0.5)\times 10^2$	$(4.3\pm 0.4)\times 10^2$	$(1.5\pm 0.2)\times 10^2$	$(5.2\pm 0.6)\times 10^1$	$(1.8\pm 0.2)\times 10^1$	—
E18	$(3.1\pm 0.3)\times 10^1$	$(6.2\pm 0.6)\times 10^1$	$(9.0\pm 1.0)\times 10^2$	$(1.3\pm 0.2)\times 10^3$	$(1.1\pm 0.2)\times 10^3$	$(10.0\pm 2.0)\times 10^2$	—	—	—	—	—	sc
E19	$(9.1\pm 0.9)\times 10^1$	$(1.1\pm 0.1)\times 10^2$	$(2.1\pm 0.3)\times 10^3$	$(2.8\pm 0.4)\times 10^3$	$(3.0\pm 0.4)\times 10^3$	$(2.8\pm 0.4)\times 10^3$	—	—	—	—	—	—
E20	$(3.2\pm 0.3)\times 10^2$	$(7.4\pm 0.7)\times 10^2$	$(1.1\pm 0.2)\times 10^4$	$(1.2\pm 0.2)\times 10^4$	$(7.0\pm 1.0)\times 10^3$	$(5.8\pm 0.9)\times 10^3$	—	—	—	—	—	—
E21	$(2.4\pm 0.2)\times 10^2$	$(7.0\pm 0.7)\times 10^2$	$(8.0\pm 1.0)\times 10^3$	$(9.0\pm 1.0)\times 10^3$	$(8.0\pm 1.0)\times 10^3$	$(7.0\pm 1.0)\times 10^3$	$(9.2\pm 0.9)\times 10^3$	$(8.5\pm 0.9)\times 10^3$	$(2.9\pm 0.3)\times 10^3$	$(1.1\pm 0.1)\times 10^3$	$(4.1\pm 0.4)\times 10^2$	—
E22	$(10.0\pm 1.0)\times 10^0$	$(8.7\pm 0.9)\times 10^0$	$(1.6\pm 0.2)\times 10^2$	$(2.5\pm 0.4)\times 10^2$	$(4.1\pm 0.6)\times 10^2$	$(4.0\pm 0.6)\times 10^2$	$(1.6\pm 0.2)\times 10^2$	$(4.3\pm 0.4)\times 10^2$	$(2.4\pm 0.2)\times 10^2$	$(1.2\pm 0.1)\times 10^2$	$(4.7\pm 0.5)\times 10^1$	—

ble 3. (Continued)

Name	Flux 9 μm [Jy] (AKARI IRC)	Flux 18 μm [Jy] (AKARI IRC)	Flux 65 μm [Jy] (AKARI FIS)	Flux 90 μm [Jy] (AKARI FIS)	Flux 140 μm [Jy] (AKARI FIS)	Flux 160 μm [Jy] (AKARI FIS)	Flux 70 μm [Jy] (Herschel PACS)	Flux 160 μm [Jy] (Herschel PACS)	Flux 250 μm [Jy] (Herschel SPIRE)	Flux 350 μm [Jy] (Herschel SPIRE)	Flux 500 μm [Jy] (Herschel SPIRE)	Notes†
E23	$(3.5\pm 0.3)\times 10^{-1}$	$(2.6\pm 0.3)\times 10^{-1}$	$(4.3\pm 0.7)\times 10^{-2}$	$(7.0\pm 1.0)\times 10^{-2}$	$(1.1\pm 0.2)\times 10^{-3}$	$(10.0\pm 2.0)\times 10^{-2}$	$(6.2\pm 0.6)\times 10^{-2}$	$(1.3\pm 0.1)\times 10^{-3}$	$(6.3\pm 0.6)\times 10^{-2}$	$(2.8\pm 0.3)\times 10^{-2}$	$(10.0\pm 1.0)\times 10^{-1}$	—
E24	$(2.1\pm 0.2)\times 10^{-2}$	$(6.5\pm 0.7)\times 10^{-2}$	$(6.3\pm 0.9)\times 10^{-3}$	$(9.0\pm 1.0)\times 10^{-3}$	$(10.0\pm 1.0)\times 10^{-3}$	$(9.0\pm 1.0)\times 10^{-3}$	—	—	—	—	—	—
E25	$(4.1\pm 0.4)\times 10^{-2}$	$(8.9\pm 0.9)\times 10^{-2}$	$(9.0\pm 1.0)\times 10^{-3}$	$(1.3\pm 0.2)\times 10^{-3}$	$(1.8\pm 0.3)\times 10^{-4}$	$(1.6\pm 0.2)\times 10^{-4}$	—	—	—	—	—	—
E26	$(3.3\pm 0.3)\times 10^{-1}$	$(3.2\pm 0.3)\times 10^{-1}$	$(2.5\pm 0.4)\times 10^{-2}$	$(3.4\pm 0.5)\times 10^{-2}$	$(8.0\pm 1.0)\times 10^{-2}$	$(8.0\pm 1.0)\times 10^{-2}$	—	—	—	—	—	—
E27	$(1.3\pm 0.1)\times 10^{-1}$	$(2.3\pm 0.2)\times 10^{-1}$	$(3.4\pm 0.5)\times 10^{-2}$	$(3.6\pm 0.5)\times 10^{-2}$	$(4.7\pm 0.7)\times 10^{-2}$	$(5.0\pm 0.8)\times 10^{-2}$	$(3.5\pm 0.3)\times 10^{-2}$	$(5.3\pm 0.5)\times 10^{-2}$	$(2.5\pm 0.2)\times 10^{-2}$	$(1.1\pm 0.1)\times 10^{-2}$	$(4.3\pm 0.4)\times 10^{-1}$	—
E28	$(1.3\pm 0.1)\times 10^{-1}$	$(1.8\pm 0.2)\times 10^{-1}$	$(5.2\pm 0.8)\times 10^{-2}$	$(6.6\pm 1.0)\times 10^{-2}$	$(7.0\pm 1.0)\times 10^{-2}$	$(8.0\pm 1.0)\times 10^{-2}$	—	—	—	—	—	—
E29	$(3.5\pm 0.4)\times 10^{-1}$	$(7.7\pm 0.8)\times 10^{-1}$	$(1.3\pm 0.2)\times 10^{-3}$	$(1.5\pm 0.2)\times 10^{-3}$	$(1.4\pm 0.2)\times 10^{-3}$	$(1.1\pm 0.2)\times 10^{-3}$	—	—	—	—	—	—
E30	$(7.0\pm 0.7)\times 10^{-1}$	$(8.1\pm 0.8)\times 10^{-1}$	$(8.0\pm 1.0)\times 10^{-2}$	$(1.4\pm 0.2)\times 10^{-3}$	$(2.6\pm 0.4)\times 10^{-3}$	$(2.6\pm 0.4)\times 10^{-3}$	$(1.4\pm 0.1)\times 10^{-3}$	$(3.5\pm 0.3)\times 10^{-3}$	$(2.0\pm 0.2)\times 10^{-3}$	$(9.9\pm 1.0)\times 10^{-2}$	$(4.1\pm 0.4)\times 10^{-2}$	—
E31	$(2.1\pm 0.2)\times 10^{-1}$	$(2.6\pm 0.3)\times 10^{-1}$	$(3.7\pm 0.6)\times 10^{-2}$	$(3.8\pm 0.6)\times 10^{-2}$	$(5.3\pm 0.8)\times 10^{-2}$	$(6.1\pm 0.9)\times 10^{-2}$	$(4.9\pm 0.5)\times 10^{-2}$	$(6.8\pm 0.7)\times 10^{-2}$	$(2.9\pm 0.3)\times 10^{-2}$	$(1.2\pm 0.1)\times 10^{-2}$	$(4.2\pm 0.4)\times 10^{-1}$	—
E32	$(4.1\pm 0.4)\times 10^{-1}$	$(5.5\pm 0.5)\times 10^{-1}$	$(7.0\pm 1.0)\times 10^{-2}$	$(9.0\pm 1.0)\times 10^{-2}$	$(1.8\pm 0.3)\times 10^{-3}$	$(1.9\pm 0.3)\times 10^{-3}$	—	—	—	—	—	—
E33	$(1.6\pm 0.2)\times 10^{-1}$	$(1.8\pm 0.2)\times 10^{-1}$	$(1.5\pm 0.2)\times 10^{-2}$	$(2.1\pm 0.3)\times 10^{-2}$	$(3.7\pm 0.6)\times 10^{-2}$	$(3.8\pm 0.6)\times 10^{-2}$	—	—	—	—	—	—
E34	$(1.7\pm 0.2)\times 10^{-1}$	$(2.1\pm 0.2)\times 10^{-1}$	$(2.8\pm 0.4)\times 10^{-2}$	$(3.9\pm 0.6)\times 10^{-2}$	$(7.0\pm 1.0)\times 10^{-2}$	$(8.0\pm 1.0)\times 10^{-2}$	—	—	—	—	—	—
E35	$(3.7\pm 0.4)\times 10^{-2}$	$(6.3\pm 0.6)\times 10^{-2}$	$(9.0\pm 1.0)\times 10^{-3}$	$(10.0\pm 2.0)\times 10^{-3}$	$(1.5\pm 0.2)\times 10^{-4}$	$(1.4\pm 0.2)\times 10^{-4}$	—	—	—	—	—	—
E36	$(2.7\pm 0.3)\times 10^{-1}$	$(2.0\pm 0.2)\times 10^{-1}$	$(5.1\pm 0.8)\times 10^{-2}$	$(5.2\pm 0.8)\times 10^{-2}$	$(6.2\pm 1.0)\times 10^{-2}$	$(5.8\pm 0.9)\times 10^{-2}$	—	—	—	—	—	—
E37	$(2.0\pm 0.2)\times 10^{-1}$	$(3.1\pm 0.3)\times 10^{-1}$	$(5.0\pm 0.7)\times 10^{-2}$	$(5.4\pm 0.8)\times 10^{-2}$	$(9.0\pm 1.0)\times 10^{-2}$	$(9.0\pm 1.0)\times 10^{-2}$	—	—	—	—	—	sc
E38	$(3.3\pm 0.3)\times 10^{-2}$	$(2.6\pm 0.3)\times 10^{-2}$	$(2.1\pm 0.3)\times 10^{-3}$	$(3.4\pm 0.5)\times 10^{-3}$	$(8.0\pm 1.0)\times 10^{-3}$	$(8.0\pm 1.0)\times 10^{-3}$	—	—	—	—	—	—
E39	$(8.2\pm 0.8)\times 10^0$	$(7.9\pm 0.8)\times 10^0$	$(1.3\pm 0.2)\times 10^{-2}$	$(1.7\pm 0.3)\times 10^{-2}$	$(2.7\pm 0.4)\times 10^{-2}$	$(2.2\pm 0.3)\times 10^{-2}$	$(2.1\pm 0.2)\times 10^{-2}$	$(3.8\pm 0.4)\times 10^{-2}$	$(1.7\pm 0.2)\times 10^{-2}$	$(7.0\pm 0.7)\times 10^{-1}$	$(2.4\pm 0.3)\times 10^{-1}$	—
E40	$(6.0\pm 0.6)\times 10^0$	$(9.1\pm 0.9)\times 10^0$	$(9.0\pm 1.0)\times 10^{-1}$	$(1.1\pm 0.2)\times 10^{-2}$	$(1.6\pm 0.2)\times 10^{-2}$	$(1.7\pm 0.3)\times 10^{-2}$	—	—	—	—	—	sc
E41	$(7.7\pm 0.8)\times 10^{-1}$	$(7.5\pm 0.7)\times 10^{-1}$	$(1.3\pm 0.2)\times 10^{-3}$	$(1.4\pm 0.2)\times 10^{-3}$	$(1.9\pm 0.3)\times 10^{-3}$	$(2.1\pm 0.3)\times 10^{-3}$	—	—	—	—	—	—
E42	$(2.3\pm 0.2)\times 10^{-1}$	$(1.9\pm 0.2)\times 10^{-1}$	$(2.1\pm 0.3)\times 10^{-2}$	$(2.6\pm 0.4)\times 10^{-2}$	$(5.2\pm 0.8)\times 10^{-2}$	$(5.1\pm 0.8)\times 10^{-2}$	—	—	—	—	—	—
E43	$(1.1\pm 0.1)\times 10^{-1}$	$(1.2\pm 0.1)\times 10^{-2}$	$(1.3\pm 0.2)\times 10^{-2}$	$(1.1\pm 0.2)\times 10^{-2}$	$(8.0\pm 1.0)\times 10^{-1}$	$(8.0\pm 1.0)\times 10^{-1}$	—	—	—	—	—	—
E44	$(1.2\pm 0.1)\times 10^{-1}$	$(9.5\pm 1.0)\times 10^0$	$(7.0\pm 1.0)\times 10^{-1}$	$(1.2\pm 0.2)\times 10^{-2}$	$(2.8\pm 0.4)\times 10^{-2}$	$(3.3\pm 0.5)\times 10^{-2}$	—	—	—	—	—	—
E45	$(5.1\pm 0.5)\times 10^{-1}$	$(3.4\pm 0.3)\times 10^{-1}$	$(2.8\pm 0.4)\times 10^{-2}$	$(4.1\pm 0.6)\times 10^{-2}$	$(1.1\pm 0.2)\times 10^{-3}$	$(1.1\pm 0.2)\times 10^{-3}$	—	—	—	—	—	sc
E46	$(3.6\pm 0.4)\times 10^{-1}$	$(4.0\pm 0.4)\times 10^{-1}$	$(1.5\pm 0.2)\times 10^{-3}$	$(1.3\pm 0.2)\times 10^{-3}$	$(10.0\pm 1.0)\times 10^{-2}$	$(8.0\pm 1.0)\times 10^{-2}$	—	—	—	—	—	—
E47	$(8.4\pm 0.8)\times 10^{-1}$	$(8.2\pm 0.8)\times 10^{-1}$	$(7.0\pm 1.0)\times 10^{-2}$	$(10.0\pm 1.0)\times 10^{-2}$	$(2.2\pm 0.3)\times 10^{-3}$	$(2.3\pm 0.3)\times 10^{-3}$	$(8.9\pm 0.9)\times 10^{-2}$	$(2.6\pm 0.3)\times 10^{-3}$	$(1.4\pm 0.1)\times 10^{-3}$	$(6.8\pm 0.7)\times 10^{-2}$	$(2.8\pm 0.3)\times 10^{-2}$	—
E48	$(6.4\pm 0.6)\times 10^{-1}$	$(5.8\pm 0.6)\times 10^{-1}$	$(5.8\pm 0.9)\times 10^{-2}$	$(8.0\pm 1.0)\times 10^{-2}$	$(1.6\pm 0.2)\times 10^{-3}$	$(1.6\pm 0.2)\times 10^{-3}$	—	—	—	—	—	—
E49	$(2.3\pm 0.2)\times 10^{-1}$	$(3.7\pm 0.4)\times 10^{-1}$	$(7.0\pm 1.0)\times 10^{-2}$	$(6.4\pm 1.0)\times 10^{-2}$	$(5.1\pm 0.8)\times 10^{-2}$	$(4.6\pm 0.7)\times 10^{-2}$	—	—	—	—	—	sc
E50	$(8.2\pm 0.8)\times 10^0$	$(9.2\pm 0.9)\times 10^0$	$(1.8\pm 0.3)\times 10^{-2}$	$(2.4\pm 0.4)\times 10^{-2}$	$(3.8\pm 0.6)\times 10^{-2}$	$(3.6\pm 0.5)\times 10^{-2}$	—	—	—	—	—	—
E51	$(2.3\pm 0.2)\times 10^{-2}$	$(2.6\pm 0.3)\times 10^{-2}$	$(2.0\pm 0.3)\times 10^{-3}$	$(2.6\pm 0.4)\times 10^{-3}$	$(5.7\pm 0.9)\times 10^{-3}$	$(6.0\pm 0.9)\times 10^{-3}$	—	—	—	—	—	—
E52	$(1.3\pm 0.1)\times 10^{-1}$	$(10.0\pm 1.0)\times 10^0$	$(7.0\pm 1.0)\times 10^{-1}$	$(1.2\pm 0.2)\times 10^{-2}$	$(2.4\pm 0.4)\times 10^{-2}$	$(2.5\pm 0.4)\times 10^{-2}$	—	—	—	—	—	—
E53	$(1.9\pm 0.2)\times 10^{-1}$	$(1.3\pm 0.1)\times 10^{-1}$	$(1.9\pm 0.3)\times 10^{-2}$	$(2.6\pm 0.4)\times 10^{-2}$	$(3.9\pm 0.6)\times 10^{-2}$	$(3.9\pm 0.6)\times 10^{-2}$	—	—	—	—	—	—
E54	$(3.9\pm 0.4)\times 10^{-2}$	$(3.5\pm 0.3)\times 10^{-2}$	$(1.3\pm 0.2)\times 10^{-4}$	$(10.0\pm 2.0)\times 10^{-3}$	$(10.0\pm 1.0)\times 10^{-3}$	$(9.0\pm 1.0)\times 10^{-3}$	—	—	—	—	—	—
E55	$(9.6\pm 1.0)\times 10^{-1}$	$(9.4\pm 0.9)\times 10^{-1}$	$(1.2\pm 0.2)\times 10^{-3}$	$(1.5\pm 0.2)\times 10^{-3}$	$(2.9\pm 0.4)\times 10^{-3}$	$(3.3\pm 0.5)\times 10^{-3}$	$(1.6\pm 0.2)\times 10^{-3}$	$(3.5\pm 0.3)\times 10^{-3}$	$(1.8\pm 0.2)\times 10^{-3}$	$(8.9\pm 0.9)\times 10^{-2}$	$(3.6\pm 0.4)\times 10^{-2}$	—
E56	$(8.0\pm 0.8)\times 10^{-1}$	$(7.0\pm 0.8)\times 10^{-1}$	$(2.2\pm 0.3)\times 10^{-3}$	$(3.0\pm 0.5)\times 10^{-3}$	$(4.1\pm 0.6)\times 10^{-3}$	$(4.3\pm 0.6)\times 10^{-3}$	$(2.0\pm 0.2)\times 10^{-3}$	$(3.9\pm 0.4)\times 10^{-3}$	$(2.0\pm 0.2)\times 10^{-3}$	$(10.0\pm 1.0)\times 10^{-2}$	$(3.9\pm 0.4)\times 10^{-2}$	—
E57	$(7.4\pm 0.7)\times 10^0$	$(7.5\pm 0.8)\times 10^0$	$(1.4\pm 0.2)\times 10^{-2}$	$(1.7\pm 0.3)\times 10^{-2}$	$(2.7\pm 0.4)\times 10^{-2}$	$(2.3\pm 0.4)\times 10^{-2}$	—	—	—	—	—	—
E58	$(1.3\pm 0.1)\times 10^{-2}$	$(1.6\pm 0.2)\times 10^{-2}$	$(2.6\pm 0.4)\times 10^{-3}$	$(2.8\pm 0.4)\times 10^{-3}$	$(4.5\pm 0.7)\times 10^{-3}$	$(4.7\pm 0.7)\times 10^{-3}$	$(2.6\pm 0.3)\times 10^{-3}$	$(4.8\pm 0.5)\times 10^{-3}$	$(2.4\pm 0.2)\times 10^{-3}$	$(1.1\pm 0.1)\times 10^{-3}$	$(4.3\pm 0.4)\times 10^{-2}$	—
E59	$(5.4\pm 0.5)\times 10^{-1}$	$(5.6\pm 0.6)\times 10^{-1}$	$(3.1\pm 0.5)\times 10^{-3}$	$(2.0\pm 0.3)\times 10^{-3}$	$(1.9\pm 0.3)\times 10^{-3}$	$(1.9\pm 0.3)\times 10^{-3}$	$(1.5\pm 0.1)\times 10^{-3}$	$(1.4\pm 0.1)\times 10^{-3}$	$(5.4\pm 0.5)\times 10^{-2}$	$(2.1\pm 0.2)\times 10^{-2}$	$(8.3\pm 0.8)\times 10^{-1}$	—
E60	$(1.2\pm 0.1)\times 10^{-2}$	$(1.1\pm 0.1)\times 10^{-2}$	$(9.0\pm 1.0)\times 10^{-2}$	$(1.5\pm 0.2)\times 10^{-3}$	$(3.9\pm 0.6)\times 10^{-3}$	$(4.2\pm 0.6)\times 10^{-3}$	—	—	—	—	—	—
E61	$(1.4\pm 0.1)\times 10^{-2}$	$(1.3\pm 0.1)\times 10^{-2}$	$(10.0\pm 2.0)\times 10^{-2}$	$(1.7\pm 0.3)\times 10^{-3}$	$(4.3\pm 0.6)\times 10^{-3}$	$(4.6\pm 0.7)\times 10^{-3}$	—	—	—	—	—	—
E62	$(7.5\pm 0.8)\times 10^{-1}$	$(7.3\pm 0.7)\times 10^{-1}$	$(1.1\pm 0.2)\times 10^{-3}$	$(1.4\pm 0.2)\times 10^{-3}$	$(2.2\pm 0.3)\times 10^{-3}$	$(2.0\pm 0.3)\times 10^{-3}$	—	—	—	—	—	—

ble 3. (Continued)

Name	Flux 9 μm [Jy] (AKARI IRC)	Flux 18 μm [Jy] (AKARI IRC)	Flux 65 μm [Jy] (AKARI FIS)	Flux 90 μm [Jy] (AKARI FIS)	Flux 140 μm [Jy] (AKARI FIS)	Flux 160 μm [Jy] (AKARI FIS)	Flux 70 μm [Jy] (Herschel PACS)	Flux 160 μm [Jy] (Herschel PACS)	Flux 250 μm [Jy] (Herschel SPIRE)	Flux 350 μm [Jy] (Herschel SPIRE)	Flux 500 μm [Jy] (Herschel SPIRE)	Notes†
E63	$(2.7\pm 0.3)\times 10^2$	$(2.8\pm 0.3)\times 10^2$	$(2.3\pm 0.3)\times 10^3$	$(3.3\pm 0.5)\times 10^3$	$(8.0\pm 1.0)\times 10^3$	$(8.0\pm 1.0)\times 10^3$	—	—	—	—	—	—
E64	$(1.2\pm 0.1)\times 10^1$	$(1.5\pm 0.1)\times 10^1$	$(1.6\pm 0.2)\times 10^2$	$(1.8\pm 0.3)\times 10^2$	$(3.2\pm 0.5)\times 10^2$	$(2.8\pm 0.4)\times 10^2$	—	—	—	—	—	—
E65	$(2.2\pm 0.2)\times 10^1$	$(4.6\pm 0.5)\times 10^1$	$(8.0\pm 1.0)\times 10^2$	$(7.0\pm 1.0)\times 10^2$	$(6.4\pm 1.0)\times 10^2$	$(6.6\pm 1.0)\times 10^2$	—	—	—	—	—	—
E66	$(3.9\pm 0.4)\times 10^1$	$(5.2\pm 0.5)\times 10^1$	$(4.6\pm 0.7)\times 10^2$	$(5.8\pm 0.9)\times 10^2$	$(1.1\pm 0.2)\times 10^3$	$(9.0\pm 1.0)\times 10^2$	—	—	—	—	—	—
E67	$(1.7\pm 0.2)\times 10^1$	$(1.5\pm 0.1)\times 10^1$	$(2.9\pm 0.4)\times 10^2$	$(2.9\pm 0.4)\times 10^2$	$(3.5\pm 0.5)\times 10^2$	$(3.3\pm 0.5)\times 10^2$	—	—	—	—	—	—
E68	$(8.1\pm 0.8)\times 10^2$	$(9.5\pm 0.9)\times 10^2$	$(1.6\pm 0.2)\times 10^4$	$(1.6\pm 0.2)\times 10^4$	$(2.7\pm 0.4)\times 10^4$	$(2.8\pm 0.4)\times 10^4$	—	—	—	—	—	—
E69	$(2.1\pm 0.2)\times 10^2$	$(2.6\pm 0.3)\times 10^2$	$(6.0\pm 0.9)\times 10^3$	$(4.8\pm 0.7)\times 10^3$	$(5.5\pm 0.8)\times 10^3$	$(5.6\pm 0.8)\times 10^3$	—	—	—	—	—	—
E70	$(2.7\pm 0.3)\times 10^1$	$(3.7\pm 0.4)\times 10^1$	$(1.7\pm 0.3)\times 10^2$	$(2.9\pm 0.4)\times 10^2$	$(8.0\pm 1.0)\times 10^2$	$(8.0\pm 1.0)\times 10^2$	$(3.0\pm 0.3)\times 10^2$	$(7.7\pm 0.8)\times 10^2$	$(4.4\pm 0.4)\times 10^2$	$(2.1\pm 0.2)\times 10^2$	$(8.5\pm 0.9)\times 10^1$	—
E71	$(3.5\pm 0.3)\times 10^1$	$(3.1\pm 0.3)\times 10^1$	$(8.0\pm 1.0)\times 10^2$	$(9.0\pm 1.0)\times 10^2$	$(10.0\pm 1.0)\times 10^2$	$(1.1\pm 0.2)\times 10^3$	—	—	—	—	—	—
E72	$(1.2\pm 0.1)\times 10^2$	$(1.1\pm 0.1)\times 10^2$	$(1.7\pm 0.2)\times 10^3$	$(2.0\pm 0.3)\times 10^3$	$(3.3\pm 0.5)\times 10^3$	$(3.6\pm 0.5)\times 10^3$	$(2.0\pm 0.2)\times 10^3$	$(3.9\pm 0.4)\times 10^3$	$(2.0\pm 0.2)\times 10^3$	$(9.0\pm 0.9)\times 10^2$	$(3.6\pm 0.4)\times 10^2$	—
E73	$(4.2\pm 0.4)\times 10^1$	$(3.8\pm 0.4)\times 10^1$	$(4.7\pm 0.7)\times 10^2$	$(5.4\pm 0.8)\times 10^2$	$(8.0\pm 1.0)\times 10^2$	$(8.0\pm 1.0)\times 10^2$	$(7.1\pm 0.7)\times 10^2$	$(1.4\pm 0.1)\times 10^3$	$(6.9\pm 0.7)\times 10^2$	$(3.1\pm 0.3)\times 10^2$	$(1.2\pm 0.1)\times 10^2$	—
E74	$(1.1\pm 0.1)\times 10^2$	$(1.9\pm 0.2)\times 10^2$	$(4.0\pm 0.6)\times 10^3$	$(4.0\pm 0.6)\times 10^3$	$(5.3\pm 0.8)\times 10^3$	$(5.4\pm 0.8)\times 10^3$	—	—	—	—	—	—
E75	$(6.1\pm 0.6)\times 10^1$	$(7.1\pm 0.7)\times 10^1$	$(1.2\pm 0.2)\times 10^3$	$(1.4\pm 0.2)\times 10^3$	$(2.5\pm 0.4)\times 10^3$	$(2.5\pm 0.4)\times 10^3$	—	—	—	—	—	—
E76	$(10.0\pm 1.0)\times 10^2$	$(1.2\pm 0.1)\times 10^3$	$(1.8\pm 0.3)\times 10^4$	$(2.1\pm 0.3)\times 10^4$	$(3.6\pm 0.5)\times 10^4$	$(3.4\pm 0.5)\times 10^4$	$(1.8\pm 0.2)\times 10^4$	$(3.5\pm 0.4)\times 10^4$	$(2.1\pm 0.2)\times 10^4$	$(9.9\pm 1.0)\times 10^3$	$(4.0\pm 0.4)\times 10^3$	—
E77	$(2.6\pm 0.3)\times 10^1$	$(3.0\pm 0.3)\times 10^1$	$(3.4\pm 0.5)\times 10^2$	$(5.2\pm 0.8)\times 10^2$	$(8.0\pm 1.0)\times 10^2$	$(7.0\pm 1.0)\times 10^2$	$(6.0\pm 0.6)\times 10^2$	$(1.1\pm 0.1)\times 10^3$	$(4.6\pm 0.5)\times 10^2$	$(2.0\pm 0.2)\times 10^2$	$(7.2\pm 0.7)\times 10^1$	—
E78	$(1.3\pm 0.1)\times 10^2$	$(2.1\pm 0.2)\times 10^2$	$(2.3\pm 0.3)\times 10^3$	$(2.9\pm 0.4)\times 10^3$	$(5.3\pm 0.8)\times 10^3$	$(5.1\pm 0.8)\times 10^3$	—	—	—	—	—	—
E79	$(5.1\pm 0.5)\times 10^0$	$(4.5\pm 0.5)\times 10^0$	$(4.8\pm 0.7)\times 10^1$	$(7.0\pm 1.0)\times 10^1$	$(1.3\pm 0.2)\times 10^2$	$(1.2\pm 0.2)\times 10^2$	—	—	—	—	—	—
E80	$(7.2\pm 0.7)\times 10^0$	$(7.1\pm 0.7)\times 10^0$	$(1.2\pm 0.2)\times 10^2$	$(1.3\pm 0.2)\times 10^2$	$(2.1\pm 0.3)\times 10^2$	$(2.1\pm 0.3)\times 10^2$	$(1.4\pm 0.1)\times 10^2$	$(2.8\pm 0.3)\times 10^2$	$(1.2\pm 0.1)\times 10^2$	$(5.2\pm 0.5)\times 10^1$	$(1.9\pm 0.2)\times 10^1$	—
E81	$(8.9\pm 0.9)\times 10^0$	$(1.1\pm 0.1)\times 10^1$	$(1.2\pm 0.2)\times 10^2$	$(1.6\pm 0.2)\times 10^2$	$(2.7\pm 0.4)\times 10^2$	$(2.1\pm 0.3)\times 10^2$	—	—	—	—	—	—
E82	$(2.8\pm 0.3)\times 10^2$	$(3.6\pm 0.4)\times 10^2$	$(3.9\pm 0.6)\times 10^3$	$(6.0\pm 0.9)\times 10^3$	$(1.2\pm 0.2)\times 10^4$	$(1.1\pm 0.2)\times 10^4$	$(5.1\pm 0.5)\times 10^3$	$(1.3\pm 0.1)\times 10^4$	$(7.7\pm 0.8)\times 10^3$	$(3.9\pm 0.4)\times 10^3$	$(1.6\pm 0.2)\times 10^3$	—
E83	$(1.1\pm 0.1)\times 10^1$	$(1.9\pm 0.2)\times 10^1$	$(3.1\pm 0.5)\times 10^2$	$(3.2\pm 0.5)\times 10^2$	$(4.9\pm 0.7)\times 10^2$	$(5.6\pm 0.8)\times 10^2$	$(2.3\pm 0.2)\times 10^2$	$(5.2\pm 0.5)\times 10^2$	$(3.1\pm 0.3)\times 10^2$	$(1.5\pm 0.1)\times 10^2$	$(6.1\pm 0.6)\times 10^1$	—
E84	$(1.1\pm 0.1)\times 10^1$	$(1.4\pm 0.1)\times 10^1$	$(1.3\pm 0.2)\times 10^2$	$(1.7\pm 0.3)\times 10^2$	$(3.2\pm 0.5)\times 10^2$	$(3.2\pm 0.5)\times 10^2$	$(1.7\pm 0.2)\times 10^2$	$(3.7\pm 0.4)\times 10^2$	$(1.7\pm 0.2)\times 10^2$	$(7.4\pm 0.7)\times 10^1$	$(2.8\pm 0.3)\times 10^1$	—
E85	$(2.5\pm 0.3)\times 10^1$	$(2.6\pm 0.3)\times 10^1$	$(2.4\pm 0.4)\times 10^2$	$(3.7\pm 0.5)\times 10^2$	$(8.0\pm 1.0)\times 10^2$	$(7.0\pm 1.0)\times 10^2$	$(3.7\pm 0.4)\times 10^2$	$(9.2\pm 0.9)\times 10^2$	$(5.1\pm 0.5)\times 10^2$	$(2.6\pm 0.3)\times 10^2$	$(1.1\pm 0.1)\times 10^2$	—
E86	$(2.8\pm 0.3)\times 10^1$	$(3.1\pm 0.3)\times 10^1$	$(2.4\pm 0.4)\times 10^2$	$(3.6\pm 0.5)\times 10^2$	$(9.0\pm 1.0)\times 10^2$	$(10.0\pm 1.0)\times 10^2$	$(3.3\pm 0.3)\times 10^2$	$(1.2\pm 0.1)\times 10^3$	$(8.2\pm 0.8)\times 10^2$	$(4.7\pm 0.5)\times 10^2$	$(2.1\pm 0.2)\times 10^2$	—
E87	$(7.2\pm 0.7)\times 10^1$	$(5.2\pm 0.5)\times 10^1$	$(7.0\pm 1.0)\times 10^2$	$(10.0\pm 2.0)\times 10^2$	$(2.0\pm 0.3)\times 10^3$	$(2.2\pm 0.3)\times 10^3$	—	—	—	—	—	—
E88	$(4.2\pm 0.4)\times 10^1$	$(3.8\pm 0.4)\times 10^1$	$(10.0\pm 2.0)\times 10^2$	$(9.0\pm 1.0)\times 10^2$	$(9.0\pm 1.0)\times 10^2$	$(9.0\pm 1.0)\times 10^2$	—	—	—	—	—	—
E89	$(1.7\pm 0.2)\times 10^1$	$(1.7\pm 0.2)\times 10^1$	$(2.2\pm 0.3)\times 10^2$	$(2.9\pm 0.4)\times 10^2$	$(4.2\pm 0.6)\times 10^2$	$(4.7\pm 0.7)\times 10^2$	$(3.1\pm 0.3)\times 10^2$	$(6.7\pm 0.7)\times 10^2$	$(3.2\pm 0.3)\times 10^2$	$(1.4\pm 0.1)\times 10^2$	$(5.9\pm 0.6)\times 10^1$	—
E90	$(1.5\pm 0.1)\times 10^1$	$(1.8\pm 0.2)\times 10^1$	$(2.5\pm 0.4)\times 10^2$	$(3.0\pm 0.5)\times 10^2$	$(3.7\pm 0.6)\times 10^2$	$(4.4\pm 0.7)\times 10^2$	—	—	—	—	—	—
E91	$(1.1\pm 0.1)\times 10^2$	$(9.7\pm 1.0)\times 10^1$	$(1.9\pm 0.3)\times 10^3$	$(2.4\pm 0.4)\times 10^3$	$(3.5\pm 0.5)\times 10^3$	$(3.5\pm 0.5)\times 10^3$	—	—	—	—	—	—
E92	$(4.1\pm 0.4)\times 10^1$	$(4.7\pm 0.5)\times 10^1$	$(4.6\pm 0.7)\times 10^2$	$(6.6\pm 1.0)\times 10^2$	$(1.2\pm 0.2)\times 10^3$	$(1.1\pm 0.2)\times 10^3$	—	—	—	—	—	—
E93	$(6.7\pm 0.7)\times 10^1$	$(9.7\pm 1.0)\times 10^1$	$(1.2\pm 0.2)\times 10^3$	$(1.4\pm 0.2)\times 10^3$	$(2.2\pm 0.3)\times 10^3$	$(2.2\pm 0.3)\times 10^3$	—	—	—	—	—	—
E94	$(1.6\pm 0.2)\times 10^2$	$(2.3\pm 0.2)\times 10^2$	$(1.6\pm 0.2)\times 10^3$	$(2.3\pm 0.3)\times 10^3$	$(5.0\pm 0.7)\times 10^3$	$(4.7\pm 0.7)\times 10^3$	—	—	—	—	—	—
E95	$(9.8\pm 1.0)\times 10^1$	$(7.5\pm 0.8)\times 10^1$	$(10.0\pm 1.0)\times 10^2$	$(1.4\pm 0.2)\times 10^3$	$(3.1\pm 0.5)\times 10^3$	$(2.9\pm 0.4)\times 10^3$	$(1.4\pm 0.1)\times 10^3$	$(3.6\pm 0.4)\times 10^3$	$(2.2\pm 0.2)\times 10^3$	$(1.1\pm 0.1)\times 10^3$	$(4.7\pm 0.5)\times 10^2$	—
E96	$(1.6\pm 0.2)\times 10^1$	$(1.5\pm 0.2)\times 10^1$	$(5.2\pm 0.8)\times 10^2$	$(4.9\pm 0.7)\times 10^2$	$(5.7\pm 0.9)\times 10^2$	$(5.7\pm 0.9)\times 10^2$	—	—	—	—	—	—
E97	$(1.7\pm 0.2)\times 10^2$	$(2.0\pm 0.2)\times 10^2$	$(2.5\pm 0.4)\times 10^3$	$(3.5\pm 0.5)\times 10^3$	$(7.0\pm 1.0)\times 10^3$	$(6.6\pm 1.0)\times 10^3$	$(3.1\pm 0.3)\times 10^3$	$(7.3\pm 0.7)\times 10^3$	$(4.0\pm 0.4)\times 10^3$	$(1.9\pm 0.2)\times 10^3$	$(7.7\pm 0.8)\times 10^2$	—
E98	$(8.2\pm 0.8)\times 10^2$	$(8.8\pm 0.9)\times 10^2$	$(8.0\pm 1.0)\times 10^3$	$(1.2\pm 0.2)\times 10^4$	$(3.0\pm 0.4)\times 10^4$	$(2.9\pm 0.4)\times 10^4$	—	—	—	—	—	—
E99	$(2.5\pm 0.2)\times 10^1$	$(1.5\pm 0.1)\times 10^1$	$(2.0\pm 0.3)\times 10^2$	$(3.0\pm 0.5)\times 10^2$	$(4.8\pm 0.7)\times 10^2$	$(5.2\pm 0.8)\times 10^2$	—	—	—	—	—	—
E100	$(9.5\pm 1.0)\times 10^1$	$(8.2\pm 0.8)\times 10^1$	$(6.4\pm 1.0)\times 10^2$	$(1.1\pm 0.2)\times 10^3$	$(3.3\pm 0.5)\times 10^3$	$(3.5\pm 0.5)\times 10^3$	—	—	—	—	—	—
E101	$(1.1\pm 0.1)\times 10^1$	$(9.3\pm 0.9)\times 10^0$	$(5.5\pm 0.8)\times 10^1$	$(8.0\pm 1.0)\times 10^1$	$(2.1\pm 0.3)\times 10^2$	$(2.1\pm 0.3)\times 10^2$	—	—	—	—	—	—
E102	$(1.2\pm 0.1)\times 10^3$	$(8.6\pm 0.9)\times 10^2$	$(1.2\pm 0.2)\times 10^4$	$(1.6\pm 0.2)\times 10^4$	$(3.0\pm 0.5)\times 10^4$	$(2.9\pm 0.4)\times 10^4$	—	—	—	—	—	—

ble 3. (Continued)

Name	Flux 9 μm [Jy] (AKARI IRC)	Flux 18 μm [Jy] (AKARI IRC)	Flux 65 μm [Jy] (AKARI FIS)	Flux 90 μm [Jy] (AKARI FIS)	Flux 140 μm [Jy] (AKARI FIS)	Flux 160 μm [Jy] (AKARI FIS)	Flux 70 μm [Jy] (Herschel PACS)	Flux 160 μm [Jy] (Herschel PACS)	Flux 250 μm [Jy] (Herschel SPIRE)	Flux 350 μm [Jy] (Herschel SPIRE)	Flux 500 μm [Jy] (Herschel SPIRE)	Notes†
E103	$(6.9\pm 0.7)\times 10^1$	$(10.0\pm 1.0)\times 10^1$	$(2.1\pm 0.3)\times 10^3$	$(2.5\pm 0.4)\times 10^3$	$(1.7\pm 0.3)\times 10^3$	$(1.6\pm 0.2)\times 10^3$	$(2.2\pm 0.2)\times 10^3$	$(2.5\pm 0.3)\times 10^3$	$(1.2\pm 0.1)\times 10^3$	$(5.2\pm 0.5)\times 10^2$	$(1.9\pm 0.2)\times 10^2$	—
E104	$(1.8\pm 0.2)\times 10^1$	$(2.0\pm 0.2)\times 10^1$	$(1.9\pm 0.3)\times 10^2$	$(2.7\pm 0.4)\times 10^2$	$(4.6\pm 0.7)\times 10^2$	$(5.5\pm 0.8)\times 10^2$	—	—	—	—	—	—
E105	$(1.4\pm 0.1)\times 10^2$	$(1.9\pm 0.2)\times 10^2$	$(3.4\pm 0.5)\times 10^3$	$(3.6\pm 0.5)\times 10^3$	$(4.0\pm 0.6)\times 10^3$	$(3.2\pm 0.5)\times 10^3$	—	—	—	—	—	—
E106	$(4.8\pm 0.5)\times 10^1$	$(5.4\pm 0.5)\times 10^1$	$(9.0\pm 1.0)\times 10^2$	$(10.0\pm 1.0)\times 10^2$	$(9.0\pm 1.0)\times 10^2$	$(7.0\pm 1.0)\times 10^2$	—	—	—	—	—	—
E107	$(3.4\pm 0.3)\times 10^2$	$(4.9\pm 0.5)\times 10^2$	$(1.6\pm 0.2)\times 10^4$	$(9.0\pm 1.0)\times 10^3$	$(9.0\pm 1.0)\times 10^3$	$(10.0\pm 2.0)\times 10^3$	—	—	—	—	—	—
E108	$(9.7\pm 1.0)\times 10^2$	$(1.2\pm 0.1)\times 10^3$	$(2.1\pm 0.3)\times 10^4$	$(2.7\pm 0.4)\times 10^4$	$(5.4\pm 0.8)\times 10^4$	$(5.2\pm 0.8)\times 10^4$	$(2.4\pm 0.2)\times 10^4$	$(5.6\pm 0.6)\times 10^4$	$(3.0\pm 0.3)\times 10^4$	$(1.5\pm 0.1)\times 10^4$	$(6.1\pm 0.6)\times 10^3$	—
E109	$(1.2\pm 0.1)\times 10^2$	$(1.4\pm 0.1)\times 10^2$	$(3.9\pm 0.6)\times 10^3$	$(4.0\pm 0.6)\times 10^3$	$(2.6\pm 0.4)\times 10^3$	$(2.1\pm 0.3)\times 10^3$	—	—	—	—	—	—
E110	$(5.4\pm 0.5)\times 10^2$	$(9.2\pm 0.9)\times 10^2$	$(1.7\pm 0.3)\times 10^4$	$(1.8\pm 0.3)\times 10^4$	$(1.3\pm 0.2)\times 10^4$	$(1.1\pm 0.2)\times 10^4$	—	—	—	—	—	—
E111	$(8.4\pm 0.8)\times 10^1$	$(8.5\pm 0.9)\times 10^1$	$(8.0\pm 1.0)\times 10^2$	$(1.2\pm 0.2)\times 10^3$	$(2.3\pm 0.3)\times 10^3$	$(2.2\pm 0.3)\times 10^3$	—	—	—	—	—	—
E112	$(2.2\pm 0.2)\times 10^1$	$(2.1\pm 0.2)\times 10^1$	$(3.1\pm 0.5)\times 10^2$	$(5.0\pm 0.7)\times 10^2$	$(8.0\pm 1.0)\times 10^2$	$(9.0\pm 1.0)\times 10^2$	$(4.9\pm 0.5)\times 10^2$	$(1.1\pm 0.1)\times 10^3$	$(4.8\pm 0.5)\times 10^2$	$(2.3\pm 0.2)\times 10^2$	$(9.6\pm 1.0)\times 10^1$	—
E113	$(4.3\pm 0.4)\times 10^2$	$(4.6\pm 0.5)\times 10^2$	$(5.2\pm 0.8)\times 10^3$	$(7.0\pm 1.0)\times 10^3$	$(1.4\pm 0.2)\times 10^4$	$(1.2\pm 0.2)\times 10^4$	—	—	—	—	—	—
E114	$(1.1\pm 0.1)\times 10^1$	$(10.0\pm 1.0)\times 10^0$	$(1.1\pm 0.2)\times 10^2$	$(1.5\pm 0.2)\times 10^2$	$(3.4\pm 0.5)\times 10^2$	$(4.1\pm 0.6)\times 10^2$	—	—	—	—	—	—
E115	$(3.3\pm 0.3)\times 10^1$	$(2.5\pm 0.2)\times 10^1$	$(2.3\pm 0.3)\times 10^2$	$(4.0\pm 0.6)\times 10^2$	$(9.0\pm 1.0)\times 10^2$	$(10.0\pm 1.0)\times 10^2$	—	—	—	—	—	—
E116	$(1.2\pm 0.1)\times 10^2$	$(1.2\pm 0.1)\times 10^2$	$(10.0\pm 1.0)\times 10^2$	$(1.5\pm 0.2)\times 10^3$	$(2.9\pm 0.4)\times 10^3$	$(3.0\pm 0.5)\times 10^3$	—	—	—	—	—	—
E117	$(1.7\pm 0.2)\times 10^1$	$(2.0\pm 0.2)\times 10^1$	$(2.3\pm 0.3)\times 10^2$	$(2.7\pm 0.4)\times 10^2$	$(5.2\pm 0.8)\times 10^2$	$(6.2\pm 0.9)\times 10^2$	$(2.8\pm 0.3)\times 10^2$	$(6.3\pm 0.6)\times 10^2$	$(3.5\pm 0.4)\times 10^2$	$(1.8\pm 0.2)\times 10^2$	$(7.7\pm 0.8)\times 10^1$	—
E118	$(7.0\pm 1.0)\times 10^0$	$(8.6\pm 0.9)\times 10^0$	$(1.4\pm 0.2)\times 10^2$	$(1.9\pm 0.3)\times 10^2$	$(3.4\pm 0.5)\times 10^2$	$(3.7\pm 0.6)\times 10^2$	$(2.0\pm 0.2)\times 10^2$	$(4.3\pm 0.4)\times 10^2$	$(2.0\pm 0.2)\times 10^2$	$(8.8\pm 0.9)\times 10^1$	$(3.2\pm 0.3)\times 10^1$	—
E119	$(3.2\pm 0.3)\times 10^1$	$(2.8\pm 0.3)\times 10^1$	$(2.0\pm 0.3)\times 10^2$	$(3.3\pm 0.5)\times 10^2$	$(10.0\pm 1.0)\times 10^2$	$(10.0\pm 2.0)\times 10^2$	—	—	—	—	—	—
E120	$(1.4\pm 0.1)\times 10^1$	$(9.4\pm 0.9)\times 10^0$	$(8.0\pm 1.0)\times 10^1$	$(1.8\pm 0.3)\times 10^2$	$(3.8\pm 0.6)\times 10^2$	$(3.3\pm 0.5)\times 10^2$	—	—	—	—	—	—
E121	$(3.5\pm 0.3)\times 10^2$	$(8.0\pm 0.8)\times 10^2$	$(1.3\pm 0.2)\times 10^4$	$(1.6\pm 0.2)\times 10^4$	$(1.7\pm 0.3)\times 10^4$	$(1.3\pm 0.2)\times 10^4$	$(1.4\pm 0.1)\times 10^4$	$(1.8\pm 0.2)\times 10^4$	$(7.5\pm 0.7)\times 10^3$	$(3.2\pm 0.3)\times 10^3$	$(1.2\pm 0.1)\times 10^3$	—
E122	$(6.4\pm 0.6)\times 10^1$	$(3.3\pm 0.3)\times 10^2$	$(2.7\pm 0.4)\times 10^3$	$(2.9\pm 0.4)\times 10^3$	$(2.7\pm 0.4)\times 10^3$	$(2.5\pm 0.4)\times 10^3$	$(3.2\pm 0.3)\times 10^3$	$(2.8\pm 0.3)\times 10^3$	$(1.1\pm 0.1)\times 10^3$	$(4.8\pm 0.5)\times 10^2$	$(1.8\pm 0.2)\times 10^2$	—
E123	$(4.8\pm 0.5)\times 10^1$	$(10.0\pm 1.0)\times 10^1$	$(1.5\pm 0.2)\times 10^3$	$(1.7\pm 0.3)\times 10^3$	$(1.9\pm 0.3)\times 10^3$	$(1.5\pm 0.2)\times 10^3$	—	—	—	—	—	—
E124	$(1.4\pm 0.1)\times 10^3$	$(2.6\pm 0.3)\times 10^3$	$(4.1\pm 0.6)\times 10^4$	$(5.4\pm 0.8)\times 10^4$	$(6.4\pm 1.0)\times 10^4$	$(5.1\pm 0.8)\times 10^4$	$(4.8\pm 0.5)\times 10^4$	$(6.8\pm 0.7)\times 10^4$	$(2.9\pm 0.3)\times 10^4$	$(1.4\pm 0.1)\times 10^4$	$(5.3\pm 0.5)\times 10^3$	—
E125	$(3.4\pm 0.3)\times 10^1$	$(4.0\pm 0.4)\times 10^1$	$(7.0\pm 1.0)\times 10^2$	$(9.0\pm 1.0)\times 10^2$	$(1.1\pm 0.2)\times 10^3$	$(1.2\pm 0.2)\times 10^3$	$(8.2\pm 0.8)\times 10^2$	$(1.1\pm 0.1)\times 10^3$	$(4.8\pm 0.5)\times 10^2$	$(2.0\pm 0.2)\times 10^2$	$(7.4\pm 0.7)\times 10^1$	—
E126	$(3.9\pm 0.4)\times 10^1$	$(8.4\pm 0.8)\times 10^1$	$(1.5\pm 0.2)\times 10^3$	$(2.0\pm 0.3)\times 10^3$	$(1.7\pm 0.3)\times 10^3$	$(1.6\pm 0.2)\times 10^3$	—	—	—	—	—	sc
E127	$(1.9\pm 0.2)\times 10^3$	$(2.4\pm 0.2)\times 10^3$	$(4.2\pm 0.6)\times 10^4$	$(5.4\pm 0.8)\times 10^4$	$(6.1\pm 0.9)\times 10^4$	$(5.0\pm 0.8)\times 10^4$	$(4.7\pm 0.5)\times 10^4$	$(6.3\pm 0.6)\times 10^4$	$(2.6\pm 0.3)\times 10^4$	$(1.1\pm 0.1)\times 10^4$	$(4.1\pm 0.4)\times 10^3$	—
E128	$(5.9\pm 0.6)\times 10^1$	$(3.6\pm 0.4)\times 10^1$	$(8.0\pm 1.0)\times 10^2$	$(1.4\pm 0.2)\times 10^3$	$(1.3\pm 0.2)\times 10^3$	$(8.0\pm 1.0)\times 10^2$	$(9.9\pm 1.0)\times 10^2$	$(1.5\pm 0.2)\times 10^3$	$(6.3\pm 0.6)\times 10^2$	$(2.7\pm 0.3)\times 10^2$	$(9.9\pm 1.0)\times 10^1$	sc
E129	$(1.5\pm 0.1)\times 10^1$	$(1.8\pm 0.2)\times 10^1$	$(1.5\pm 0.2)\times 10^2$	$(2.0\pm 0.3)\times 10^2$	$(2.7\pm 0.4)\times 10^2$	$(2.6\pm 0.4)\times 10^2$	—	—	—	—	—	—
E130	$(5.3\pm 0.5)\times 10^1$	$(7.4\pm 0.7)\times 10^1$	$(8.0\pm 1.0)\times 10^2$	$(10.0\pm 1.0)\times 10^2$	$(1.5\pm 0.2)\times 10^3$	$(1.4\pm 0.2)\times 10^3$	—	—	—	—	—	—
E131	$(3.8\pm 0.4)\times 10^1$	$(4.5\pm 0.4)\times 10^1$	$(9.0\pm 1.0)\times 10^2$	$(1.1\pm 0.2)\times 10^3$	$(1.2\pm 0.2)\times 10^3$	$(10.0\pm 2.0)\times 10^2$	$(1.1\pm 0.1)\times 10^3$	$(1.3\pm 0.1)\times 10^3$	$(5.0\pm 0.5)\times 10^2$	$(2.0\pm 0.2)\times 10^2$	$(7.5\pm 0.8)\times 10^1$	—
E132	$(1.8\pm 0.2)\times 10^1$	$(1.3\pm 0.1)\times 10^1$	$(1.9\pm 0.3)\times 10^2$	$(3.0\pm 0.5)\times 10^2$	$(5.5\pm 0.8)\times 10^2$	$(5.6\pm 0.8)\times 10^2$	$(2.8\pm 0.3)\times 10^2$	$(5.9\pm 0.6)\times 10^2$	$(2.7\pm 0.3)\times 10^2$	$(1.1\pm 0.1)\times 10^2$	$(4.1\pm 0.4)\times 10^1$	—
E133	$(4.9\pm 0.5)\times 10^1$	$(5.1\pm 0.5)\times 10^1$	$(1.1\pm 0.2)\times 10^3$	$(1.5\pm 0.2)\times 10^3$	$(1.2\pm 0.2)\times 10^3$	$(1.2\pm 0.2)\times 10^3$	—	—	—	—	—	—
E134	$(5.4\pm 0.5)\times 10^1$	$(1.2\pm 0.1)\times 10^2$	$(1.8\pm 0.3)\times 10^3$	$(2.2\pm 0.3)\times 10^3$	$(1.5\pm 0.2)\times 10^3$	$(1.3\pm 0.2)\times 10^3$	$(1.7\pm 0.2)\times 10^3$	$(1.7\pm 0.2)\times 10^3$	$(6.7\pm 0.7)\times 10^2$	$(2.7\pm 0.3)\times 10^2$	$(10.0\pm 1.0)\times 10^1$	—
E135	$(5.8\pm 0.6)\times 10^1$	$(1.3\pm 0.1)\times 10^2$	$(2.0\pm 0.3)\times 10^3$	$(2.2\pm 0.3)\times 10^3$	$(1.7\pm 0.3)\times 10^3$	$(1.5\pm 0.2)\times 10^3$	—	—	—	—	—	—
E136	$(1.4\pm 0.1)\times 10^1$	$(1.1\pm 0.1)\times 10^1$	$(2.7\pm 0.4)\times 10^2$	$(3.5\pm 0.5)\times 10^2$	$(5.8\pm 0.9)\times 10^2$	$(6.3\pm 0.9)\times 10^2$	$(3.0\pm 0.3)\times 10^2$	$(6.2\pm 0.6)\times 10^2$	$(3.1\pm 0.3)\times 10^2$	$(1.5\pm 0.2)\times 10^2$	$(6.2\pm 0.6)\times 10^1$	—
E137	$(2.1\pm 0.2)\times 10^1$	$(1.7\pm 0.2)\times 10^1$	$(3.0\pm 0.5)\times 10^2$	$(3.7\pm 0.6)\times 10^2$	$(5.9\pm 0.9)\times 10^2$	$(5.7\pm 0.9)\times 10^2$	$(3.9\pm 0.4)\times 10^2$	$(6.2\pm 0.6)\times 10^2$	$(2.6\pm 0.3)\times 10^2$	$(1.1\pm 0.1)\times 10^2$	$(3.7\pm 0.4)\times 10^1$	—
E138	$(2.9\pm 0.3)\times 10^1$	$(2.0\pm 0.2)\times 10^1$	$(2.7\pm 0.4)\times 10^2$	$(4.4\pm 0.7)\times 10^2$	$(9.0\pm 1.0)\times 10^2$	$(9.0\pm 1.0)\times 10^2$	—	—	—	—	—	sc
E139	$(10.0\pm 1.0)\times 10^1$	$(1.5\pm 0.2)\times 10^2$	$(1.4\pm 0.2)\times 10^3$	$(1.7\pm 0.3)\times 10^3$	$(2.0\pm 0.3)\times 10^3$	$(1.7\pm 0.2)\times 10^3$	—	—	—	—	—	—
E140	$(6.1\pm 0.6)\times 10^1$	$(7.6\pm 0.8)\times 10^1$	$(10.0\pm 2.0)\times 10^2$	$(1.2\pm 0.2)\times 10^3$	$(2.8\pm 0.4)\times 10^3$	$(3.1\pm 0.5)\times 10^3$	$(1.3\pm 0.1)\times 10^3$	$(2.8\pm 0.3)\times 10^3$	$(1.4\pm 0.1)\times 10^3$	$(6.7\pm 0.7)\times 10^2$	$(2.7\pm 0.3)\times 10^2$	—
E141	$(1.3\pm 0.1)\times 10^2$	$(1.4\pm 0.1)\times 10^2$	$(1.8\pm 0.3)\times 10^3$	$(2.4\pm 0.4)\times 10^3$	$(3.4\pm 0.5)\times 10^3$	$(3.0\pm 0.4)\times 10^3$	—	—	—	—	—	—

† We considered random and systematic errors as flux uncertainties (see text for detail).

sc: Targets with source contamination in their background regions, where areas larger than 10% suffer source contamination.

Table 4. Summary of the luminosities of the IR bubbles obtained by the SED fitting.

Name	$\log(L_{\text{TIR}}/L_{\odot})$	$\log(L_{\text{PAH}}/L_{\text{TIR}})$	$\log(L_{\text{warm}}/L_{\text{TIR}})$	$\log(L_{\text{cold}}/L_{\text{TIR}})$
N2	6.95±0.36	-0.94±0.02	-0.26±0.04	-0.47±0.03
N4	5.17±0.11	-0.71±0.02	-0.25±0.04	-0.61±0.03
N5	5.41±0.26	-0.81±0.03	-0.27±0.05	-0.51±0.05
N6	5.82±0.11	-0.70±0.02	-0.34±0.04	-0.47±0.03
N10	5.65±0.12	-1.03±0.02	-0.14±0.04	-0.73±0.03
N12	5.85±0.11	-0.76±0.02	-0.36±0.05	-0.41±0.03
N14	5.28±0.12	-0.87±0.02	-0.16±0.04	-0.78±0.03
N16	6.09±0.11	-0.84±0.02	-0.45±0.05	-0.30±0.03
N18	5.83±0.11	-0.91±0.02	-0.34±0.04	-0.38±0.03
N20	–	-0.67±0.02	-0.29±0.04	-0.57±0.03
N24	6.80±0.12	-0.85±0.02	-0.21±0.04	-0.61±0.03
N30	4.32±0.27	-0.92±0.02	-0.16±0.04	-0.73±0.03
N34	5.77±0.12	-0.88±0.02	-0.24±0.04	-0.53±0.03
N35	6.69±0.12	-1.07±0.02	-0.19±0.04	-0.57±0.03
N36	6.33±0.12	-1.15±0.02	-0.20±0.04	-0.53±0.03
N37	5.09±0.12	-0.77±0.02	-0.18±0.04	-0.75±0.03
N39	6.49±0.12	-1.03±0.03	-0.14±0.04	-0.74±0.03
N40	5.63±0.12	-1.07±0.02	-0.12±0.04	-0.81±0.03
N44	4.46±0.11	-0.68±0.02	-0.33±0.05	-0.49±0.03
N45	5.80±0.12	-0.94±0.02	-0.21±0.04	-0.57±0.03
N46	4.69±0.12	-1.04±0.02	-0.16±0.04	-0.67±0.03
N47	5.64±0.11	-1.11±0.02	-0.31±0.04	-0.36±0.03
N49	5.33±0.12	-0.98±0.02	-0.23±0.04	-0.52±0.03
N50	5.66±0.11	-1.12±0.02	-0.23±0.04	-0.47±0.03
N51	4.44±0.12	-0.89±0.02	-0.22±0.04	-0.57±0.03
N52	6.88±0.12	-1.28±0.02	-0.10±0.04	-0.81±0.03
N54	5.05±0.11	-0.89±0.02	-0.40±0.05	-0.32±0.03
N56	5.00±0.11	-0.74±0.02	-0.39±0.04	-0.38±0.03
N59	6.61±0.11	-0.77±0.02	-0.43±0.05	-0.34±0.03
N61	5.92±0.12	-1.26±0.02	-0.15±0.04	-0.61±0.03
N64	5.29±0.11	-0.85±0.02	-0.34±0.04	-0.40±0.03
N65	4.88±0.11	-0.86±0.02	-0.34±0.05	-0.40±0.03
N68	6.61±0.12	-1.10±0.02	-0.27±0.04	-0.41±0.03
N69	5.83±0.11	-0.68±0.02	-0.49±0.05	-0.33±0.03
N71	5.93±0.11	-0.91±0.02	-0.39±0.04	-0.33±0.03
N73	5.16±0.11	-0.89±0.02	-0.38±0.05	-0.34±0.03
N77	4.36±0.11	-0.67±0.02	-0.35±0.04	-0.47±0.03
N79	5.59±0.12	-0.91±0.02	-0.29±0.05	-0.44±0.03
N80	3.40±0.11	-0.94±0.02	-0.26±0.04	-0.47±0.03
N81	6.22±0.11	-0.73±0.02	-0.39±0.04	-0.39±0.03
N82	5.47±0.12	-0.77±0.02	-0.26±0.05	-0.55±0.03
N84	3.35±0.12	-0.67±0.02	-0.38±0.06	-0.43±0.03
N91	5.88±0.11	-0.67±0.02	-0.35±0.04	-0.48±0.03
N92	4.65±0.11	-0.61±0.02	-0.40±0.05	-0.46±0.03
N95	4.70±0.11	-0.83±0.02	-0.23±0.04	-0.59±0.03
N98	4.74±0.11	-0.81±0.02	-0.27±0.04	-0.50±0.03
N101	6.03±0.12	-1.13±0.02	-0.09±0.04	-0.92±0.03
N107	6.11±0.15	-0.78±0.02	-0.33±0.04	-0.44±0.03
N109	6.83±0.08	-0.53±0.02	-0.41±0.05	-0.50±0.03

Table 4. (Continued)

Name	$\log(L_{\text{TIR}}/L_{\odot})$	$\log(L_{\text{PAH}}/L_{\text{TIR}})$	$\log(L_{\text{warm}}/L_{\text{TIR}})$	$\log(L_{\text{cold}}/L_{\text{TIR}})$
N114	5.65±0.05	-0.79±0.02	-0.27±0.04	-0.53±0.03
N115	5.34±0.11	-0.63±0.02	-0.29±0.04	-0.60±0.03
N117	5.50±0.11	-0.85±0.02	-0.22±0.04	-0.60±0.03
N120	3.25±0.27	-0.70±0.02	-0.35±0.04	-0.45±0.03
N123	5.43±0.12	-0.84±0.02	-0.19±0.04	-0.67±0.03
N126	4.48±0.11	-0.62±0.02	-0.33±0.04	-0.54±0.03
N127	3.02±0.11	-0.58±0.02	-0.36±0.04	-0.53±0.03
N128	4.03±0.11	-0.74±0.02	-0.28±0.04	-0.53±0.03
N133	4.80±0.12	-0.86±0.02	-0.17±0.04	-0.73±0.03
S1	5.92±0.22	-0.86±0.02	-0.23±0.05	-0.56±0.03
S7	4.98±0.11	-0.79±0.02	-0.24±0.04	-0.57±0.03
S8	5.56±0.05	-0.88±0.02	-0.26±0.05	-0.50±0.03
S11	5.13±0.12	-1.03±0.02	-0.21±0.04	-0.53±0.03
S13	5.34±0.11	-0.82±0.02	-0.36±0.04	-0.39±0.03
S14	5.09±0.11	-0.77±0.02	-0.51±0.05	-0.28±0.03
S15	4.91±0.20	-0.90±0.02	-0.29±0.04	-0.45±0.03
S17	5.73±0.12	-0.91±0.02	-0.14±0.04	-0.79±0.03
S18	5.24±0.06	-1.05±0.02	-0.16±0.04	-0.65±0.03
S20	3.83±0.12	-0.93±0.02	-0.16±0.04	-0.72±0.03
S23	4.97±0.11	-0.92±0.02	-0.19±0.04	-0.64±0.03
S29	5.80±0.16	-0.97±0.02	-0.16±0.04	-0.70±0.03
S36	6.17±0.11	-1.14±0.02	-0.14±0.04	-0.68±0.03
S41	6.25±0.12	-1.09±0.02	-0.15±0.04	-0.69±0.03
S44	5.23±0.10	-0.74±0.02	-0.32±0.05	-0.47±0.03
S51	6.05±0.12	-1.04±0.02	-0.13±0.04	-0.79±0.03
S54	—	-0.71±0.02	-0.29±0.05	-0.54±0.03
S62	5.69±0.10	-0.94±0.02	-0.20±0.05	-0.59±0.03
S64	5.86±0.12	-1.18±0.02	-0.17±0.04	-0.59±0.03
S66	6.29±0.08	-0.89±0.02	-0.24±0.04	-0.52±0.03
S70	5.62±0.04	-0.80±0.02	-0.33±0.05	-0.43±0.03
S71	5.80±0.08	-0.85±0.02	-0.18±0.04	-0.69±0.03
S73	4.93±0.15	-0.84±0.02	-0.29±0.05	-0.46±0.03
S74	4.55±0.15	-0.75±0.02	-0.24±0.05	-0.60±0.03
S76	5.97±0.16	-1.22±0.02	-0.11±0.04	-0.78±0.03
S79	5.43±0.24	-0.94±0.03	-0.13±0.04	-0.83±0.03
S91	4.79±0.12	-0.74±0.02	-0.35±0.04	-0.43±0.03
S92	6.40±0.05	-0.88±0.02	-0.21±0.04	-0.59±0.03
S96	5.30±0.24	-0.87±0.02	-0.17±0.04	-0.74±0.03
S97	4.85±0.23	-0.81±0.02	-0.17±0.04	-0.76±0.03
S104	4.72±0.23	-0.93±0.03	-0.16±0.04	-0.72±0.03
S109	5.67±0.27	-1.06±0.02	-0.17±0.04	-0.62±0.03
S110	5.81±0.23	-1.09±0.02	-0.11±0.04	-0.84±0.03
S111	6.00±0.27	-1.09±0.02	-0.10±0.04	-0.91±0.03
S116	5.98±0.13	-0.84±0.02	-0.25±0.05	-0.54±0.03
S123	4.95±0.31	-0.71±0.02	-0.35±0.05	-0.44±0.03
S133	5.68±0.05	-0.89±0.02	-0.22±0.05	-0.57±0.03
S137	5.68±0.19	-0.61±0.02	-0.38±0.05	-0.47±0.03
S141	5.11±0.29	-0.88±0.02	-0.19±0.04	-0.66±0.03
S145	6.37±0.15	-0.88±0.02	-0.15±0.04	-0.80±0.03

Table 4. (Continued)

Name	$\log(L_{\text{TIR}}/L_{\odot})$	$\log(L_{\text{PAH}}/L_{\text{TIR}})$	$\log(L_{\text{warm}}/L_{\text{TIR}})$	$\log(L_{\text{cold}}/L_{\text{TIR}})$
S150	5.18±0.24	-0.94±0.02	-0.17±0.04	-0.67±0.03
S156	6.52±0.20	-1.11±0.03	-0.07±0.04	-1.16±0.04
S163	5.60±0.05	-0.84±0.02	-0.27±0.04	-0.49±0.03
S181	6.05±0.12	-1.06±0.03	-0.10±0.04	-0.92±0.04
S186	5.79±0.12	-1.03±0.02	-0.16±0.04	-0.67±0.03
CN60	6.36±0.12	-1.21±0.02	-0.14±0.04	-0.67±0.03
CN63	5.90±0.05	-0.88±0.02	-0.40±0.05	-0.33±0.03
CN71	5.41±0.07	-0.95±0.02	-0.17±0.04	-0.68±0.03
CN73	4.24±0.07	-1.18±0.02	-0.14±0.04	-0.67±0.03
CN88	5.39±0.26	-0.74±0.02	-0.22±0.04	-0.66±0.03
CN90	5.00±0.26	-0.76±0.02	-0.21±0.04	-0.69±0.03
CN99	6.50±0.05	-0.96±0.02	-0.21±0.04	-0.57±0.03
CN107	6.59±0.05	-1.04±0.02	-0.14±0.04	-0.73±0.03
CN108	6.24±0.11	-0.79±0.02	-0.37±0.04	-0.38±0.03
CN111	5.08±0.06	-0.81±0.02	-0.33±0.05	-0.43±0.03
CN114	5.36±0.08	-0.84±0.02	-0.22±0.04	-0.60±0.03
CN138	4.44±0.12	-0.92±0.02	-0.22±0.04	-0.57±0.03
CN139	5.65±0.14	-0.69±0.02	-0.40±0.05	-0.40±0.03
CN148	5.49±0.12	-1.16±0.02	-0.11±0.04	-0.82±0.03
CS2	4.65±0.12	-1.05±0.02	-0.15±0.04	-0.69±0.03
CS33	5.92±0.03	-0.99±0.02	-0.19±0.04	-0.61±0.03
CS39	–	-0.66±0.02	-0.33±0.04	-0.51±0.03
CS51	5.75±0.12	-0.98±0.02	-0.19±0.04	-0.60±0.03
CS62	5.30±0.18	-1.13±0.03	-0.10±0.04	-0.88±0.03
CS81	6.58±0.04	-1.19±0.03	-0.11±0.04	-0.79±0.03
EN1	–	-0.92±0.03	-0.11±0.05	-0.99±0.06
EN2	4.61±0.12	-0.67±0.03	-0.20±0.05	-0.83±0.06
EN3	4.50±0.12	-0.66±0.03	-0.27±0.05	-0.62±0.05
EN4	4.29±0.12	-0.62±0.03	-0.27±0.05	-0.65±0.06
EN5	4.25±0.12	-0.65±0.03	-0.33±0.06	-0.51±0.05
EN6	4.93±0.12	-0.84±0.03	-0.21±0.05	-0.62±0.05
EN7	3.34±0.12	-0.39±0.02	-0.48±0.06	-0.59±0.05
EN8	–	-0.50±0.02	-0.48±0.06	-0.45±0.05
EN9	5.14±0.12	-0.62±0.02	-0.29±0.05	-0.62±0.05
EN10	–	-0.76±0.03	-0.22±0.05	-0.66±0.05
EN11	3.77±0.12	-0.70±0.03	-0.21±0.05	-0.72±0.06
EN12	4.73±0.12	-0.67±0.03	-0.15±0.05	-1.11±0.07
EN13	5.96±0.12	-0.78±0.03	-0.13±0.05	-1.00±0.07
EN14	6.04±0.12	-0.86±0.03	-0.12±0.05	-0.98±0.07
EN15	–	-0.64±0.03	-0.29±0.05	-0.58±0.05
EN16	5.28±0.12	-0.61±0.03	-0.36±0.06	-0.50±0.05
EN17	5.31±0.12	-0.68±0.03	-0.30±0.05	-0.54±0.05
EN18	4.59±0.12	-0.66±0.03	-0.26±0.05	-0.62±0.05
EN19	–	-0.77±0.03	-0.29±0.05	-0.50±0.05
EN20	–	-0.65±0.02	-0.36±0.05	-0.47±0.05
EN21	4.43±0.12	-0.54±0.02	-0.40±0.05	-0.51±0.05
EN22	5.15±0.12	-0.80±0.03	-0.21±0.05	-0.66±0.05
ES1	5.91±0.12	-0.86±0.03	-0.16±0.05	-0.76±0.06
ES2	4.63±0.12	-0.52±0.02	-0.36±0.05	-0.58±0.05

Table 4. (Continued)

Name	$\log(L_{\text{TIR}}/L_{\odot})$	$\log(L_{\text{PAH}}/L_{\text{TIR}})$	$\log(L_{\text{warm}}/L_{\text{TIR}})$	$\log(L_{\text{cold}}/L_{\text{TIR}})$
ES3	5.06±0.12	-0.59±0.02	-0.33±0.05	-0.56±0.05
ES4	5.33±0.12	-0.85±0.03	-0.15±0.05	-0.84±0.06
ES5	4.24±0.12	-0.48±0.02	-0.44±0.06	-0.51±0.05
ES6	–	-0.56±0.03	-0.27±0.05	-0.72±0.05
ES7	–	-0.57±0.02	-0.32±0.05	-0.60±0.05
ES8	–	-0.64±0.03	-0.22±0.05	-0.77±0.06
ES9	3.89±0.12	-0.46±0.02	-0.48±0.06	-0.50±0.05
ES10	–	-0.61±0.03	-0.29±0.05	-0.62±0.05
ES11	–	-0.63±0.03	-0.28±0.05	-0.61±0.05
ES12	–	-0.53±0.02	-0.44±0.06	-0.46±0.05
ES13	–	-0.74±0.03	-0.37±0.06	-0.40±0.05
ES14	–	-0.96±0.03	-0.19±0.05	-0.61±0.06
ES15	–	-0.80±0.03	-0.22±0.05	-0.62±0.06
ES16	6.22±0.12	-0.84±0.03	-0.12±0.05	-0.98±0.06
E1	4.44±0.11	-0.39±0.02	-0.56±0.06	-0.50±0.05
E2	4.06±0.12	-0.66±0.03	-0.15±0.05	-1.14±0.08
E3	5.28±0.11	-0.67±0.02	-0.32±0.04	-0.51±0.03
E4	–	-0.86±0.02	-0.21±0.04	-0.62±0.03
E5	6.06±0.12	-0.95±0.03	-0.13±0.05	-0.84±0.06
E7	5.06±0.11	-0.72±0.02	-0.26±0.04	-0.59±0.03
E8	4.56±0.12	-0.78±0.03	-0.18±0.05	-0.75±0.06
E9	–	-1.25±0.02	-0.08±0.04	-0.93±0.03
E10	4.02±0.12	-0.58±0.02	-0.33±0.05	-0.57±0.05
E11	5.52±0.12	-0.77±0.03	-0.17±0.05	-0.81±0.06
E12	–	-1.37±0.03	-0.06±0.05	-1.04±0.06
E13	5.97±0.12	-0.90±0.03	-0.13±0.05	-0.86±0.06
E14	–	-0.82±0.02	-0.26±0.04	-0.52±0.03
E15	–	-0.93±0.02	-0.19±0.04	-0.63±0.03
E16	–	-0.59±0.02	-0.42±0.05	-0.44±0.03
E18	4.00±0.12	-0.88±0.03	-0.15±0.05	-0.78±0.06
E19	5.03±0.12	-0.77±0.03	-0.20±0.05	-0.71±0.06
E20	5.03±0.12	-0.91±0.03	-0.09±0.05	-1.14±0.07
E21	5.78±0.12	-0.89±0.02	-0.21±0.05	-0.59±0.03
E22	–	-0.67±0.02	-0.38±0.05	-0.43±0.03
E23	–	-0.61±0.02	-0.38±0.05	-0.47±0.03
E24	5.45±0.12	-0.94±0.03	-0.16±0.05	-0.71±0.05
E25	4.95±0.12	-0.84±0.03	-0.21±0.05	-0.63±0.05
E26	–	-0.50±0.02	-0.40±0.05	-0.55±0.05
E27	4.65±0.11	-0.82±0.02	-0.21±0.04	-0.62±0.03
E28	4.77±0.12	-0.95±0.03	-0.18±0.05	-0.63±0.06
E29	3.69±0.12	-0.96±0.03	-0.12±0.05	-0.87±0.06
E32	4.73±0.12	-0.73±0.03	-0.31±0.05	-0.49±0.05
E33	4.41±0.12	-0.56±0.02	-0.33±0.05	-0.60±0.05
E34	2.93±0.12	-0.74±0.03	-0.31±0.05	-0.48±0.05
E35	5.68±0.12	-0.81±0.03	-0.21±0.05	-0.64±0.05
E36	4.63±0.12	-0.65±0.03	-0.22±0.05	-0.75±0.06
E37	2.98±0.12	-0.82±0.03	-0.23±0.05	-0.60±0.05
E38	3.82±0.12	-0.47±0.02	-0.46±0.06	-0.51±0.05
E40	4.53±0.12	-0.68±0.03	-0.25±0.05	-0.65±0.05

Table 4. (Continued)

Name	$\log(L_{\text{TIR}}/L_{\odot})$	$\log(L_{\text{PAH}}/L_{\text{TIR}})$	$\log(L_{\text{warm}}/L_{\text{TIR}})$	$\log(L_{\text{cold}}/L_{\text{TIR}})$
E41	5.04±0.12	-0.66±0.03	-0.24±0.05	-0.68±0.06
E42	4.36±0.12	-0.53±0.02	-0.35±0.05	-0.59±0.05
E43	4.37±0.12	-0.86±0.03	-0.08±0.05	-1.45±0.06
E44	4.00±0.12	-0.47±0.02	-0.48±0.06	-0.49±0.05
E45	4.57±0.12	-0.41±0.02	-0.50±0.06	-0.52±0.05
E46	4.88±0.12	-0.89±0.03	-0.10±0.05	-1.07±0.08
E47	4.29±0.11	-0.55±0.02	-0.38±0.04	-0.53±0.03
E48	4.32±0.12	-0.54±0.02	-0.37±0.05	-0.55±0.05
E49	4.13±0.12	-0.88±0.03	-0.11±0.05	-1.02±0.07
E50	3.90±0.12	-0.76±0.03	-0.27±0.05	-0.53±0.05
E51	5.07±0.12	-0.54±0.02	-0.36±0.05	-0.55±0.05
E52	3.68±0.11	-0.44±0.02	-0.46±0.06	-0.54±0.05
E53	3.89±0.12	-0.53±0.03	-0.33±0.06	-0.62±0.05
E54	4.93±0.12	-0.79±0.03	-0.14±0.05	-0.91±0.07
E55	4.93±0.11	-0.64±0.02	-0.30±0.04	-0.56±0.03
E56	4.99±0.11	-0.78±0.02	-0.31±0.04	-0.46±0.03
E57	3.57±0.12	-0.71±0.03	-0.26±0.05	-0.60±0.05
E58	5.11±0.11	-0.72±0.02	-0.26±0.04	-0.59±0.03
E60	4.89±0.12	-0.52±0.02	-0.47±0.06	-0.44±0.05
E61	4.94±0.12	-0.52±0.02	-0.47±0.06	-0.45±0.05
E62	4.79±0.12	-0.64±0.03	-0.28±0.05	-0.61±0.05
E63	5.23±0.12	-0.55±0.02	-0.40±0.05	-0.49±0.05
E64	4.20±0.12	-0.64±0.03	-0.26±0.05	-0.66±0.05
E65	4.84±0.12	-0.89±0.03	-0.13±0.05	-0.90±0.06
E66	4.68±0.12	-0.62±0.02	-0.29±0.05	-0.62±0.05
E67	4.37±0.12	-0.65±0.03	-0.22±0.05	-0.76±0.06
E68	5.19±0.12	-0.71±0.03	-0.25±0.05	-0.62±0.05
E69	4.60±0.12	-0.78±0.03	-0.16±0.05	-0.83±0.06
E71	4.52±0.12	-0.71±0.03	-0.22±0.05	-0.69±0.06
E72	4.62±0.11	-0.64±0.02	-0.30±0.04	-0.57±0.03
E74	4.89±0.12	-0.91±0.03	-0.18±0.05	-0.67±0.06
E75	4.85±0.12	-0.74±0.03	-0.27±0.05	-0.55±0.05
E76	5.73±0.11	-0.70±0.02	-0.27±0.04	-0.59±0.03
E78	5.24±0.12	-0.74±0.03	-0.26±0.05	-0.56±0.05
E79	3.69±0.12	-0.55±0.02	-0.36±0.05	-0.56±0.05
E80	4.03±0.11	-0.66±0.02	-0.30±0.04	-0.56±0.03
E81	4.11±0.12	-0.65±0.03	-0.27±0.05	-0.63±0.05
E82	5.68±0.11	-0.72±0.02	-0.32±0.04	-0.49±0.03
E83	4.62±0.11	-0.81±0.02	-0.24±0.04	-0.58±0.03
E84	4.16±0.11	-0.63±0.02	-0.31±0.04	-0.55±0.03
E86	4.66±0.11	-0.63±0.02	-0.35±0.04	-0.49±0.03
E87	4.52±0.12	-0.54±0.02	-0.41±0.06	-0.49±0.05
E88	4.99±0.12	-0.73±0.03	-0.17±0.05	-0.85±0.06
E90	4.53±0.12	-0.69±0.03	-0.23±0.05	-0.68±0.05
E91	3.95±0.12	-0.68±0.03	-0.27±0.05	-0.60±0.05
E92	4.72±0.12	-0.61±0.02	-0.32±0.05	-0.56±0.05
E93	5.05±0.12	-0.72±0.03	-0.24±0.05	-0.63±0.05
E94	4.48±0.12	-0.60±0.02	-0.33±0.05	-0.55±0.05
E95	5.09±0.11	-0.60±0.02	-0.36±0.04	-0.50±0.03

Table 4. (Continued)

Name	$\log(L_{\text{TIR}}/L_{\odot})$	$\log(L_{\text{PAH}}/L_{\text{TIR}})$	$\log(L_{\text{warm}}/L_{\text{TIR}})$	$\log(L_{\text{cold}}/L_{\text{TIR}})$
E96	–	-0.82 ± 0.03	-0.18 ± 0.05	-0.73 ± 0.06
E97	–	-0.71 ± 0.02	-0.30 ± 0.04	-0.51 ± 0.03
E98	5.80 ± 0.12	-0.59 ± 0.02	-0.40 ± 0.05	-0.46 ± 0.05
E99	3.69 ± 0.12	-0.47 ± 0.02	-0.41 ± 0.06	-0.57 ± 0.05
E100	–	-0.51 ± 0.02	-0.52 ± 0.06	-0.41 ± 0.05
E101	3.24 ± 0.11	-0.43 ± 0.02	-0.47 ± 0.06	-0.53 ± 0.05
E102	4.49 ± 0.12	-0.53 ± 0.02	-0.37 ± 0.06	-0.55 ± 0.05
E103	–	-0.86 ± 0.02	-0.17 ± 0.04	-0.72 ± 0.03
E104	–	-0.60 ± 0.02	-0.33 ± 0.05	-0.55 ± 0.05
E105	4.07 ± 0.12	-0.76 ± 0.03	-0.17 ± 0.05	-0.82 ± 0.06
E106	–	-0.68 ± 0.03	-0.17 ± 0.05	-0.92 ± 0.06
E107	–	-0.89 ± 0.03	-0.12 ± 0.05	-0.98 ± 0.07
E108	–	-0.80 ± 0.02	-0.28 ± 0.04	-0.49 ± 0.03
E109	–	-0.85 ± 0.03	-0.11 ± 0.05	-1.07 ± 0.07
E110	5.66 ± 0.12	-0.87 ± 0.03	-0.11 ± 0.05	-1.03 ± 0.07
E111	–	-0.57 ± 0.02	-0.35 ± 0.05	-0.55 ± 0.05
E113	5.54 ± 0.12	-0.62 ± 0.03	-0.32 ± 0.05	-0.56 ± 0.05
E114	–	-0.58 ± 0.02	-0.40 ± 0.05	-0.47 ± 0.05
E115	3.12 ± 0.12	-0.49 ± 0.02	-0.48 ± 0.06	-0.45 ± 0.05
E116	–	-0.54 ± 0.02	-0.37 ± 0.05	-0.55 ± 0.05
E117	–	-0.68 ± 0.02	-0.27 ± 0.04	-0.59 ± 0.03
E119	–	-0.50 ± 0.02	-0.50 ± 0.06	-0.44 ± 0.05
E120	2.56 ± 0.12	-0.48 ± 0.02	-0.52 ± 0.06	-0.44 ± 0.05
E121	–	-0.93 ± 0.02	-0.21 ± 0.04	-0.57 ± 0.03
E122	5.10 ± 0.12	-1.06 ± 0.02	-0.13 ± 0.04	-0.77 ± 0.03
E123	–	-0.90 ± 0.03	-0.14 ± 0.05	-0.81 ± 0.06
E124	6.72 ± 0.12	-0.88 ± 0.02	-0.22 ± 0.04	-0.57 ± 0.03
E125	4.88 ± 0.12	-0.71 ± 0.02	-0.29 ± 0.05	-0.54 ± 0.03
E126	5.29 ± 0.12	-0.95 ± 0.03	-0.14 ± 0.05	-0.78 ± 0.06
E127	6.07 ± 0.12	-0.73 ± 0.02	-0.27 ± 0.05	-0.55 ± 0.03
E128	–	-0.57 ± 0.02	-0.43 ± 0.06	-0.45 ± 0.03
E129	–	-0.58 ± 0.02	-0.26 ± 0.05	-0.72 ± 0.05
E130	–	-0.69 ± 0.03	-0.24 ± 0.05	-0.66 ± 0.05
E131	–	-0.76 ± 0.02	-0.28 ± 0.05	-0.53 ± 0.03
E133	–	-0.74 ± 0.03	-0.18 ± 0.05	-0.80 ± 0.06
E134	5.62 ± 0.12	-0.86 ± 0.02	-0.21 ± 0.05	-0.61 ± 0.03
E135	–	-0.96 ± 0.03	-0.11 ± 0.05	-0.94 ± 0.06
E136	–	-0.71 ± 0.02	-0.31 ± 0.04	-0.50 ± 0.03
E137	–	-0.61 ± 0.02	-0.34 ± 0.05	-0.52 ± 0.03
E138	–	-0.56 ± 0.02	-0.43 ± 0.06	-0.46 ± 0.05
E139	4.68 ± 0.12	-0.65 ± 0.03	-0.20 ± 0.05	-0.83 ± 0.06
E140	–	-0.73 ± 0.02	-0.28 ± 0.04	-0.53 ± 0.03
E141	–	-0.63 ± 0.03	-0.26 ± 0.05	-0.66 ± 0.05

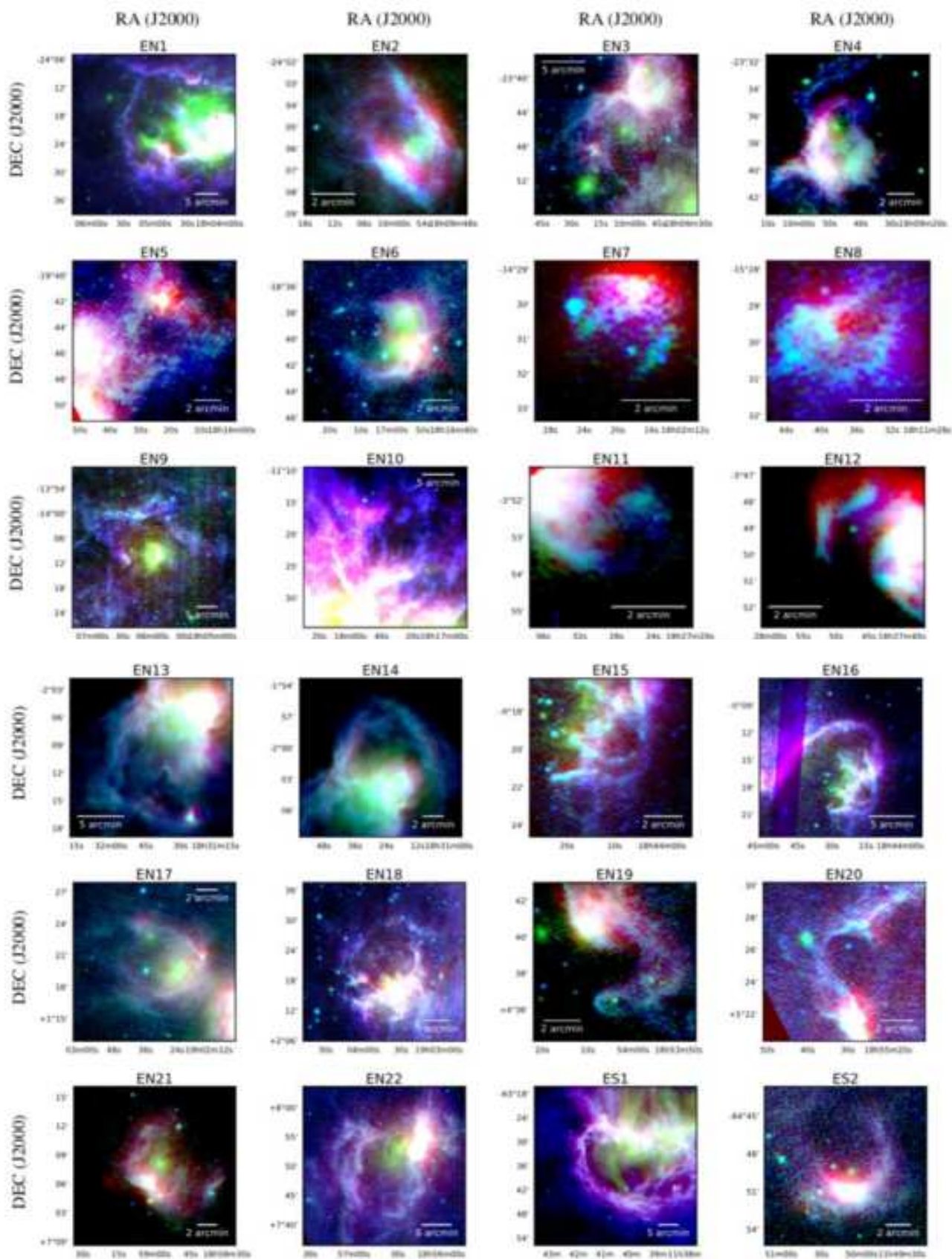


Fig. 12. Images of the IR bubbles newly found in this study. The blue, green and red correspond to the AKARI 9 μm, 18 μm and 90 μm band images, respectively.

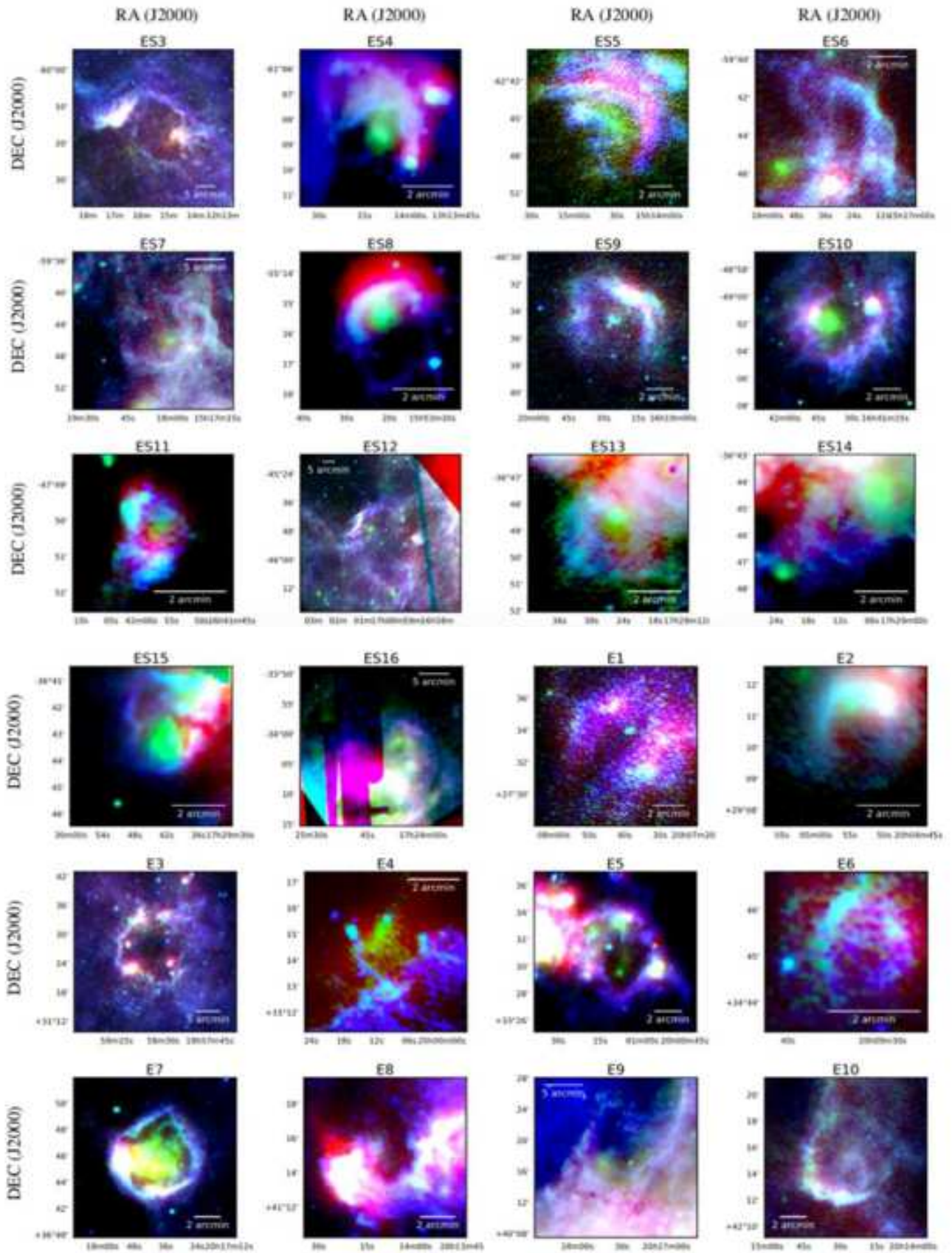


Fig. 12. Continued.

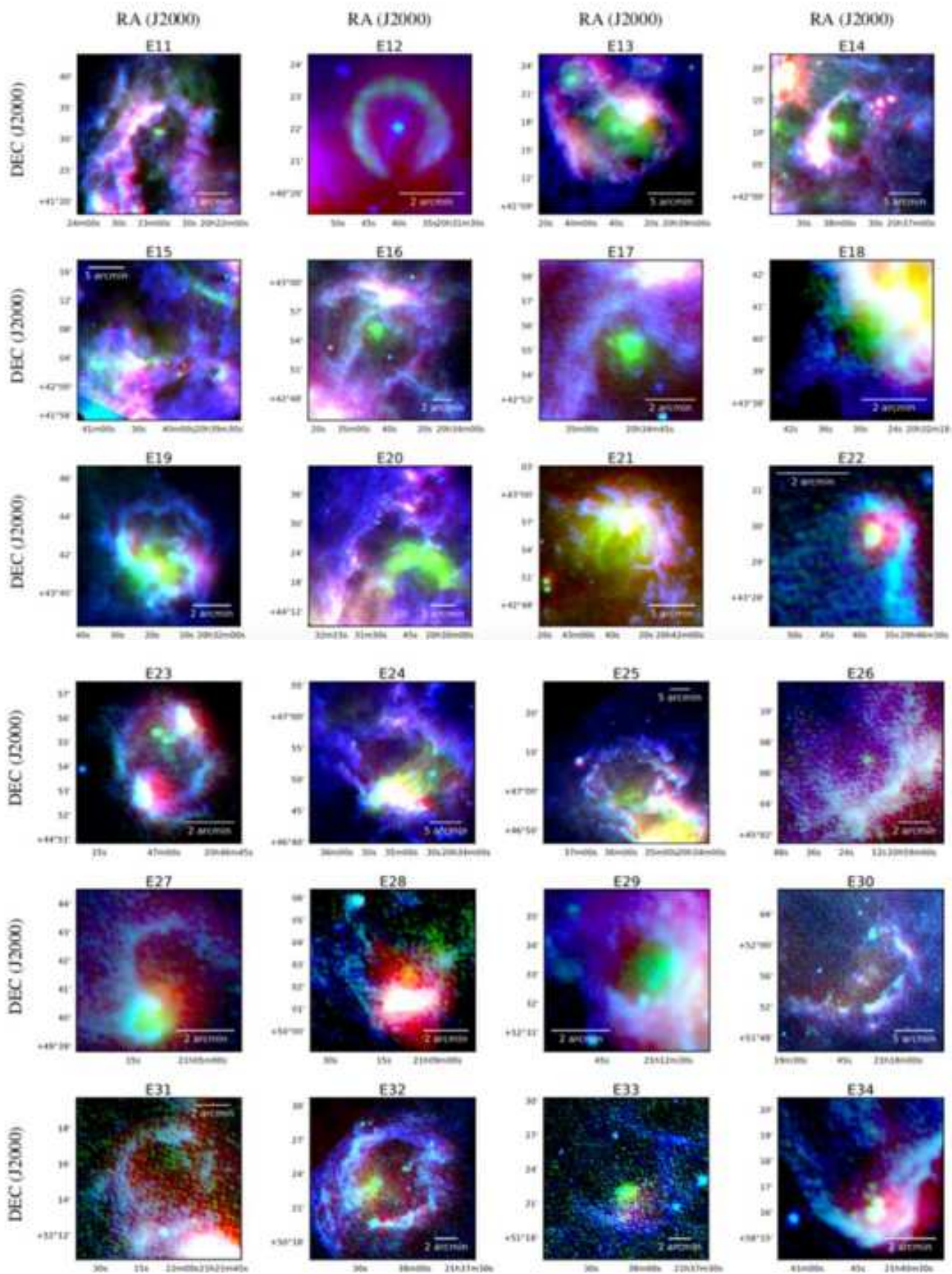


Fig. 12. Continued.

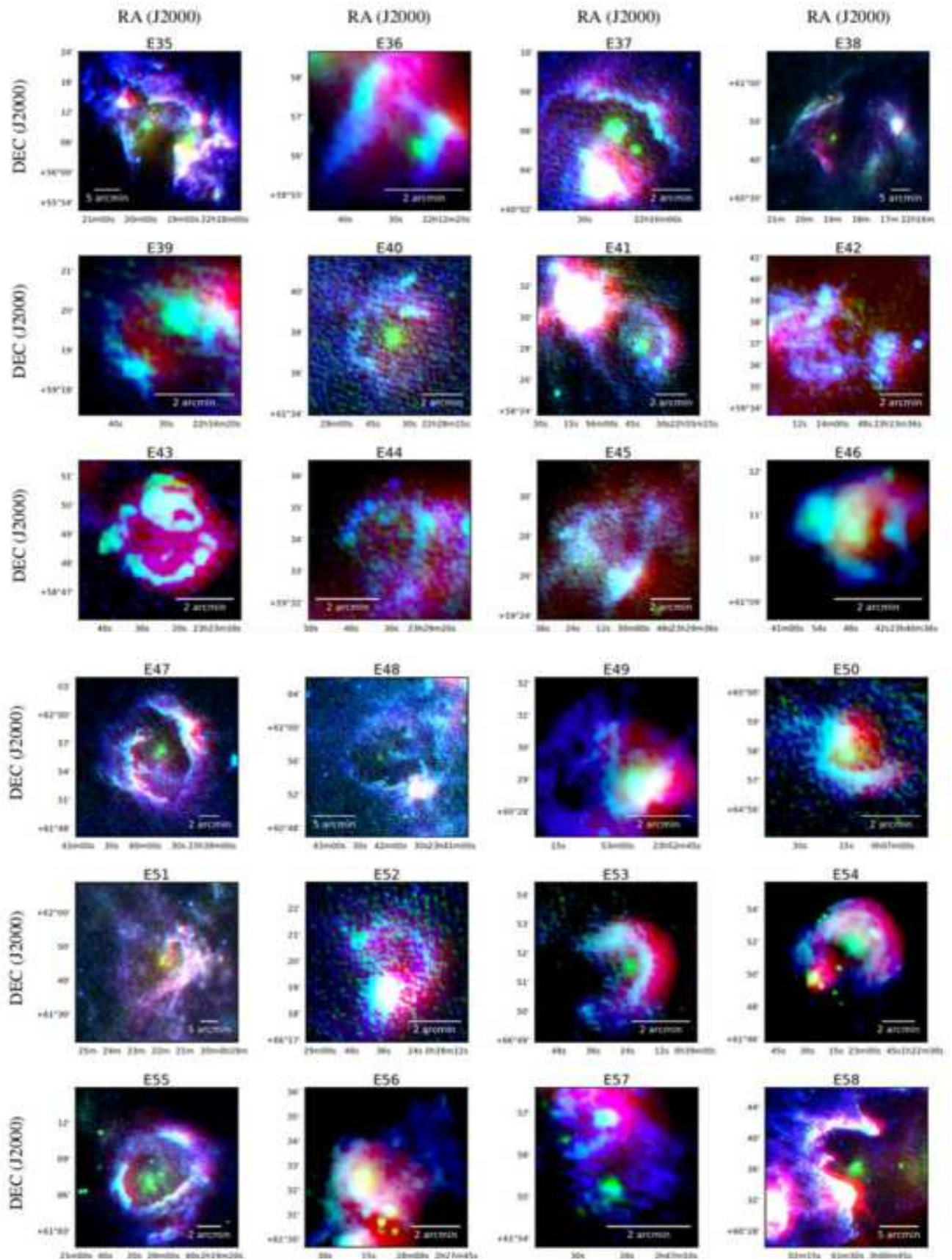


Fig. 12. Continued.

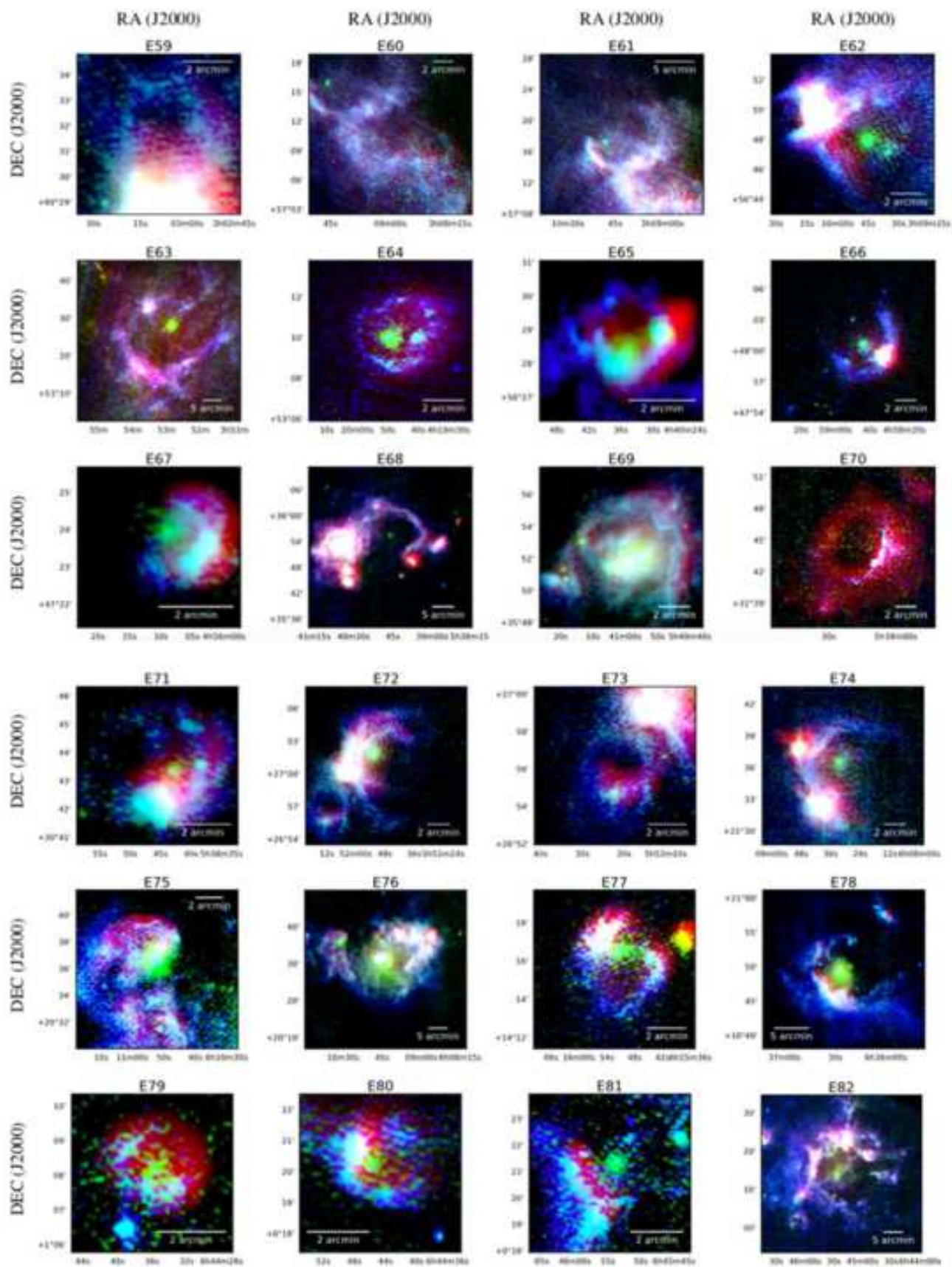


Fig. 12. Continued.

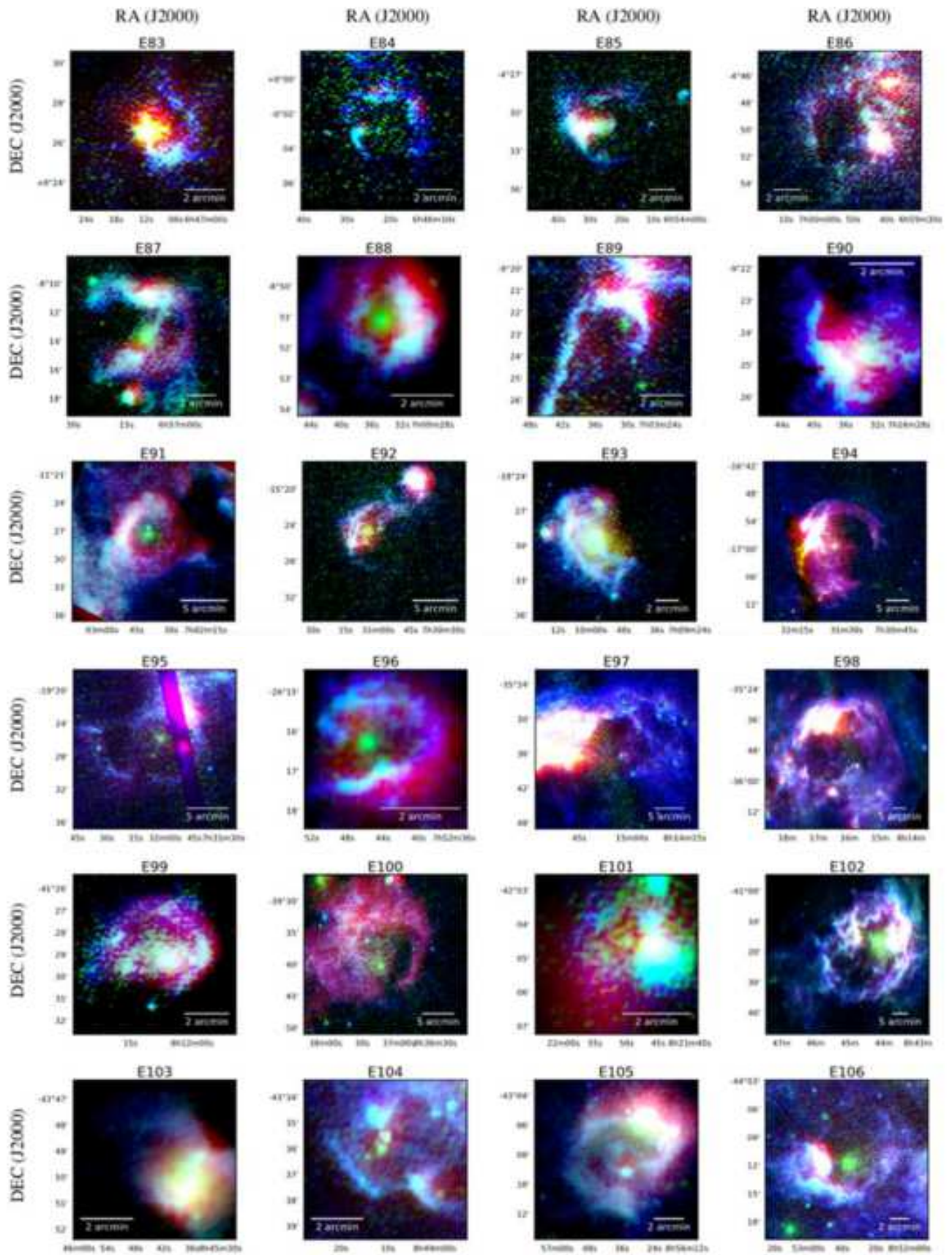


Fig. 12. Continued.

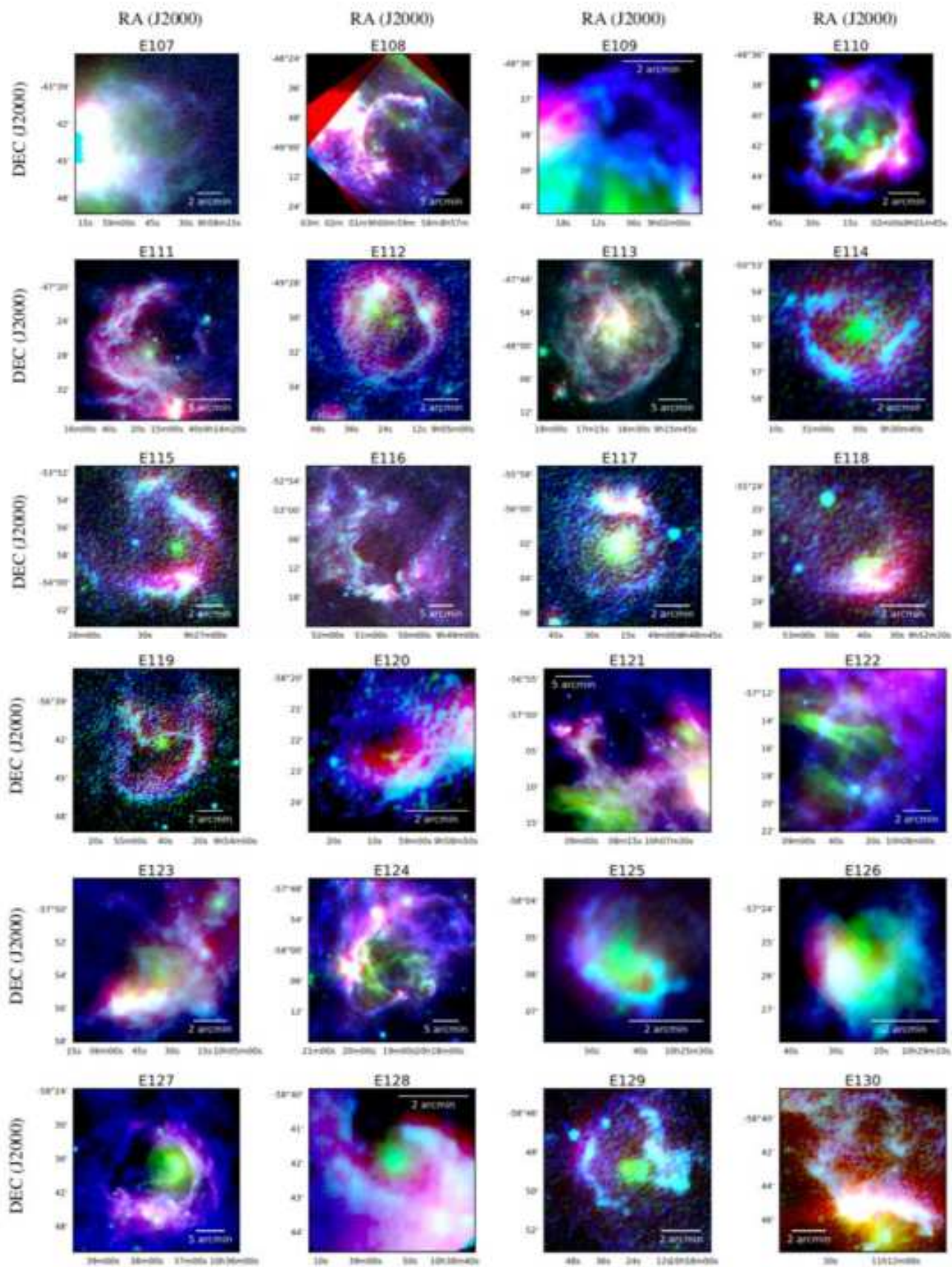


Fig. 12. Continued.

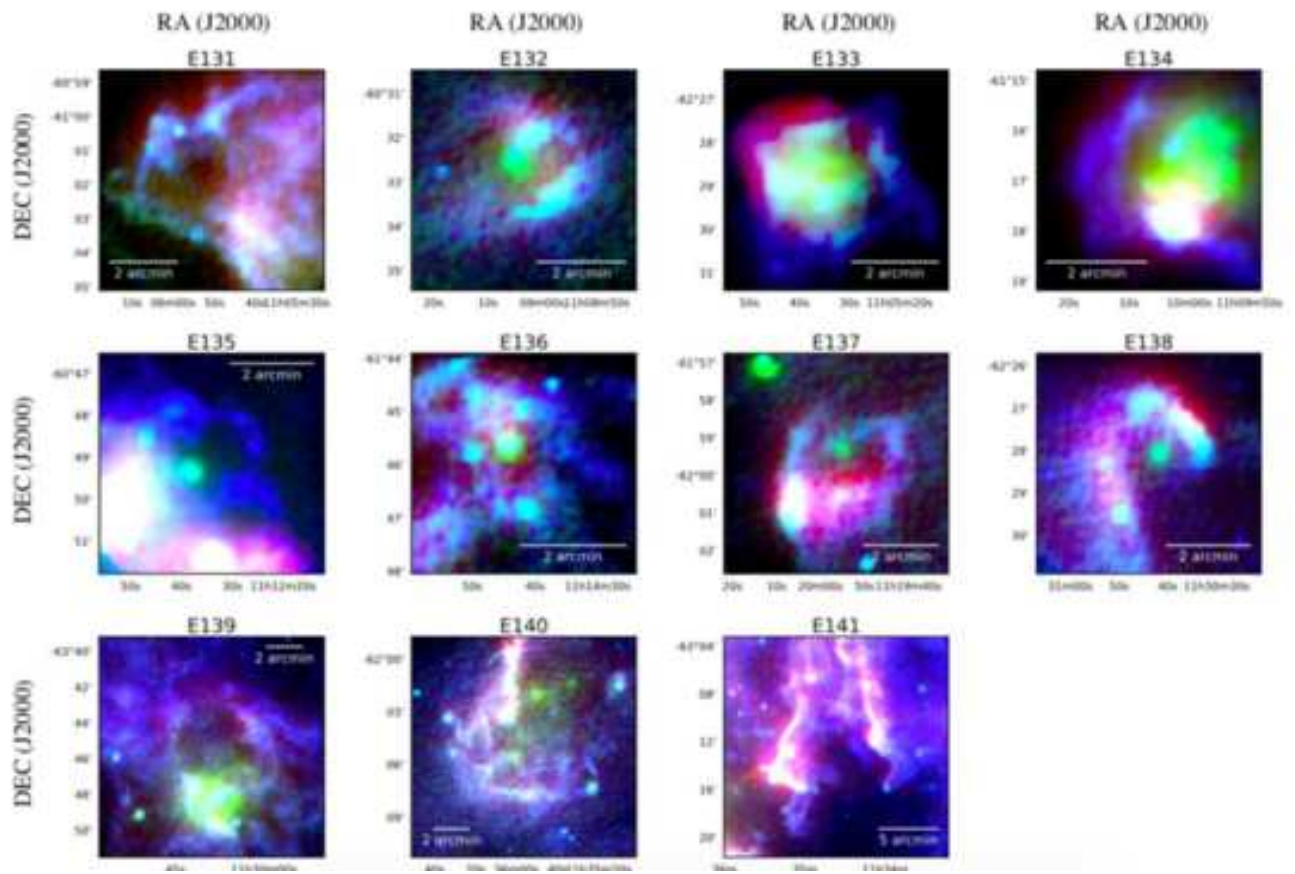


Fig. 12. Continued.

References

- Acero, F., et al. 2016, *ApJS*, 224, 8
- Ackermann, M., et al. 2012, *ApJ*, 750, 3
- Arendt, R.G., et al. 1998, *ApJ*, 508, 74
- Anderson, L.D., et al. 2012, *A&A*, 542, A10
- Bally, J., Snell, R.L., & Predmore, R. 1983, *ApJ*, 272, 154
- Bassino, L.P., Dessaunet, V.H., Muzzio, J.C., & Waldhausen, S. 1982, *MNRAS*, 201, 885
- Baug, T., Dewangan, L.K., Ojha, D.K., & Ninan, J.P. 2016, *ApJ*, 833, 85
- Beaumont, C.N., & Williams, J.P. 2010, *ApJ*, 709, 791
- Benjamin, R.A., et al. 2003, *PASP*, 115, 953
- Bronfman, L., Casassus, S., May, J., & Nyman, L. 2000, *A&A*, 358, 521
- Case, G.L., & Bhattacharya, D. 1998, *ApJ*, 504, 761
- Churchwell, E., et al. 2006, *ApJ*, 649, 759
- Churchwell, E., et al. 2007, *ApJ*, 670, 428
- Churchwell, E., et al. 2009, *PASP*, 121, 213
- Dale, J.E., Bonnell, I.A., & Whitworth, A.P. 2007, *MNRAS*, 375, 1291
- Dalglish, H.S., Longmore, S.N., Peters, T., Henshaw, J.D., Veitch-Michaelis, J.L., & Urquhart, J.S. 2018, *MNRAS*, 478, 3530
- Deharveng, L., Zavagno, A., Schuller, F., Caplan, J., Pomarès, M., & Breuck, C.D. 2009, *A&A*, 496, 177
- Deharveng, L., et al. 2010, *A&A*, 523, A6
- Deharveng, L., et al. 2012, *A&A*, 546, A74
- Deharveng, L., et al. 2015, *A&A*, 582, A1
- Dewangan, L.K., Ojha, D.K., Grave, J.M.C., & Mallick, K.K. 2015, *MNRAS*, 446, 2640
- Dewangan, L.K., Ojha, D.K., Zinchenko, I., Janardhan, P., Ghosh, S.K., & Luna, A. 2016, *ApJ*, 833, 246
- Doi, Y., et al. 2015, *PASJ*, 67, 50
- Draine, B.T. 2003, *ARA&A*, 41, 241
- Draine, B.T., & Li, A. 2007, *ApJ*, 657, 810
- Draine, B.T. 2011, *Physics of the Interstellar and Intergalactic Medium*, Princeton University Press
- Dubner, G., Giacani, E., Cappa de Nicolau, C., & Reynoso, E. 1992, *A&AS*, 96, 505
- Elmegreen, B.G. 1998, in *ASP Conf. Ser.*, 148, *Origins*, ed. C.E. Woodward et al. (San Francisco: ASP), 150
- Fukui, Y., et al. 2018, *PASJ*, 70, S46
- Gennaro, M., et al. 2012, *A&A*, 542, A74
- Guesten, R., & Mezger, P.G. 1982, *Vistas Astron.*, 26, 159
- Habe, A., & Ohta, K. 1992, *PASJ*, 44, 203
- Han, J.L., Manchester, R.N., Lyne, A.G., Qiao, G.J., & van Straten, W. 2006, *ApJ*, 642, 868
- Hattori, Y., et al. 2016, *PASJ*, 68, 37
- Heiles, C., & Crutcher, R. 2005, *Cosmic Magnetic Fields (Lect. Notes Phys. vol.664)*, 137
- Hou, L.G., & Gao, X.Y. 2014, *MNRAS*, 438, 426
- Hou, L.G., & Han, J.L. 2014, *A&A*, 569, A125
- Ishihara, D., Kaneda, H., Onaka, T., Ita, Y., Matsuura, M., & Matsunaga, N. 2011, *A&A*, 534, A79
- Kaneda, H., et al. 2013, *A&A*, 556, A92
- Kawada, M., et al. 2007, *PASJ*, 59, S389
- Kennicutt, R.C., & Evans, N.J. 2012, *ARA&A*, 50, 531
- Kraemer, K.E., et al. 2010, *AJ*, 139, 2319
- Kokusho, T., Kaneda, H., Bureau, M., Suzuki, T., Murata, K., Kondo, A., & Yamagishi, M. 2017, *A&A*, 605, A74
- Kuchar, T.A. & Bania, T.M. 1994, *ApJ*, 436, 117
- Latter, W.B. 1991, *ApJ*, 377, 187
- Lorimer, D.R., et al. 2006, *MNRAS*, 372, 777
- Mallick, K.K., Kumar, M.S.N., Ojha, D.K., Bachiller, R., Samal, M.R., & Pirogov, L. 2013, *ApJ*, 779, 113
- Martins, F., Schaerer, D., & Hillier, D.J. 2005, *A&A*, 436, 1049
- Mathis, J.S., Metzger, P.G., & Panagia, N. 1983, *A&A*, 128, 212
- Matsuura, M., et al. 2009, *MNRAS*, 396, 918
- Misiriotis, A., Xilouris, E.M., Papamastorakis, J., Boumis, P., & Goudis, C.D. 2006, *A&A*, 459, 113
- Miszalski, B., Parker, Q.A., Acker, A., Birkby, J.L., Frew, D.J., & Kovacevic, A. 2008, *MNRAS*, 384, 525
- Molinari, S., et al. 2010, *PASP*, 122, 314
- Molinari, S., et al. 2016, *A&A*, 591, A149
- Nakanishi, H., & Sofue, Y. 2006, *PASJ*, 58, 847
- Nakanishi, H., & Sofue, Y. 2016, *PASJ*, 68, 5
- Ohama, A., et al. 2018, *PASJ*, 70, S45
- Onaka, T., Yamamura, I., Tanabe, T., Roellig, T.L., & Yuen, L. 1996, *PASJ*, 48, L59
- Onaka, T., et al. 2007, *PASJ*, 59, S401
- Osterbrock, D.E. 1989, *Astrophysics of gaseous nebulae and active galactic nuclei*, Mill Valley, CA: University Science Books
- Parker, Q.A., et al. 2006, *MNRAS*, 373, 79
- Pavel, M.D., & Clemens, D.P. 2012, *ApJ*, 760, 150
- Rahman, M., & Murray, N. 2010, *ApJ*, 719, 1104
- Rodríguez-Esnard, T., Trinidad, M.A., & Migenes, V. 2012, *ApJ*, 761, 158
- Samal, M.R., Deharveng, L., Zavagno, A., Anderson, L.D., Molinari, S., & Russeil, D. 2018, *A&A*, 617, A67
- Simpson, R.J., et al. 2012, *MNRAS*, 424, 2442
- Smith, J.D.T., et al. 2007, *ApJ*, 656, 770
- Stierwalt, S., et al. 2014, *ApJ*, 790, 124
- Strömgren, B. 1939, *ApJ*, 89, 526
- Takita, S., et al. 2015, *PASJ*, 67, 51
- Tenorio-Tagle, G. 1979, *A&A*, 71, 59
- Tielens, A.G.G.M. 2008, *ARA&A*, 46, 289
- Torii, K., et al. 2015, *ApJ*, 806, 7
- Watson, C., Corn, T., Churchwell, E.B., Babler, B.L., Povich, M.S., Meade, M.R., & Whitney, B.A. 2009, *ApJ*, 694, 546
- Watson, C., Hanspal, U., & Mengistu, A. 2010, *ApJ*, 716, 1478
- Webber, W.R., & Yushak, S.M. 1983, *ApJ*, 275, 391
- Whitworth, A., Lomax, O., Balfour, S., Mège, P., Zavagno, A., & Deharveng, L. 2018, *PASJ*, 70, S55
- Wolfire, M.G., Mckee, C.F., Hollenbach, D., & Tielens, A.G.G.M. 2003, *ApJ*, 587, 278
- Zhang, C.-P., Wang, J.-J., & Xu, J.-L. 2013, *A&A*, 550, A117
- Zinnecker, H., & Yorke, H.W. 2007, *ARA&A*, 45, 481